The Dissertation Committee for Christopher Lee Schardon Certifies that this is the approved version of the following dissertation:

Tuning halopyridines for covalent protein modification and applying a novel DDAH mutant to quantify methylated arginines

Committee:

Walter Fast, Supervisor

David Hoffman

Edward Mills

Rick Russell

Chris Whitman

Tuning halopyridines for covalent protein modification and applying a novel DDAH mutant to quantify methylated arginines

by

Christopher Lee Schardon, B.S.

Dissertation

Presented to the Faculty of the Graduate School of

The University of Texas at Austin

in Partial Fulfillment

of the Requirements

for the Degree of

Doctor of Philosophy

The University of Texas at Austin

December 2016

Dedication

To my better half, Rachael, for her love, support, and understanding. I am better everyday because you are by my side.

To my loving parents, for helping provide every opportunity for me to pursue my dreams.

To the philosophers, scientists, and thinkers that continue to spur my intellectual curiosity. "If I have seen further, it is by standing on ye shoulders of giants."

Acknowledgements

I would like to start by thanking my very first research mentor Dr. Michelle Bushey. As a young undergraduate at Trinity University I was introduced to analytical biochemistry in her lab. I will always remember that time as the moment science became tangible for me. I would also like to thank Dr. Adam Urbach. My second mentor and the professor who demonstrated a focused drive in research that has helped me to understand and overcome setbacks throughout my research career. I'd like to thank the graduate students I have had the pleasure and honor to share time, drinks, ideas, and laughs with. Ashley Solmonson, Joseph Taft, Tyler Stack, Jake LeVieux, Alex Bean, and more, you have all been an important part of this journey. I'd like to specifically thank the members of the Fast Lab past and present for thoughtful conversation both within and outside of 6.202E BME.

Dr. Rick Russell, Dr. David Hoffman, Dr. Christian Whitman, and Dr. Edward 'Ted' Mills, I'd like to thank you for being a part of my dissertation committee. I chose all of you because I have a high regard and respect for your scientific opinion. Finally, I would like to thank my PhD advisor, Dr. Walter Fast. Walt, you are an incredibly gifted scientist and thinker. Your thoughtful reflection and meticulous attention to detail have been important influences in my growth as a scientist. It has been an honor to be a part of your lab and I am fortunate to call you a friend. Thank you for providing me the opportunity to study at the interface of enzymology and drug discovery.

Tuning halopyridines for covalent protein modification and applying a novel DDAH mutant to quantify methylated arginines

Christopher Lee Schardon, Ph.D.

The University of Texas at Austin, 2016

Supervisor: Walter L. Fast

2- and 4-Halopyridines were previously identified as a novel class of protein modifiers. These weakly electrophilic fragment sized molecules were shown to act as quiescent affinity labels that selectively and covalently modify some protein thiols. Covalent modification can occur when a carboxylate side chain is found at a certain distance and orientation from a cysteine thiol. This arrangement of residues catalyzes covalent bond formation by stabilizing the active, protonated form of the pyridine, which allows subsequent attack by the cysteine thiol. This need for catalysis imparts a unique selectivity that sets 2- and 4-halopyridines apart from most electrophilic fragments since efficient modification is not only derived from inherent reactivity and proximity to the target nucleophile, but also by way of a protonation 'switch' catalyzed by two residues at the binding site of the target protein. The inherent selectivity of these fragment sized molecules and their relatively straightforward derivitization at multiple positions on the pyridine ring have prompted further study to characterize their unique features as a class of covalent protein modifiers and to explore their utility to engage therapeutic targets.

In this work, the features that set 4-halopyridines apart from other fragment-sized electrophiles are identified and characterized. These studies revealed the protonation 'switch' allows modulation of halopyridine reactivity through catalysis whereas the non-enzymatic reactivity remains low an effect not obtainable with other electrophilic fragments. After definition of the general requirements for protein modification and identification of methods to alter reactivity, additional protein targets that meet the requirements for 4-halopyridine modification are identified and validated. Modification of one of the identified targets for 4-halopyridines, V-Ki-ras2 Kristen rat sarcoma viral oncogene (KRas), is characterized in detail. It is demonstrated that the 4-halopyridine fragment represents a starting point to selectively modify this historically difficult drug target in cells.

In a separate project, enzyme inhibition is studied and applied in a different way. The utility of a substrate-inactivatable *Pseudomonas aeruginosa* dimethylarginine dimethylaminiohydrolase (*Pa*DDAH) mutant enzyme, *Pa*DDAH T165L, for the quantitative measurement of asymmetric dimethylarginine (ADMA) is evaluated. The catalytic partitioning between normal turnover and self-inactivation enables a low cost quantitative means for measurement of the clinically-relevant biomarker ADMA.

Table of Contents

List of Tables

List of Figures

Chapter 1. Introduction

The medicinal use of small molecules that function through the formation of covalent bonds has a long and storied history. Acetylsalicyclic acid (aspirin) is one of the best-known and most widely used drugs that work by covalent inhibition of its target. The recorded origins of aspirin can be traced back to as early as 200 B.C. when the Greek physician Hippocrates prescribed willow tree extracts for pain relief. While the use of willow bark to combat pain and fever continued into the 19th century, the main active ingredient, salicyclic acid, was not isolated until 1838 by Italian chemist Raffaele Piria.[1] Within a half-century, the production, distribution, and use of salicyclic acid was widespread as was the gastric irritation that accompanied its regular use.[2] A Bayer chemist, Felix Hoffmann, in 1897 synthesized a derivative of salicyclic acid, which effectively relieved the gastrointestinal distress associated with regular consumption of salicyclic acid.[3] This derivative, acetylsalicyclic acid, was coined aspirin and while its use continues to this day, its mechanism of action remained a mystery for almost a century longer.

In 1971, it was revealed that aspirin inhibits prostaglandin biosynthesis.[4,5] Synthesis of prostaglandins increases in response to local trauma. This causes elevated body temperature, inflammation, and pain. Aspirin was shown to act in part by acetylating, and irreversibly inactivating, both cyclooxygenase isoforms (COX-1 and COX-2), which are essential for prostaglandin synthesis.[6]

The history of aspirin highlights many of the themes associated with the development of covalent drugs, one of the most common themes being serendipitous

discovery and confirmation of the covalent mode of action only long after the clinical utility had been well established. For example, some of the most famous antibiotics (penicillin, cephalosporin(s), and fosfomycin) were discovered by fortuitous accident.[7] In the case of aspirin, the original acetylation of salicyclic acid was conducted not to convey any additional pharmacological effect when compared to the salicyclic acid, but merely to create a more palatable medicine. Incredibly, acetylsalicyclic acid not only served as a prodrug for salicyclic acid, which has been shown to have its own COX-1/2 independent anti-inflammatory effects, but also conferred irreversible inhibition of two principal proteins responsible for the local inflammatory response.[8]

Regardless of the serendipitous circumstances surrounding their discovery, these examples clearly demonstrate the therapeutic utility of covalent drugs. These early successes however, did not spur the rational development of covalent drugs in the modern era due to safety concerns surrounding irreversible and off-target binding. Irreversible binding presents potential risks of idiosyncratic toxicity and/or immune-mediated drug hypersensitivity. This response can cause the production of antibodies that target elements of the drug molecule itself or autoantibodies that recognize epitopes on drug-modified proteins that are now rendered "foreign".[9,10] These rare adverse reactions, in addition to the ever-present (associated with both covalent and non-covalent drug development) risk of generating reactive drug metabolites during normal metabolism, have been enough to deter pharmaceutical companies from considering their development.[11] In theory, the risks associated with off-target reactivity should decrease with decreased electrophilicity of the drug compound. Evidence for this idea is

demonstrated by the successful development of acrylamide- and nitrile-containing compounds compared to compounds containing more reactive electrophilic functional groups such as epoxides and reactive Michael acceptors.[10]

In the current landscape of structure based drug design, the incorporation and use of less-reactive electrophiles in targeted covalent inhibitor development has received renewed interest. Structural information of the drug target aids in the optimization of a drug candidate's non-covalent interaction in concert with placing a minimally reactive electrophile near a nucleophile of interest.[9] The optimization of non-covalent interactions with the target is not only important for target selectivity, but also essential for efficacy because the low inherent reactivity of the electrophilic moieties (e. g. acrylamide) necessitates a high effective molarity of the electrophile for a facile reaction. This development strategy continues to be used with moderate success, but the number of electrophilic moieties that fulfill the necessary requirements for incorporation into targeted covalent inhibitors and/or covalent drugs remains limited. Expanding the number of well-characterized electrophiles available for the development of future targeted covalent inhibitors would be advantageous, but few novel protein-modifying electrophilic moieties have been discovered and applied in the last quarter century.

In 2010, a high-throughput screen of fragment-sized inhibitors was carried out in an attempt to discover novel covalent modifiers of dimethylarginine dimethylaminohydrolase (DDAH).[12] This screen identified 4-halopyridines (4-bromo-2-methylpyridine and 4-chloro-2-hydroxymethylpyridine) as covalent inactivators of DDAH and were shown to represent a class of fragment-sized molecules that had not

been previously identified as covalent protein modifiers. Characterization of the 4-bromo-2-methylpyridine inactivation mechanism revealed that this fragment acts as a quiescent affinity label of DDAH meaning that inactivation is catalyzed by an off-pathway mechanism by the target protein. While unreactive towards non-specific nucleophiles (e.g. glutathione) in solution, the pyridine's reactivity is greatly enhanced when the pyridinium form can be stabilized through protein binding and interaction with a nearby carboxylate. Only when a protein nucleophile (e.g. thiol) is also correctly positioned at this binding site can modification occur.[13] These constraints create an inherent selectivity for targets where all requirements are met. Moreover, the necessity for pyridinium stabilization (termed the protonation 'switch') to promote nucleophilic aromatic substitution opens up the potential to modulate the electrophilic reactivity of the halopyridine scaffold in ways not available using other electrophiles.

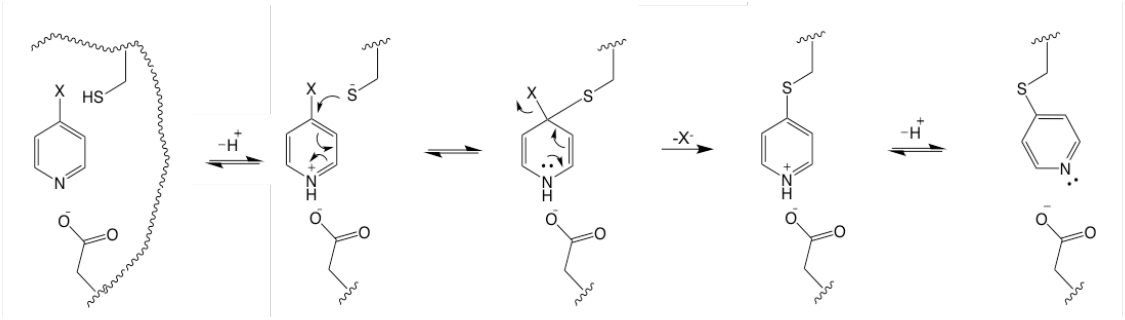

Figure 1.1 General Mechanism of 4-halopyridine protein modification.

In **Chapter 2**, two methods in which the reactivity of the halopyridine scaffold can be modulated are explored. The protonation 'switch' is hypothesized to allow reactivity to be uniquely tuned using pyridine nitrogen pK_a modulation and halogen

identity. Derivitization of typical electrophiles to increase reactivity also drastically increases non-selective reactions.[14] However, 4-halopyridine ring derivitization is shown to lead to only slight changes in non-enzymatic reactivity, but to significantly tune the reactivity for its targets. While the catalytic residues and the features of halopyridines required for protein modification have been characterized for inactivation of DDAH, they are not expected to be unique to the DDAH enzyme family. To confirm that not only DDAH, but also a wider subset of the proteome can be targeted using this scaffold, *Escherichia coli (E. Coli)* lysates were treated with 4-halopyridine derivatives containing a latent handle for Western blot visualization. The results provide evidence for our hypothesis and further highlight how the requirements for binding, pyridinium stabilization, and proximity to the nucleophile influence the scaffold's reactivity.

Affinity purification combined with mass spectrometry was previously used to identify primary screening 'hits' within the 2- and 4-chloropyridine proteomic subsets (unpublished).[15] In **Chapter 3,** verification of selected targets within this dataset is carried out. Of three targets chosen for validation, detailed characterization of the 4-halopyridine target KRas is studied in detail. KRas remains an elusive target for the treatment of cancer, but recent evidence suggests that covalent targeting strategies may provide a means to overcome some of the previously recognized hurdles in the development of direct Ras inhibitors.[16,17] Characterization of modification by 4-halopyridine derivatives revealed that KRas modification is similar to the mechanism previously shown for DDAH and *E. Coli* inosine monophosphate dehydrogenase (unpublished).[15] However, unlike these previously characterized targets, the covalent

adduct to KRas is not stable in solution due to subsequent hydrolysis. Following *in vitro* characterization, the effects of 4-chloropyridine treatment of cultured MiaPaca2 cells harboring oncogenic KRas and validation of target engagement with KRas in cell culture were tested. Although 4-halopyridine modification of KRas G12C was observed in this pancreatic carcinoma cell line, a robust functional effect on cell proliferation did not accompany 4-chloropyridine treatment. An *in vitro* test for the extent of KRas modification suggests that one factor may be due to only a small fraction of total KRas being modified in cells. This work demonstrates the ability to target and engage KRas using an inherently selective electrophilic fragment and represents a promising new strategy and starting point for KRas targeting.

Chapters 2 and 3 study enzyme inactivation for the purpose of blocking their physiological activity. In, contrast, **Chapter 4** presents work that uses enzyme inactivation as a quantitative analysis tool. The use of enzyme inactivation as a means for small molecule quantification is, to the best of our knowledge, a novel application not previously explored by others. Preliminary work conducted by Dr. Tom Linsky and Dr. Corey Johnson in our laboratory showed a mutant form of DDAH, T165L, was covalently inactivated by its own substrate over time due to partitioning between normal substrate turnover and self-inactivation (unpublished).[18] In Chapter 4, a methodology is developed to quantify N^{ω}- N^{ω}-L-dimethylarginine (ADMA), which is the native *Pa*DDAH T165L substrate and is also a clinically relevant biomarker. As it pertains to assay development, the experimental partition ratios for the DDAH substrates, ADMA, N^{ω}-monomethyl-L-argnine (NMMA), and *S*-methyl-L-thiocitrulline (SMTC) are

measured, and the influences on *Pa*DDAH T165L reactivation (following inactivation by substrate) are evaluated. Proof-of-principal experiments demonstrate the feasibility of this approach for ADMA quantification. The general assay workflow is experimentally optimized and applied to the quantification of ADMA in clinical blood-plasma samples. The concept of using mutation-induced substrate-inactivation as a means for small molecule quantification introduced here, may be applicable to other biomarkers of interest where substrate partitioning has been reported or can be engineered.

1.1 REFERENCES

1. Piria R. Sur de neuveaux produits extraits de la salicine (On new products extracted from salicine). *Comptes rendus*. **6**, 620-624 (1838).

2. Jeffreys D. *Aspirin: The Remarkable Story of a Wonder Drug*. Bloomsbury, 2004.

3. Dreser H. Pharmacologisches über Aspirin (Acetylsalicyl-saüre). *Pflügers Arch Gesamte Physiol Menschen Tiere*, **76**, 306–318 (1899).

4. Vane J. R. Inhibition of Prostaglandin Synthesis as a Mechanism of Action for Aspirin-like Drugs. *Nature New Biol*. **231**, 232 –235 (1971).
5. Mizuno K., Yamamoto S., Lands W. E. Effects of non-steroidal anti-inflammatory drugs on fatty acid cyclooxygenase and prostaglandin hydroperoxidase activities. *Prostaglandins*. **23,** 743-757 (1982).

6. Drahl C., Cravatt B. F., Sorensen E. J. Protein-Reactive Natural Products. *Angew. Chem. Int. Ed*. **44,** 5788-5809 (2005).

7. Wright P.M., Seiple I. B., Myers A. G. The evolving role of chemical synthesis in antibacterial drug discovery. *Angew. Chem. Int. Ed*. **53**, 8840–8869 (2014).

8. Amann R., Peskar B. A. Anti-inflammatory effects of aspiring and sodium salicylate. *Eur. J. Pharmacol*. **447,** 1-9 (2002).

9. Singh J., Petter R. C., Baillie T. A., Whitty A., The resurgence of covalent drugs. *Nature Reviews Drug Discovery*. **10**, 307-317 (2011).

10. Bauer R. Covalent inhibitors in drug discovery: from accidental discoveries to avoided liabilities and designed therapies. *Drug Discovery Today*. **20**, 1061-1073 (2015).

11. Park B. K., Boobis A., Clarke S., Goldring C. E., Jones D., Kenna J.G., Lambert C., Laverty H. G., Naisbitt D. J. , Nelson S, Nicoll-Griffith D. A., Obach R. S., Routledge P., Smith D. A., Tweedie D. J., Vermeulen N., Williams D. P., Wilson I. D. & Baillie T. A. Managing the challenge of chemically reactive metabolites in drug development. *Nature Reviews Drug Discovery*. **10**, 292-306 (2011).

12. Johnson, C. M., Linsky, T. W., Yoon, D. W., Person, M. D., Fast, W. Discovery of Halopyridines as Quiescent Affinity Labels: Inactivation of Dimethylarginine Dimethylaminohydrolase. *J. Am. Chem. Soc*. **133**, 1553 (2011).

13. Johnson C. M., Monzingo A. F., Ke Z., Yoon D., Linsky T. W., Guo H., Robertus J. D., Fast W. On the Mechanism of Dimethylarginine Dimetheylaminohydrolase Inactivation by 4-Halopyridines. *J. Am. Chem. Soc*. **133**, 10951-10959 (2011).

14. Kathman S. G., Xu, Z., Statsyuk A. V. A Fragment-Based Method to Discover Irreversible Covalent Inhibitors of Cysteine Proteases. *Journal of Med. Chem*. **57**, 4969-4974 (2014).

15. Er, J. A. The design of halopyridine-based activity-based probes and mechanistic studies of succinylarginine dihydrolase. Ph. D. Dissertation, University of Texas, Austin, TX, 2015.

16. Ostrem, J. M., Peters, U., Sos, M. L., Wells, J. A., & Shokat, K. M. K-Ras (G12C) inhibitors allosterically control GTP affinity and effector interactions. *Nature*. **503.** 548-551 (2013)

17. Lim, S. M., Westover, K. D., Ficarro, S. B., Harrison, R. A., Choi, H. G., Pacold, M. E., Carrasco, M., Hunter, J., Kim, N. D., Xie, T., Sim, T., Janne, P. A., Meyerson, M., Marto, J. A., Engen, J. R. & Gray, N. S. Therapeutic Targeting of Oncogenic K-Ras by a Covalent Catalytic Site Inhibitor. *Angew. Chem. Int. Ed*., ***53***, 199-204 (2014).

18. Linsky, T. W. Studies on the mechanism and inhibition of enzymes in the pentein superfamily. Ph. D. Dissertation, University of Texas, Austin, TX, 2012.

Chapter 2: 4-Halopyridines: Selectively Electrophilic Fragments with a Tunable Switch[1]

2.1 INTRODUCTION

Fragment-based drug discovery (FBDD) describes the method of identifying small molecules (ca. ≤250 Da) that bind a protein target and serve as starting points for further elaboration. The effectiveness of this approach towards non-covalent inhibitor development is now well documented among a diverse set of protein classes including kinases, proteases, chaperones, and others.[1-4]

The FBDD strategy is also advantageous in the design of targeted covalent inhibitors (TCI's). In practice, once a non-covalent fragment scaffold is identified, structure-based and computational methods can be used to guide the elaboration of the compound in order to place an electrophilic moiety near a nucleophile of interest.[5] Optimizing non-covalent binding affinity first, enables less reactive electrophiles to be used, in turn, increasing the likelihood of quickly developing a selective inhibitor. This approach has been especially effective towards the design of kinase inhibitors that target non-conserved cysteine residues.[6]

Recent drug development studies using TCIs often use acrylamides or substituted acrylamides as the electrophilic moiety to target the thiol of interest. The relatively poor electrophilicity of acrylamides make them an attractive choice compared to other more

[1] Chapter 2 was adapted from the following manuscript: Schardon CL, Tuley A, Er J, Kenefick H, Swartzel J, Fast W. (2016) 4-Halopyridines: Selectively Electrophilic Fragments with a Tunable Switch. *In preparation*. A. Tuley , J. Er, J. Swartzel contributed to compound synthesis and H. Kenefick to experimental design.

reactive electrophilic moieties to avoid off target effects. The increased reactivity of cyanoacrylamide derivatives also increases the reversibility of modification reducing some concerns about off-target modification.[7] Still, it is unlikely that all thiols of interest can be effectively targeted using the acrylamide moiety due to the trade-offs between optimizing non-covalent interactions and properly orienting the electrophile for thiol attack. The application of other fragments with advantages similar to those afforded by acrylamide (e.g. low inherent reactivity), but with enhanced selectivity would be advantageous.

One scaffold, 4-halopyridine, was recently identified in an effort to find novel inhibitors of the nitric oxide-controlling enzyme dimethylarginine dimethylaminohydrolase (DDAH).[8-10] For inhibition of DDAH, the 4-halopyridines were classified as quiescent affinity labels, indicating that catalysis (but not the normal DDAH mechanism) is needed for nucleophilic aromatic substitution at the 4- position under biological conditions. In the case of DDAH, covalent modification can only occur because a carboxylate side chain is found at a certain distance and orientation from a cysteine thiol. This arrangement of residues stabilizes the active, protonated form of the pyridine, and subsequent attack by the cysteine thiol is thus catalyzed.[10] Concisely, the reactivity and the selectivity of this fragment sized small molecule are interdependent, producing an inherent selectivity for targets where all requirements are met.

These requirements set 2- and 4-halopyridines apart from most electrophilic fragments. For example, when other weak electrophiles, like acrylamide, are incorporated into TCI's, efficient modification is derived not from any change in

reactivity, but solely from the high effective concentration brought on through non-covalent binding to the target. In contrast, modification by the 4-halopyridine fragment relies on catalysis in addition to non-covalent binding and proper orientation. As such, the 4-halopyridine scaffold represents a unique electrophilic fragment (≤250 Da) whose reactivity and selectivity is defined by a simple protonation 'switch', catalyzed by residues in its target binding site.

The simple structure and activation mechanism of 4-halopyridines suggest that this scaffold may be useful for a much wider array of applications in the design of molecular probes, enzyme inhibitors, and therapeutics.[9] In this chapter, several aspects of this scaffold are explored and characterized in detail in order to facilitate their development as covalent modifying agents. Specifically, we aimed to (1) define the rate enhancement afforded by the protonation 'switch', (2) determine the influences halogen species and (3) pyridine nitrogen pK_a modulation have on inactivation and/or thiol modification rates (using hDDAH1 as a model enzyme), and (4) ultimately confirm the applicability of 4-halopyridines for use on a broader set of targets.

2.2 MATERIALS AND METHODS

Materials

Unless noted otherwise, all chemicals are from Sigma- Aldrich Chemical Co. (St. Louis, MO). hDDAH1 was purified and assayed as described previously.[11] 4-Chloro-2-metheyl-pyridine, 3-amino-4-bromo-pyridine, and 2-amino-4-bromo-pyridine were obtained from Chem-Impex International, Inc. (Wood Dale, IL). 3-Amino-4-iodo-

pyridine and 4-bromo-2-methylpyridine were from Oakwood Chemical (Estill, SC). 2-Trifluoromethyl-4-chloropyridine was from Ark Pharm Inc. (Libertyville, IL). and 4-Chloro-3-carboxypyridine was from Enamine LLC. (Monmouth Jct., NJ).

4-Halopyridine pK_a Calculation

Pyridine nitrogen aqueous ionization constants (pK_a) for all 4-halopyridines and derivatives used in this study were calculated using the pK_a calculator plugin (default settings) in MarvinSketch Version 15.11.16.0.[12-14]

Determination of 4-Halopyridine Relative Reactivity with Glutathione

Reduced glutathione was incubated with compounds **1-8, and 29** at a 1:1 ratio (1 mM each) in buffer containing 0.1 M NaCl, 0.15 M KH_2PO_4, 1 mM ethylenediaminetetracetic acid (EDTA) at pH 7.5 for 45 min. Samples were quenched upon addition of 5,5'-dithiobis-2-nitrobenzoic acid (DTNB) to a final concentration of 1.85 mM. Buffer was added to each sample resulting in a total volume of 1.25 mL. The absorbance at 412 nm was read for each sample to determine the amount of reduced glutathione remaining after the 45 min incubation. The amount of reduced glutathione was calculated using the extinction coefficient for DTNB at 412 nm in dilute buffer solutions, ε_{412}= 14,150 $M^{-1}cm^{-1}$.[15]

Determination of Reaction Rate for Thiophenol with Halopyridines

Reduced thiophenol (1 mM) was incubated with compounds **8-16, 16m**, **22-25**, and **29** (10 mM) in buffer containing 0.1 M NaCl, 0.15 M KH_2PO_4, 1 mM EDTA at pH 7.5. Aliquots were removed from the incubations at various time points (20 uL, 0-80

min) and diluted into buffer solution containing DTNB (1.85 mM) for a final sample volume of 1 mL. The absorbance at 412 nm was read for each time point to determine the amount of free thiol remaining (ε_{412}= 14,150 $M^{-1}cm^{-1}$). The observed reaction rates (k_{obs}) were determined by fitting the percent reduced thiol remaining over time to a single-exponential equation. All fits were calculated using KaleidaGraph (Synergy Software, Reading, PA)

Time and Concentration Dependent Inactivation Assays

Assays were carried out as previously described[10]. The observed inactivation rates (k_{obs}) were determined by fitting the percent remaining activity over time to a single-exponential equation. The resulting k_{obs} values were then plotted against inactivator concentration to determine the second order rate constant for each compound tested. All fits were calculated using KaleidaGraph (Synergy Software, Reading, PA)

Preparation of Naïve *Escherichia coli* Lysates

BL21(DE3) *Escherichia coli (E. Coli)* was grown in 500 mL Lysogeny Broth (LB) medium at 37 °C with shaking and harvested by centrifugation 1 h after transition into stationary phase (OD_{600} = 1.5).[16] Cells were suspended in buffer containing 100 mM KCl / K_2HPO_4 at pH 8 supplemented with protease inhibitor cocktail (170 μg/mL phenylmethylsulfonyl fluoride (PMSF), 1 μg/mL Pepstatin A, 1 μg/mL Leupeptin) and lysed by sonication (210 s total, 10 s pulse on/45 s pulse off, 70% amplitude).

Labeling of Naïve *E. coli* Lysates

Naïve *E. coli* lysates (80 μg total protein, determined by Bradford Assay) were

treated with **30** or **31** (1 mM each) in buffer containing 100 mM KCl / K_2HPO_4 at pH 8 at room temperature for 3 h.[17] Following incubation, a biotin tag was selectively attached to alkyne groups via the click reaction described below.

General Procedure for Cu(I)-catalyzed Azide-alkyne Click Reaction.

A biotin tag was selectively appended to alkynes in the reaction mixture by treating samples with *N*-[2-[2-[2-(2-azidoethoxy)ethoxy]ethoxy]ethyl]hexahydro-2-oxo-(3*aS*,4*S*,6*aR*)- 1H-thieno[3,4-*d*]imidazole-4-pentanamide (Biotin-PEO_3-azide, 100 μM), tris(2-carboxyethyl)phosphine (TCEP, 1 mM), tris[(1-benzyl-1H-1,2,3-trazol-4-yl)methyl]amine (TBTA, 100 μM), and $CuSO_4$ (1 mM), making the final reaction volume 50 μL. Samples were gently vortexed and allowed to react for 1 h at room temperature. Reactions were quenched by adding standard 4 × sodium dodecyl sulfate polyacrylamide gel electrophoresis (SDS-PAGE) loading buffer. Samples were separated by 1D SDS-PAGE and analyzed by Western blot as described below.

Western Bloting

Western blots were performed by standard procedures using two primary antibodies, IgG fraction monoclonal mouse anti-biotin (1:200, Jackson ImmunoResearch, West Grove, PA) coupled with the Odyssey IR Dye Western Blot Kit I (Li-Cor Biosciences, Lincoln, NE), which contains IR Dye 800CW goat anti-mouse secondary antibody (1:10000). Images were scanned using an Odyssey Infrared Imaging System (Li-Cor Biosciences, Lincoln, NE) at the core DNA Facility (University of Texas, Austin).

2.3 RESULTS AND DISCUSSION

Despite the concerns involving off-target-reactivity and the potential for drug-induced toxicity associated with the development of covalent drugs, their utility for improving human health has become more widely appreciated in recent years.[5] This is reflected by both the increase in clinical trials for, and FDA approvals of, covalent drugs.[18,19] As mentioned, a number of current covalent inhibitors use acrylamide as the electrophilic moiety because of its low reactivity compared to other electrophiles. The adoption of alternative electrophilic fragments for the development of TCIs would call for the conservation of low intrinsic reactivity as well as the offer of other advantages. We reason that the 4-halopyridine scaffold represents a novel tool in this respect based on its simple, tunable, protonation 'switch'.

Glutathione Reactivity Comparison

In an attempt to relate the reactivity of 4-halopyridines with other electrophilic fragments including acrylamide, representative electrophile fragments from FDA approved drugs, as well as more reactive electrophiles commonly used in protein modification, were tested for their ability to be modified by reduced glutathione (GSH) at pH 8. [20-23] Both 4-chloropyridine (**8**) and drug fragment representatives showed no observable modification by GSH under these conditions. In contrast, the protein modification reagents showed modification by GSH and the extent of reaction reflected each compound's relative reactivity (Figure 2.1).

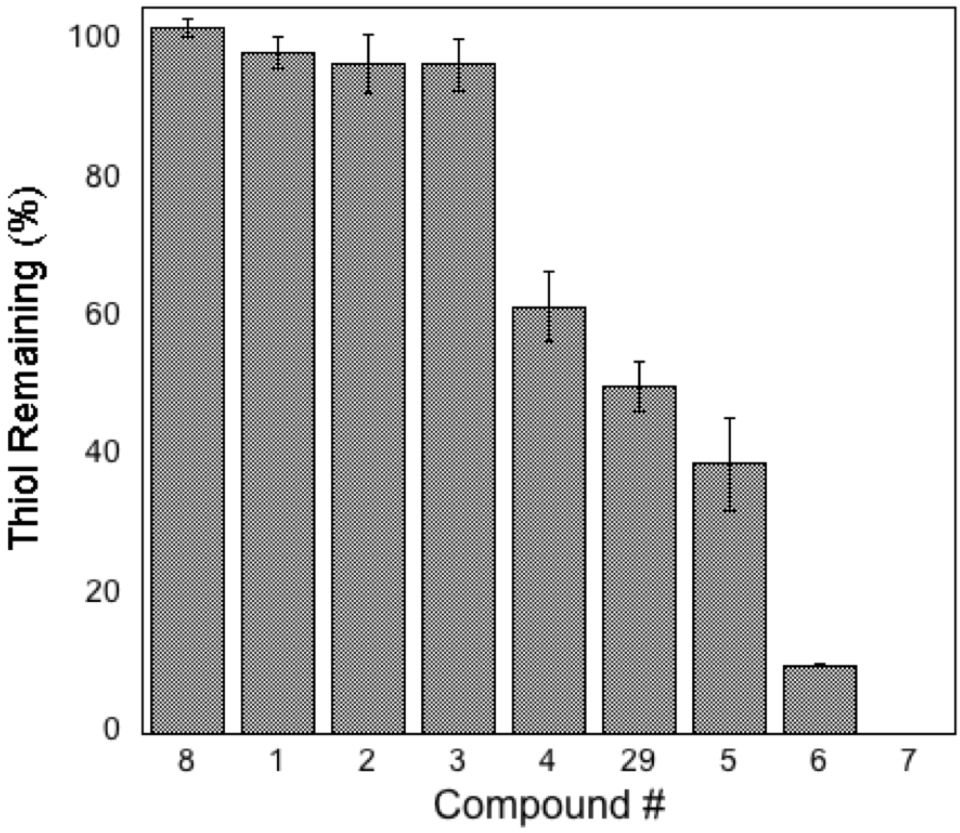

Figure 2.1 Relative reactivity of electrophiles against glutathione. Percentage of reduced glutathione remaining after 45 min incubation at equimolar concentrations (1 mM) of compound and glutathione normalized to a no compound control. (Compound names and structures can be found in Table 2.1 and 2.2)

One of the unique features of the 4-halopyridine scaffold is the necessity for stabilization of the pyridinium (the protonated pyridine) to catalyze nucleophilic attack. This protonation 'switch' can be mimicked chemically through *N*-methylation. To represent the fully reactive 4-halopyridine, 4-chloro-*N*-methyl-pyridine (**29**) was tested for the ability to be modified by GSH. When the pyridinium form is fixed by *N*-methylation, the halopyridine compounds instead showed increased reactivity comparable to protein modification reagents such as iodoacetamide (**5**).

These results highlight the 'quiescent' quality of this scaffold. At physiological pH values the 4-halopyridines show no measurable reactivity, similar to the low

reactivity of electrophiles currently used in TCIs. However, unlike classical affinity labels, substantial selectivity is achieved just by the fragment moiety itself. In other words, its electrophilicity is enhanced by the binding pocket (enzyme stabilization of the pyridinium form), and thus has enhanced reactivity through catalysis, not just by a high effective concentration.

Protonation 'Switch' Rate Enhancement Quantification

This 4-halopyridine protonation 'switch' represents a simple catalytic step that greatly influences the reactivity (and selectivity) of the 4-halopyridine scaffold. We reasoned that by quantifying the maximum possible rate enhancement afforded by this 'switch', we could define an upper limit on the effect catalysis can have on promoting modification. That is, when the optimal conditions are encountered, what increase in reactivity can be expected? To accomplish this, an analogous assay to the one used in the electrophilic fragment comparison panel was employed. As previously noted above, GSH is not able to modify the 4-chloropyridine to any observable extent under these experimental conditions. Therefore, the stronger thiol nucleophile thiophenol (pK_a = ~6.6) was used instead.[24] Reaction of thiophenol with 4-chloropyridine (**8**) was observable under these experimental conditions, using saturating amounts of **8** over long time periods (0-80 min). To measure the maximum rate enhancement achieved by the pyridinium form, 4-chloro-*N*-methylpyridine (**29**) was used. A $3.7 \pm 0.2 \times 10^3$-fold increase in k_{obs} was observed when comparing the k_{obs} of **8** to the protonated mimic**, 29**

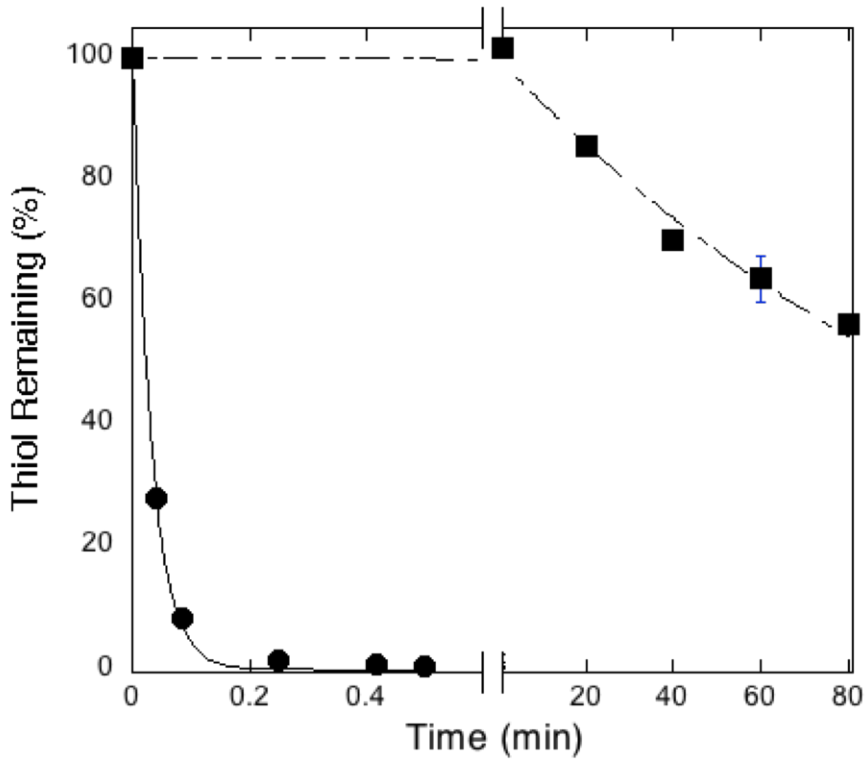

Figure 2.2 Reaction rate of thiolphenol (1 mM) under saturating conditions of compounds 8 (● , 10 mM) and 30 (■, 10 mM). Single exponential fits of compound 8 and compound 30 give kobs values of -7.58 +/- 0.37 x 10^{-3} min^{-1} and -3.13 +/- 0.07 x 10^{1} min^{-1}, respectively.

(Figure 2.2). At the concentration of **8** used in these experiments (10 mM), approximately 3 μM will be found in the protonated form. Interestingly, the k_{obs} ratio between **8** and **29** is in the same range as the ratio of protonated to deprotonated fractions of **8** at neutral pH suggesting the *N*-methyl analog is a good mimic for the protonated pyridinium.

In this simplified, non-enzymatic model reaction, a rate enhancement of almost 4,000-fold is achieved upon formation of the pyridinium ion. In this case, we used a highly reactive nucleophile under saturating conditions of **8** in order to quantify this non-

specific background reactivity. This analysis gives an approximation of the reactivity enhancement that can be achieved by way of the protonation 'switch'.

With respect to further development and use of this scaffold, these results show that unactivated 4-halopyridines, like acrylamide, are weakly electrophiles likely to show little non-specific off target reactivity. However, modification by the 4-halopyridine scaffold upon pyridinium stabilization, as catalyzed by the target protein, can enhance reactivity approximately 4,000-fold. The protonation 'switch' affords additional selectivity as well as unique ways to tune its reactivity. Specifically, we reason that through derivitization of the pyridine ring and substitution of the halogen species, the reactivity, and thus the value of the protonation 'switch' can be tuned. In future embodiments, this tunable electrophilic fragment can be combined with other non-covalent binding moieties to construct very selective TCIs.

Halogen Dependence on Inactivation

The inactivation of *Pseudomonas aeruginosa* dimethylarginine dimethylaminohydrolase (*Pa*DDAH) by both a 4-bromo and 4-chloropyridine derivatives was reported previously during the discovery of the 4-halopyridine scaffold as a novel covalent protein modifier.[11, 12] Therefore, it was apparent that the *Pa*DDAH active site could accommodate different halogens, but its influence was not characterized. Here we investigate this influence in detail to provide data on how halogen substitution can be expected to effect covalent modification in the development of 4-halopyridine based covalent modifiers.

To explore the effect of halogen identity on enzyme inactivation, the 4-X-pyridine (X = Cl, Br, I) series was tested for the ability to inactivate human dimethylarginine dimethylaminohydrolase isoform 1 (hDDAH1). Of note, 4-fluoropyridine was found to be unstable in aqueous solution over the time period of the experiment and was therefore excluded from the series (data not shown). All 4-halopyridines showed time- and concentration-dependent inactivation. The concentration dependence of inactivation rates did not show saturation kinetics, but rather showed a linear dependence on inhibitor concentration (Figure 2.3). 4-Bromopyridine (**9**) was shown to be the most effective

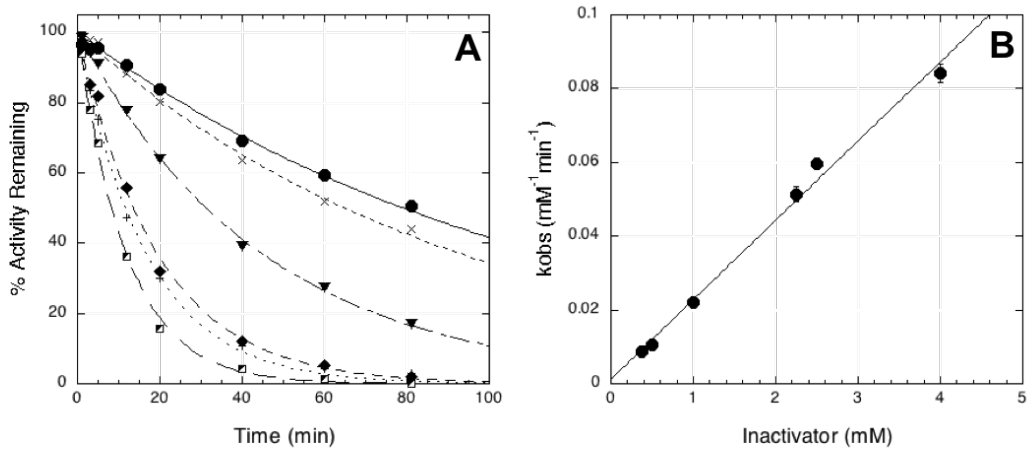

Figure 2.3 Time and concentration-dependent inactivation of hDDAH1 by 9. (A) Exponential fits to the observed hDDAH1 inactivation at concentrations of 9: 375 µM (●), 500 µM (×), 1 mM (▼), 2.25 mM (◆), 2.5 mM (+), 4 mM(◤) (B) Concentration dependence of the pseudofirst-order k_{obs} values give a second order rate constant of 0.36 +/- 0.02 $M^{-1}sec^{-1}$. The observed y-intercept is 0.001 +/- 0.002 min^{-1}.

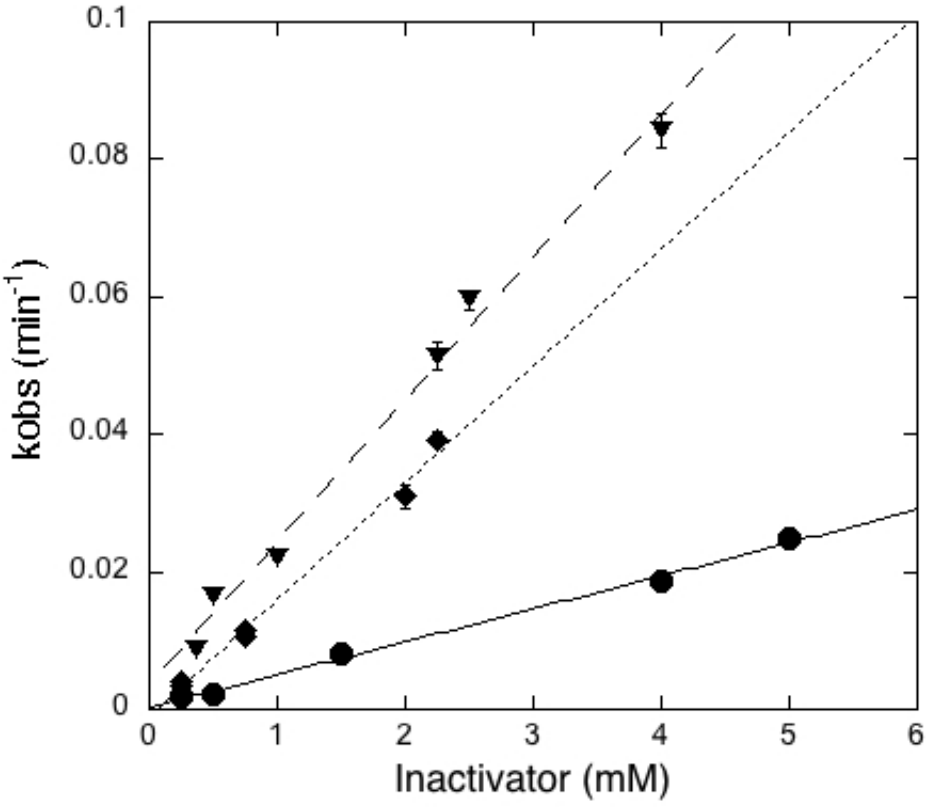

Figure 2.4 Concentration-dependent inactivation of hDDAH1 by 8 (●), 9 (▼), and 10 (◆) at pH 7.5. Concentration dependence of the pseudo first-order k_{obs} values for compounds 8-10 give second order rate constants of 7.67 +/- 0.83 x 10^{-2} $M^{-1}sec^{-1}$, 3.58 +/- 0.22 x 10^{-1} $M^{-1}sec^{-1}$, 2.83 +/- 0.18 x 10^{-1} $M^{-1}sec^{-1}$, respectively.

hDDAH1 inactivator. The k_{obs} for inactivation by 4-iodopyridine (**10**) showed a 20% reduction when compared to 4-bromo, and 4-chloropryidine (**8**) was found to be significantly slower than either 4-bromo or 4-iodopyridine (Figure 2.4).

The calculated pK_a of these 4-halopyridines only deviates by an estimated 0.05 units, suggesting insignificant differences between the protonated fractions of each halogen species in solution.[12] If the first step in the mechanism, nucleophilic attack by

the cysteine thiol, were rate limiting one would not expect to see a difference in the inactivation rates of **8-10**. (Figure 2.5) Conversely, if sigma complex (tetrahedral reaction adduct between the 4-halopyridine and cysteine thiol) collapse and concomitant halogen ion release were rate limiting, a halogen dependent effect would be expected. These experiments revealed a significant halogen dependent effect on inactivation (Br > I >> Cl), suggesting halogen ion release is indeed rate limiting.[24] However, the fact that 4-bromopyridine inactivates hDDAH1 faster than 4-iodopyridine could mean that there are size constraints imparted by the hDDAH1 active site that limit the rate of inactivation by 4-iodopyridine. Alternatively, if the rate of formation of the sigma complex and the rate of subsequent collapse and halogen release are comparable in this simple catalytic mechanism, 4-bromopyridine may represent the optimal halogen yielding both an

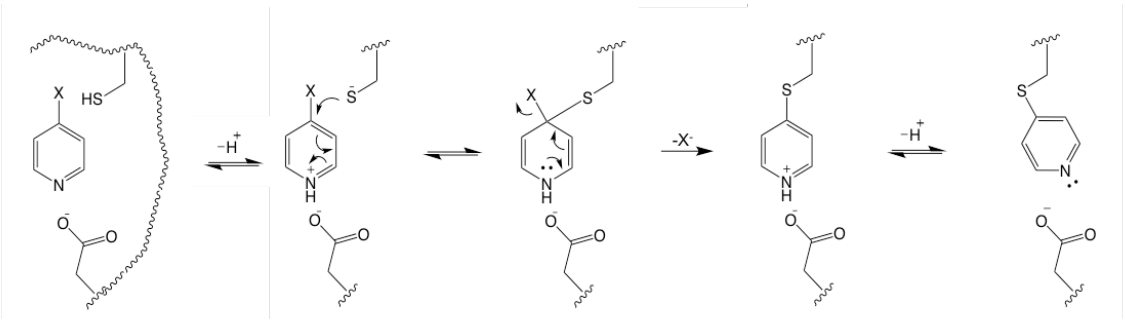

Figure 2.5 General mechanism of 4-halopyridine protein modification.

electron deficient 4-carbon (compared to 4-iodopyridine) and providing adequate leaving group stability (compared to 4-chloropyridine). While the underlying reasons for this observed order were not investigated in depth, these results do illustrate that the halogen species plays a significant role on the rate of catalysis. The results are also in agreement

with our current understanding of the mechanism. Specifically, cysteine nucleophilicity is not the predominating factor in reactivity. As such, stabilization of the pyridinium form could effectively lower the energy barrier to the point that nucleophilic attack, and formation of the sigma complex, is no longer rate limiting.

A broader search of literature describing the influence of halogen species during nucleophilic aromatic substitution reactions involving 4-halopyridine compounds found conditions almost entirely limited to reaction in organic solvents, using potent ionized nucleophiles, at high temperatures.[25-27] These are drastically different conditions than our experiments, making direct comparisons potentially problematic. Still, it is worth noting our observed trend is opposite to what might be expected on the basis of non-enzymatic S_NAr reactions with pyridine, as measured in organic solvents, wherein polarization of the carbon-halogen bond is the determining factor in halogen replacement.[25] Enzymatically, a similar reverse trend was reported for inactivation of *Actinobacter* sp. 4-CB-1 4-chlorobenzoyl-CoA dehalogenase, but in this case the S_NAr reaction involves catalysis by an enzyme specific for this reaction carried out on a benzene ring (i.e. no protonated species stabilization required).[28] Here we describe a simple protonation event, not likely to be specific to any particular enzyme class. Therefore, to the best of our knowledge, our results detail the first report of halogen influence on enzyme catalyzed 4-halopyridine modification under biologically relevant conditions.

hDDAH1 inactivation by a Diverse Set of Substituted Halopyridine Derivatives

Given the importance of protonation for activating the pyridine electrophile, we sought to understand how this proton 'switch' can be tuned by substituents on the

pyridine ring and how this modulation is potentially advantageous in the development of TCI's and other covalent modifiers.

We hypothesized that increasing nitrogen pK_a through ring derivitization would lead to increased inactivation rates by decreasing the barrier to protonation. To test this hypothesis, a series of commercially available substituted 4-halopyridine derivatives were purchased. Time-dependent inactivation of hDDAH1 was carried out at several concentrations for each compound in order to define the second order inactivation rate for each derivative (Table 2.1, 2.2, end of chapter). In all cases, there was no evidence of saturation kinetics at the concentrations tested (≤4 mM). Of the derivatives tested, the 2-methyl, 2-methanol, and 3-amino substitutions resulted in increased second order inactivation rate constants ($M^{-1}sec^{-1}$) compared to their respective un-substituted scaffolds (Figure 2.6). Regardless of substituent the same halogen dependence was observed. That is, for derivatives with common ring substituents the inactivation rates always followed the trend Br > I > Cl. As mentioned, a small set of substituents tested resulted in increased inactivation, however, the relationship between inactivation rates and calculated pK_a values was not straightforward. Although only small substituents were used to minimize unfavorable steric effects, the steric and charge effects of the

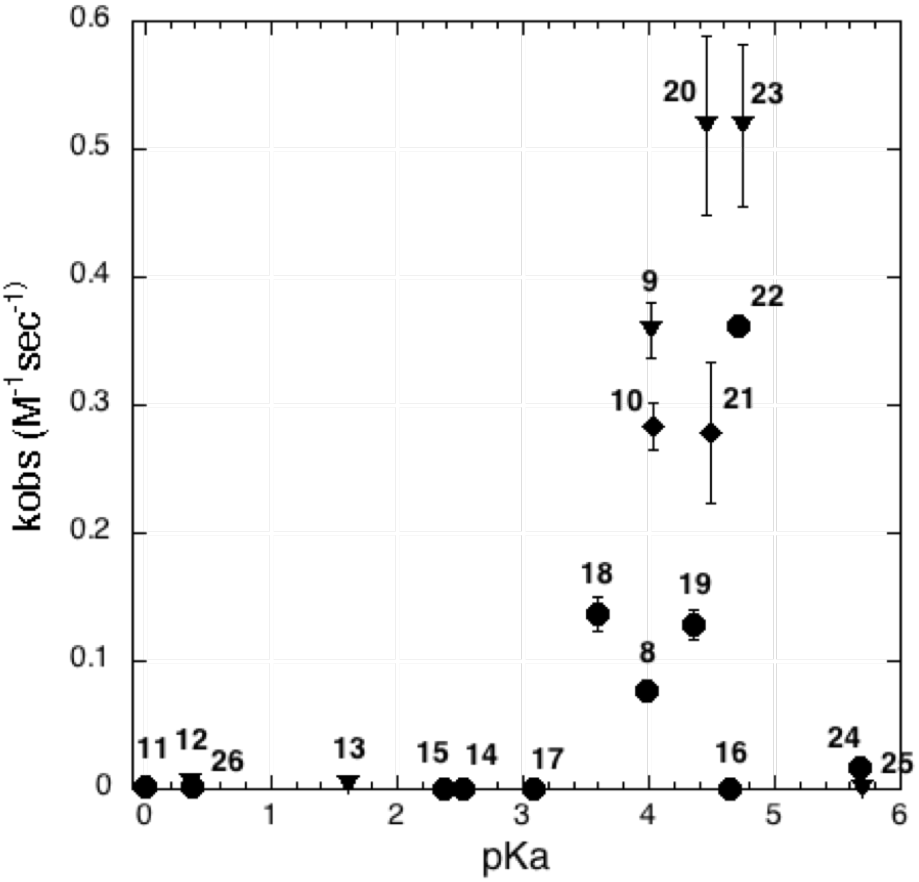

Figure 2.6 Second order rate constants ($M^{-1}sec^{-1}$) of commercially available 4-halo-pyridine derivatives by pyridine nitrogen p*Ka*. Compounds are organized by halogen species 4-Cl (●), 4-Br (▼), and 4-I (◆). Second order rate constants were defined by exponential fits of time-dependent inactivation of hDDAH1 at multiple concentrations up to or >4 mM. 2-pyridinyl-MeOH, 2-methyl, and 3-amino containing derivatives resulted in enhanced inactivation compared to their parent 4-X-pyr scaffolds.

derivatives may not be completely eliminated with hDDAH1 and may complicate the observed trends.

The influence of ionized 4-halopyridine substituents on interactions with the hDDAH1 active site was demonstrated by the inactivation rates of **16** and **16m**. These 4-chloropyridine derivatives only differ by conversion of the carboxylic acid to the methyl ester (Table 2.2). Therefore, compound **16** and **16m** have similar sterics, but **16m** is not

anionic. The calculated pK_a values of **16** and **16m** are 4.65 and 1.15, respectively.[12] In terms of the pyridinium switch, based on our hypothesis we would expect the inactivation rate of **16** to be significantly increased when compared to **16m**. However, we see the opposite. **16** does not show any measurable inactivation at 4 mM, instead, **16m** shows inactivation under the same conditions. (Figure 2.7) One interpretation of these results would be that potential pK_a modulation via substituent identity is counterproductive if the derivitization blocks productive binding and orientation at the active site. The hDDAH1 active site has two carboxylates that presumable disfavor interaction with **16,** but not with **16m.** Ideally, optimization of 4-halopyridine inactivators can be guided with respect to both non-covalent target affinity and by modulating the sensitivity of the protonation 'switch'. Since small, uncharged substituents at the 2- position appear to be tolerated, we next focused on a series of 2-substituted 4-halopyridines to determine the effect of pK_a modulation and avoid the steric issues described above.

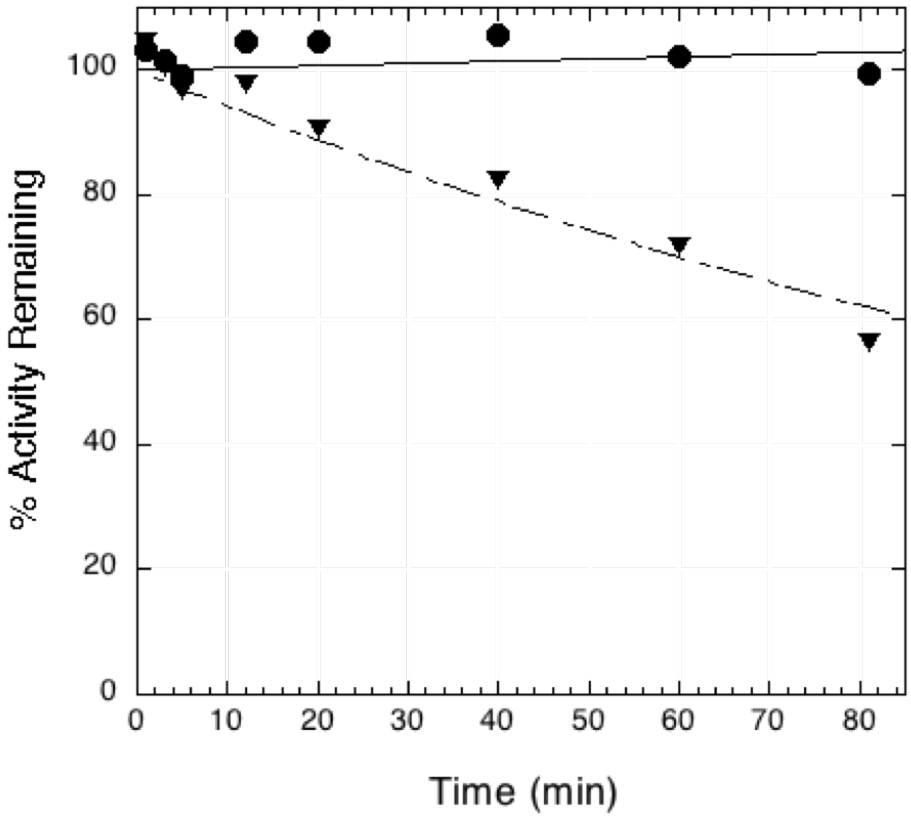

Figure 2.7 Time-dependent inactivation of hDDAH1 by 16 and 16m at 16 shows no inactivation of hDDAH1 (●). Elimination of the negative charge through conversion to the carboxy methyl ester (▼) results in inactivation at the same concentration and gives a k_{obs} value of -5.91 +/- 0.05 x 10^{-3} min^{-1}.

hDDAH1 Inactivation by a Fluoro-methyl Series

To more directly characterize the effect of nitrogen pK_a modulation on enzymatic inactivation, a series of 4-chloro-2-fluoromethylpyridines were synthesized and tested. Fluorine is much more electronegative than hydrogen, but is comparable to hydrogen with respect to both van der Waals radius and carbon-bond length. Replacing a hydrogen atom for a fluorine atom can be expected to have a large electronic effect on nearby carbon centers with little overall change in steric bulk. After reviewing potential steric

interactions described above, this set of halopyridines allowed us to plot the log(k_{obs}) versus pK_a for this series and a linear relationship was observed over 4 orders of magnitude (Figure 2.8). This relationship describes how an increase or decrease in pyridine nitrogen pK_a affects reactivity, as gauged by k_{obs}. Interestingly, when the

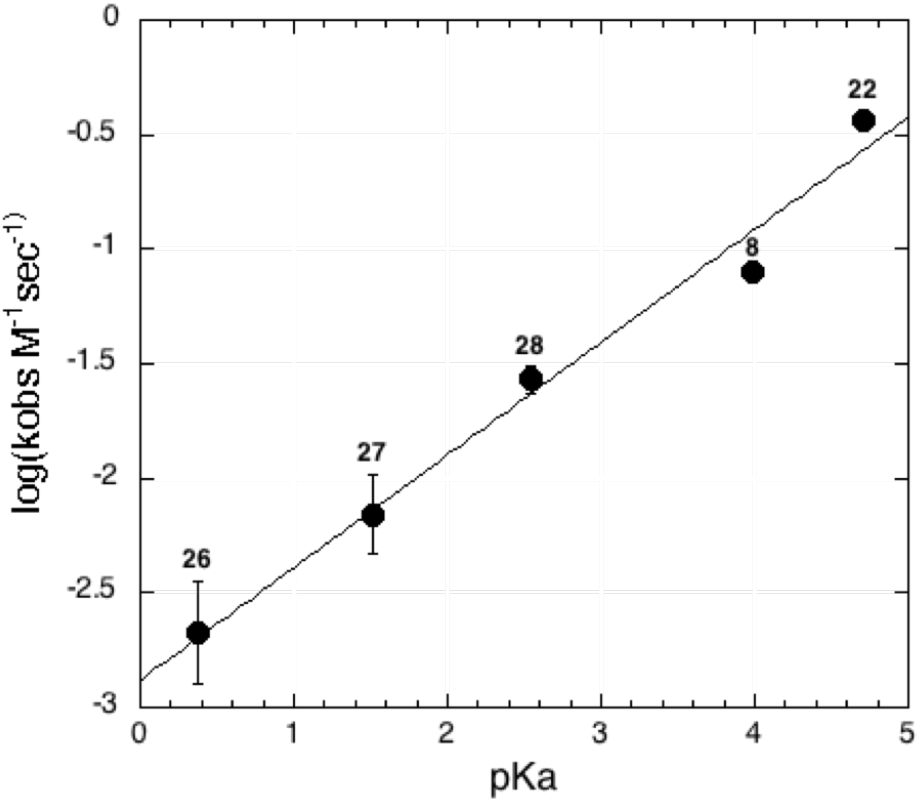

Figure 2.8 log(k_{obs}) v pK_a for conservative 2-Fluoro-Methyl Series and parent scaffold, 8. log(k_{obs}) dependence on pK_a is defined by the linear relationship, y=-2.9 + (0.49+/-0.4)x.

commercial derivatives that did show measurable inactivation are revisited and plotted in the same way, respective of their halogen species, similar slopes are observed (Figure

2.9). These results further support our hypothesis and the mechanism for 4-halopyridine activation, in that tuning the pK_a to high values can increase reactivity predictably.

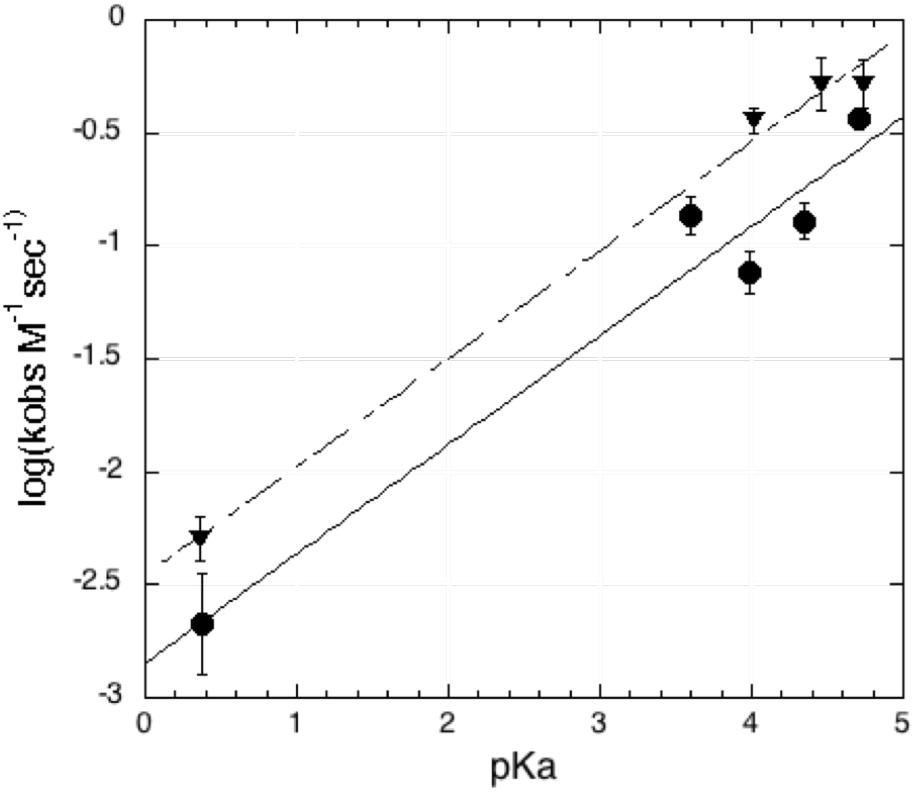

Figure 2.9 log(k_{obs}) v pK_a for commercially available 4-halo-pyridine derivatives with measureable inactivation rates. The linear relationship between log(k_{obs}) and pK_a for 4-Cl-R-pyr (●) is defined by y=-2.8 + (0.48 +/- 0.06)x and y=-2.5 + (0.48 +/- 0.03)x for 4-Br-R-pyr (▼).

Careful consideration of the tunable nature of the protonation 'switch' suggests potential applications for this scaffold. Our data supports our hypothesis that increasing or decreasing nitrogen pK_a through ring derivitization can modulate reactivity by adjusting the barrier to protonation both when target bound and when free in solution.

Increasing or decreasing the fraction protonated in solution will in practice reduce or increase the necessity for catalysis by the target to form the pyridinium during modification. This is a powerful tool for the design of a variety of different tools from TCI's to proteomic profiling agents. In practice, elaboration of this scaffold can be used to target specific enzymes and the reactivity of the scaffold can be tuned based on the selectivity needed for any particular application.

Substituent Effects on Non-Enzymatic versus Enzymatic Reactivity

Using the same experimental conditions described earlier for model studies to quantify the value of the protonation 'switch', the effects of 4-halopyridine derivitives used for hDDAH1 inactivation above, were now tested non-enzymatically (Compound **19** and **20** were excluded due to solubility issues at >5 mM). These experiments were carried out to determine whether derivitization also affects non-enzymatic reactivity and if the same relative reactivity trends are observed. If the same increases and/or decreases in reactivity are seen across all compounds (or at least those shown to inactivate enzymatically) this would suggest that derivitization affects general reactivity rather than having an effect specific to catalysis by hDDAH1.

While no substituent-based change in reactivity was seen when using GSH as the small molecule thiol, differences in reactivity can be observed by using a better nucleophile, thiophenol (Figure 2.10, 2.11A). Non-enzymatically, compounds **12** and **16** showed the highest k_{obs} values at $2.5 \pm 0.1 \times 10^{-2}$ min^{-1}, $4.8 \pm 0.2 \times 10^{-2}$ min^{-1} respectively. However, enzymatically these two compounds showed little and no hDDAH1 inactivation (Figure 11B). With respect to **16,** this difference is most likely due to

unfavorable charge interactions between the compound and the active site, as discussed above. Based on our hypothesis, compound **12** was not predicted to be a strong hDDAH1 inactivator due to a large downward pK_a shift exerted by the 3-carbonitrile group. For hDDAH1 inactivation **12** accordingly had a k_{obs} value two orders of magnitude

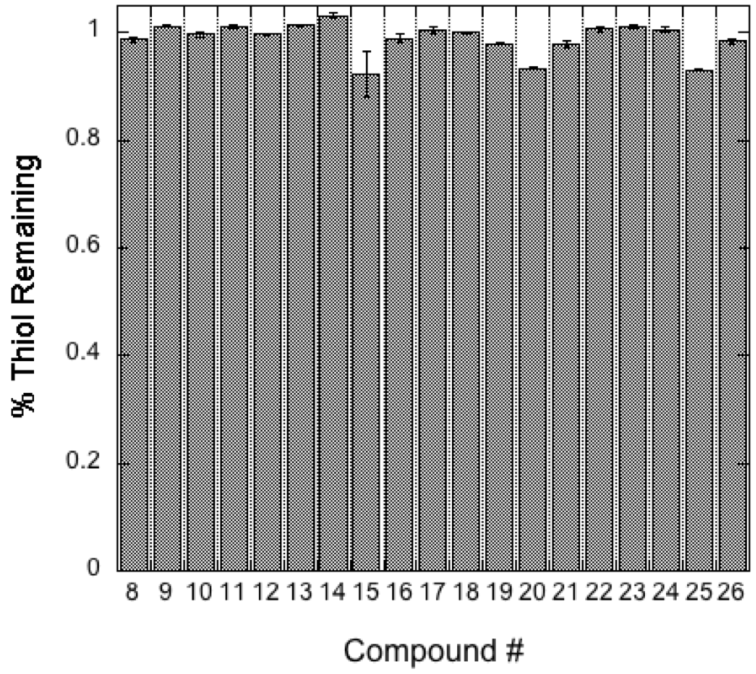

Figure 2.10 Relative reactivity of halo-pyridine derivatives toward glutathione. Percentage of reduced glutathione remaining after 45 min incubation at equimolar concentrations (1 mM) of compound and glutathione normalized to a no compound control. No significant changes in reactivity are observed as a function of derivitization.

lower than 4-bromopyridine. However, the non-enzymatic reactivity of **12** with thiophenol is relatively high (Figure 2.11A). All other compounds are clustered between k_{obs} values of 0-0.015 min^{-1}. One interpretation of the data is that because of the demand for pyridinium stabilization to promote modification, the protonation 'switch' is acting in

a gated manner. That is, without pyridinium stabilization, nucleophilic attack is rate limiting and represents a large energy barrier regardless of the given compounds pK_a. Only when the protonated form can be stabilized through target binding is the effect of pK_a modulation realized. However, from this data alone, we cannot exclude the possibility that a different mechanism may be at work non-enzymatically versus enzymatically.

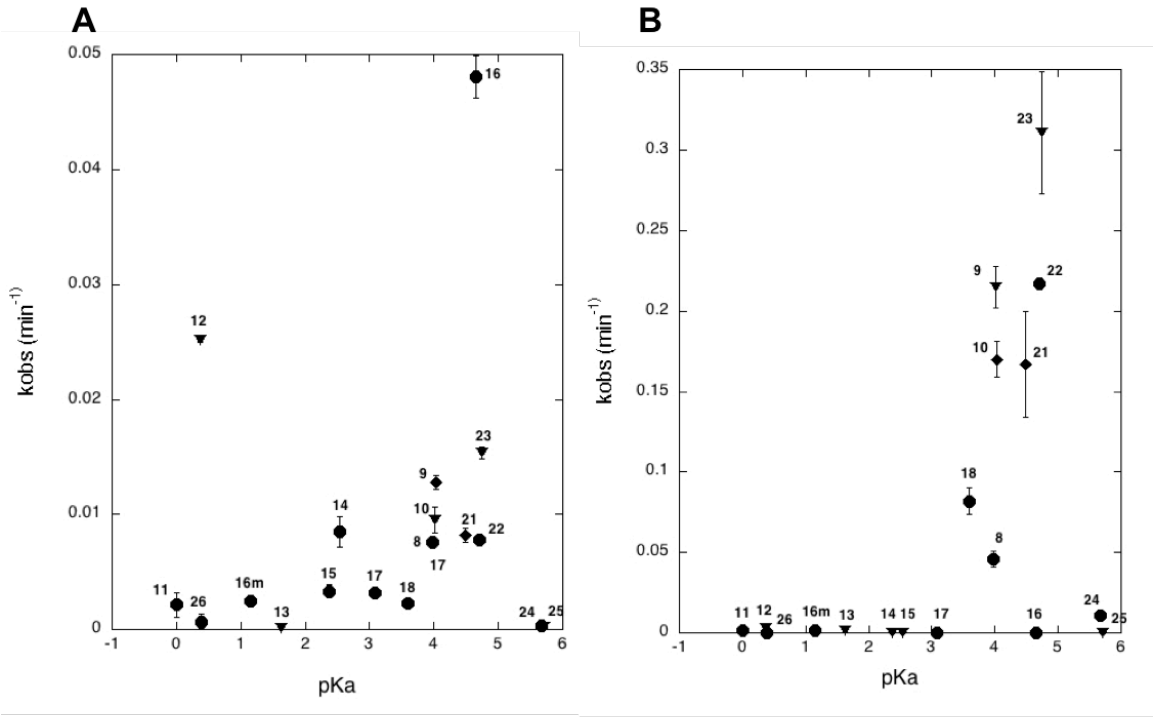

Figure 2.11 (A) k_{obs} (min^{-1}) of thiol reactivity for commercially available 4-halo-pyridine derivatives by pyridine nitrogen pK_a. k_{obs} rate constants were defined by single exponential fits of remaining thiol over time (0-80 min). (B) hDDAH1 inactivation k_{obs} (min^{-1}) at 10 mM for comparison. k_{obs} rate constants were estimated based on second order rate constants. Compounds are organized by halogen species 4-Cl (●), 4-Br (▼), and 4-I (◆).

Above, we assumed a nucleophilic S_NAr reaction, but radical reactions might also be possible as have been reported for 2-halopyridines using a benzenethiolate anion in organic solvent. So, to quench any radicals produced in the reaction, we preformed experiments in the presence of narengenin, a bio-available free-radical scavenger (Figure 2.12A).[27, 29,30] The results showed no change in reactivity trends indicating that this mechanism is not radical dependent in aqueous solution and the assumption of the nucleophilic S_NAr reaction mechanism is reasonable.

Differences in compound reactivity trends between enzymatic and non-enzymatic studies might indicate that different rate determining steps matter in each case. However,

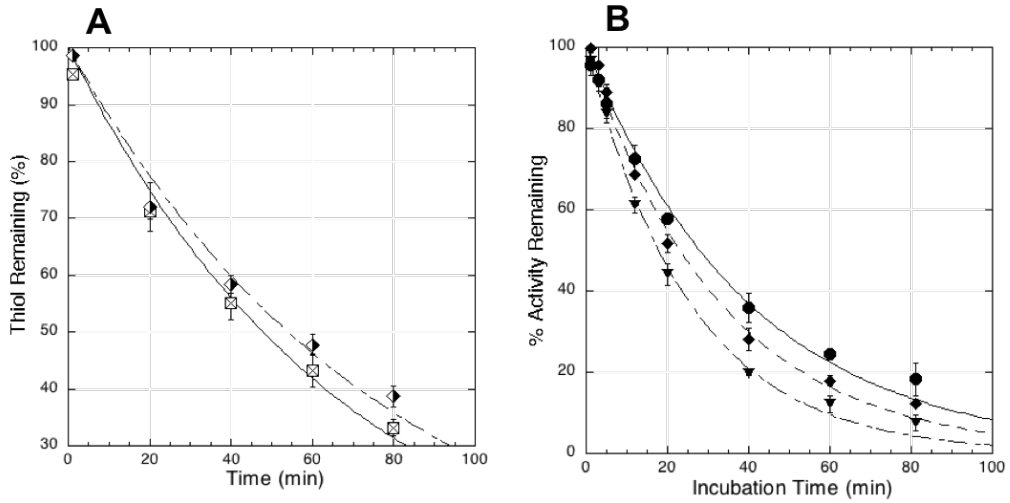

Figure 2.12 Halo-pyridine non-enzymatic and enzymatic reactivity in the presence of a free-radical scavenger. (A) Reaction rate of thiolphenol (1 mM) under saturating conditions of 9 (☒ ,10 mM) and 9 + Narengenin (◁▶ , 10 mM). (B) Time-dependent inactivation of hDDAH1 by 8-10 + Narengenin (10 mM). Single exponential fits of 8 (●, 5 mM), 9 (▼, 2 mM), and 10 (◆, 2 mM) give k_{obs} values of -0.025 +/- 0.001 min^{-1}, -0.039 +/- 0.001 min^{-1}, and -0.030 +/-0.001 min^{-1}, respectively. Both the halogen dependence and inactivation rates are consistent with experiments lacking narengenin.

the individual rate constants for reactivity of the 4-halopyridines with thiophenol were not investigated and the lack of published literature on non-enzymatic S_NAr reactions involving pyridine in aqueous solution limits the ability to draw conclusions on the nature of **12** and **16's** enhanced reactivity. What can be said is that both **12** and **16** contain strong electron-withdrawing groups (EWG). The enhanced reactivity of these derivatives is in agreement to what is observed with respect to organic synthesis, where replacement of halogen atoms in aryl halides by RS groups is facilitated when the aromatic ring contains strong EWGs, like those found in **12** and **16**, but is in stark contrast to the electron-donating group (EDG) substituents that result in increased hDDAH1 inactivation (2-MeOH, 2-Me, 3-amino).

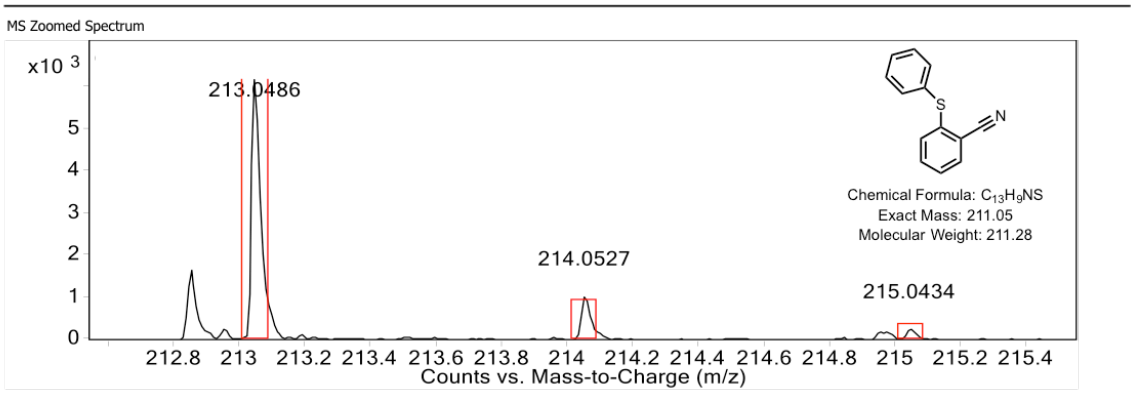

MS Spectrum Peak List

Obs. m/z	Calc. m/z	Charge	Abund	Formula	Ion/Isotope	Tgt Mass Error (ppm)
213.04860	213.04810	1	6218	C12H8N2S	(M+H)+	-2.44
214.05270	214.05090	1	1039.75	C12H8N2S	(M+H)+	-8.06
215.04340	215.04570	1	257.95	C12H8N2S	(M+H)+	10.5
216.04270	216.04750	1	36.38	C12H8N2S	(M+H)+	22.19
959.96660			119312.24			

Figure 2.13 MS Zoomed Spectrum of thiophenol and 4-bromo-3-carbonitrile incubated overnight.

One alternative explanation of the enhanced reactivity of **12** is that thiophenol is not replacing the halogen, but instead reacting with the carbonitrile, resulting in imine formation. We preformed mass spectrometry (MS) analysis on incubations of **12** with thiophenol to determine if the imine adduct was formed overnight. (Figure 2.13) No *m/z* corresponding to the imine adduct was found, only the reaction product produced upon halogen replacement by thiophenol.

What can be said with confidence in the comparison of these two data sets is that, excluding compounds **12** and **16,** non-enzymatic reactivity was weak and clustered across a broad pK_a range trending proportionally with increased pK_a. In addition, the compounds that did show increased non-enzymatic reactivity were not in agreement with those found to be increased enzymatically. While our data supports our pK_a modulation hypothesis with respect to enzymatic modification, where protonation plays a key role, other factors may have a stronger influence on non-enzymatic reactivity, but the underlying reasons were not investigated fully here.

Proteomic Profiling by 4-Chloropyridine and 4-Chloro-*N*-Methyl-pyridine Probes

To this point, we have explored the characteristics and unique features of halo-pyridines as electrophilic scaffolds for use in the development of TCIs and other covalent probes, using a model enzyme studied extensively in our laboratory. However, the requirements for protein modification by 4-halopyridines are not expected to be unique to the DDAH enzyme family, but would be expected to impart an inherent selectivity for an unknown subset of targets where all requirements are met. A recent communication investigating the proteomic reactivity and selectivity of aryl halides, including both 2-

chloropyridine and 2,4-chloropyridine probes, initially confirmed their broader application, but noted their significantly decreased reactivity relative to the other aryl halides tested.[31] While this report provides strong evidence for our hypothesis, here we sought to determine other targets of 4-halopyridine modification.

To do so, *E. Coli* lysates were treated with either an alkyne-bearing 4-chloropyridine probe (**30**) or a fully activated *N*-methyl version of the same (**31**). Following incubation, a biotin moiety was appended to the alkyne using standard Cu(I)-catalyzed azide-alkyne cycloaddition. Lysates were then separated by SDS-PAGE, and

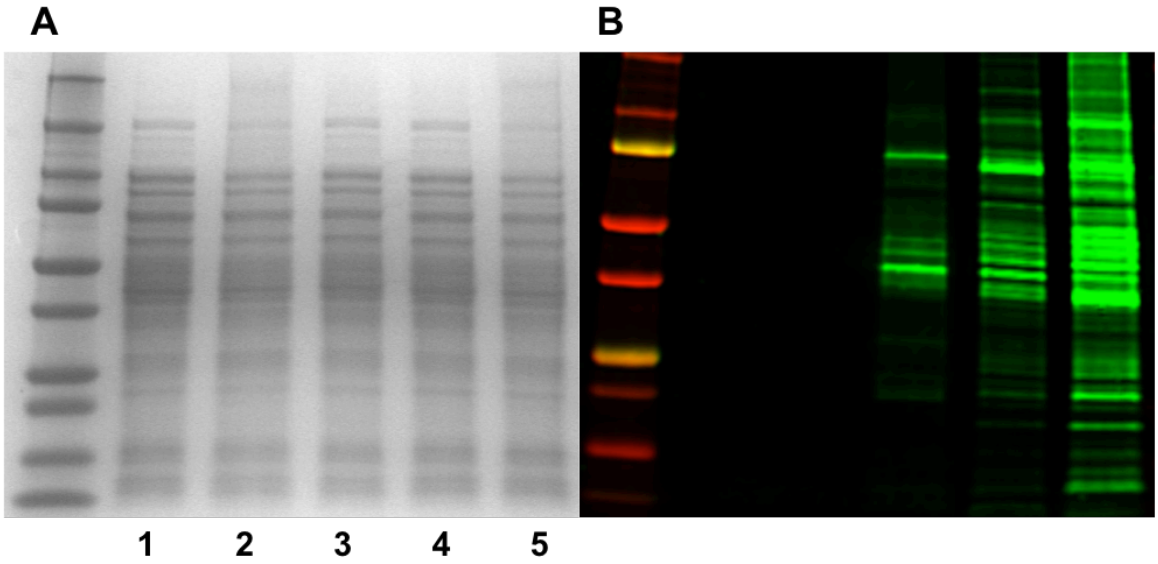

Figure 2.14 Covalent modification of proteins in *E. coli* lysates by 30 and 31. Lysates were treated with Compound (1 mM) for 3 h, followed by biotinylation. (A) Coomassie Stain of *E. Coli* Lysates treated with (1) No compound, (2) Compound 30 following heat treatment, (3) Compound 30, (4) Compound 31, (5) Compound 31 following heat treatment. (B) Western blot of naïve *E. coli* lysate of the same. Visualization using an Mouse α-Biotin mAb and GαM Secondary Ab detection (green signal) , MW Ladder (red signal)

visualized via Western Blot using an anti-biotin fluorescently conjugated antibody. In order to demonstrate the necessity of target binding and pyridinium stabilization for protein modification by **30**, but not **31,** *E. Coli* lysates were heat treated in parallel prior to treatment with compounds **30** and **31**. Visualization of the Western Blot shows a subset of the proteome is modified by the alkyne bearing 4-halopyridine probe. Furthermore, this subset is significantly less than that labeled by the fully activated *N*-methyl version. Finally, heat denaturation resulted in a loss of labeling with **30,** but an increase of labeling by **31**. (Figure 2.14B)

These results confirm that there is a distinct subset of the proteome that can be targeted using this scaffold. An important observation is that only a small portion of the proteome is labeled with **30** as compared to **31** and that no proteins are labeled by 30 after heat treatment. Therefore, if the protonation 'switch' is always on, eliminating the need for pyridinium stabilization all together, the probe becomes non-selectively reactive as evidenced by increased protein labeling. Along the same lines, if protein structure is compromised, eliminating proper target binding and catalysis by the correctly positioned cysteine thiol, modification by **30** is lost. Conversely, heat denaturation does not eliminate modification when pyridinium stabilization is not necessary (**31**), but results in a further increase in labeling. Most likely, the increase in labeling is due to increased accessibility to protein thiols upon denaturation. It is therefore reasonable to conclude that for the modified proteins visualized using **30**, the basic requirements for 4-halo-pyridine modification are fulfilled.

2.4 CONCLUSIONS

In this chapter we have identified and characterized the features of the 4-halopyridine scaffold that allow its reactivity to be tuned including halogen identity and pyridine nitrogen pK_a modulation. The protonation 'switch' provides a potential 4,000-fold tunable switch to enhance reactivity that can be catalyzed by the target, This property sets the 4-halopyridines apart from other fragment electrophiles. In other cases, derivitization of electrophilic fragments to increase electrophilicity will also increase non-selective reactions. In contrast, 4-halopyridine ring derivitization leads to only slight changes in non-enzymatic reactivity toward biological nucleophiles like GSH. However, it can change the ability for the target to catalyze protonation. The requirements for protein modification by the 4-halopyridine scaffold limit the number of possible targets, but uniquely allow for modulation of its reactivity through catalysis independent of drastic changes in non-enzymatic reactivity as would be unavoidable with other electrophilic fragments.[32]

While these features have been elucidated using hDDAH1, it is likely that the general guidelines outlined here will be applicable to other enzymes modified by 4-halopyridines. Identifying and evaluating other therapeutically relevant targets within this subset is one goal of our current research efforts. Along with the ability to achieve high effective concentrations through non-covalent elaboration as is done with other TCIs, the 4-halopyridine scaffold's unique selectivity and tunable features make it a valuable tool for fragment-based approaches. The insights gained herein will help to guide the development of 4-halopyridine based covalent modifiers.

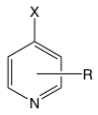

#	Compound	Calc.pKa[12]	k_{obs} ($M^{-1}sec^{-1}$)
1	Ampicillin	N/A	N/A
2	Styrene Oxide	N/A	N/A
3	Acrylamide	N/A	N/A
4	Iodoacetic acid	N/A	N/A
5	Iodoacetamide	N/A	N/A
6	Phenyl Vinylsulfonate	N/A	N/A
7	*N*-Ethylmaleimide	N/A	N/A
8	4-Chloropyridine	3.98	7.7 +/- 0.8 E-02
9	4-Bromopyridine	4.01	3.6 +/- 0.2 E-01
10	4-Iodopyridine	4.03	2.8 +/- 0.2 E-01
11	4-Cl-2-CN-pyridine	0	ND
12	4-Br-3-CN-pyridine	0.36	5.0 +/- 0.6 E-03
13	4-Br-2-F-pyridine	1.62	ND
14	3-Br-4-Cl-pyridine	2.53	ND
15	4-Cl-3-COOH-pyridine	2.37	ND
16	2-COOH-4-Cl-pyridine	4.65	ND
16m	2-COOMe-4-Cl-pyridine	1.15	2.5 +/- 0.1 E-02
17	4-Cl-3-Carboxyaldehyde-pyridine	3.08	ND
18	4-Cl-pyridinyl-2-MeOH	3.6	1.4 +/- 0.1 E-01
19	3-amino-4-Cl-pyridine	4.35	1.3 +/- 0.1 E-01
20	3-amino-4-Br-pyridine	4.46	5.2 +/- 0.7 E-01
21	4-Iodo-3-aminopyridine	4.49	2.8 +/- 0.6 E-01
22	4-Chloro-2-Me-pyridine	4.71	3.62 +/- 0.05 E-01
23	4-Bromo-2-Me-pyridine	4.74	5.2 +/- 0.6 E-01
24	2-amino-4-Cl-pyridine	5.68	1.8 +/- 0.1 E-02
25	2-amino-4-Br-pyridine	5.7	0.00E+00
26	2-TFM-4-Cl-pyridine	0.38	2.1 +/- 0.5 E-03
27	4-Cl-2-Difluorometheyl-pyridine	1.51	7.0 +/- 1.0 E-03
28	4-Cl-2-Monofluoromethyl-pyridine	2.54	2.7 +/- 0.2 E-02
29	4-Cl-N-methyl-pyridine		2.8 +/- 0.1
30	4-Cl-Probe		ND
31	4-Cl-*N*-Me-Probe		ND

Table 2.1 Summary of halo-pyridines evaluated to investigate influence of halogen species and pK_a modulation on inactivation rates.

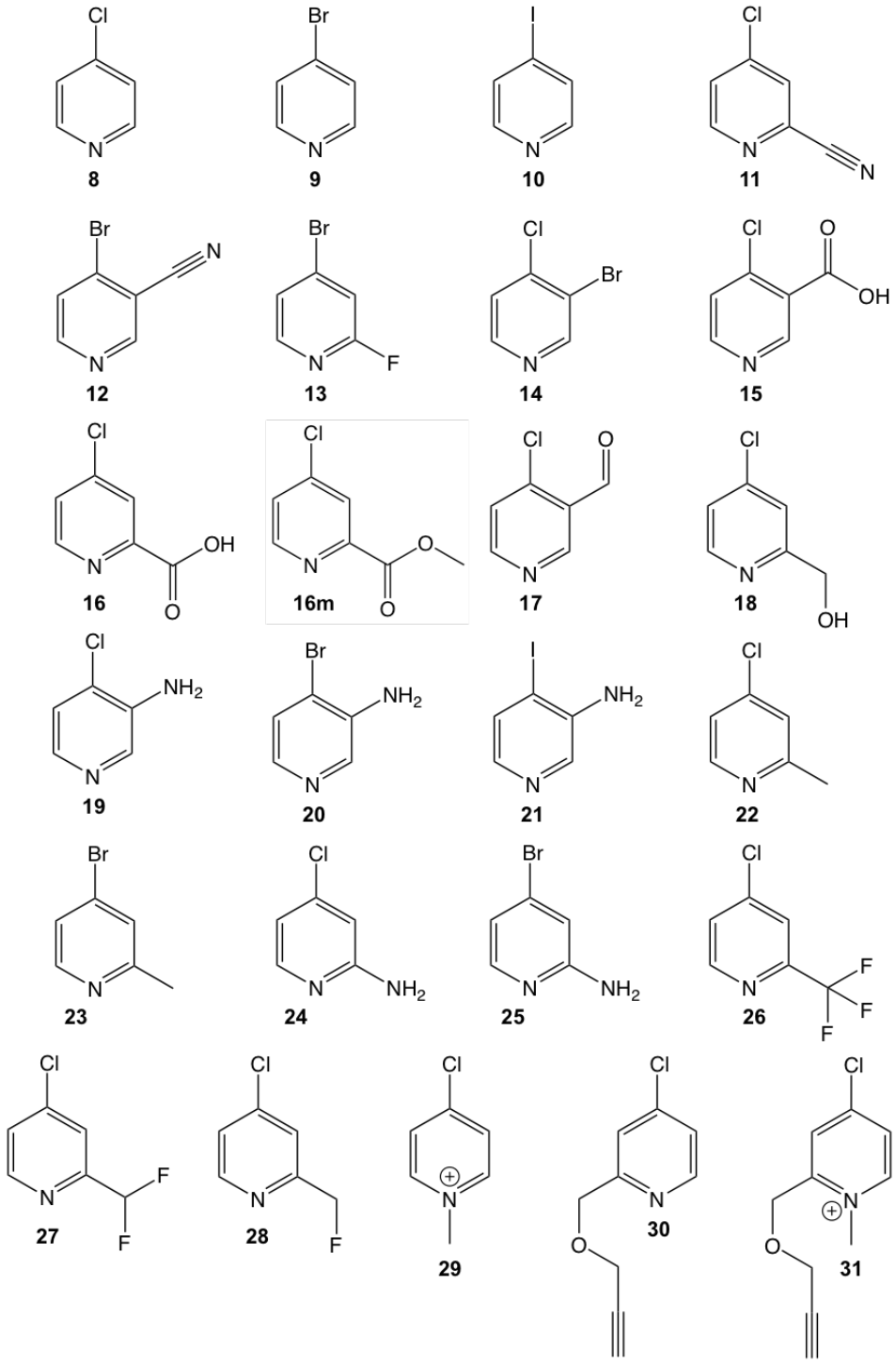

Table 2.2 Structures of 4-halopyridine derivatives evaluated for hDDAH1 inactivation (**8**-**29**) or proteomic labeling (**30**-**31**).

2.5 REFERENCES

1. Scott D. E., Coyne A. G., Hudson S. A., Abell C. Fragment-Based Approaches in Drug Discovery and Chemical Biology. *Biochemistry*. **51**, 4990-5003 (2012).

2. Huth, J. R., Park, C., Petros, A. M., Kunzer, A. R., Wendt, M. D., Wang, X., Lynch, C. L., Mack, J. C., Swift, K. M., Judge, R. A., Chen, J., Richardson, P. L., Jin, S., Tahir, S. K., Matayoshi, E. D., Dorwin, S. A., Ladror, U. S., Severin, J. M., Walter, K. A., Bartley, D. M., Fesik, S. W., Elmore, S. W., and Hajduk, P. J. Discovery and Design of Novel HSP90 Inhibitors Using Multiple Fragment-based Design Strategies. *Chem. Biol. Drug Des*. **70**, 1–12 (2007).

3. Congreve, M., Aharony, D., Albert, J., Callaghan, O., Campbell, J., Carr, R. A., Chessari, G., Cowan, S., Edwards, P. D., Frederickson, M., McMenamin, R., Murray, C. W., Patel, S., and Wallis, N. Application of fragment screening by X-ray crystallography to the discovery of amino pyridines as inhibitors of β-secretase *J. Med. Chem*. **50**, 1124–1132 (2007).

4. Miller R. M., Paavilainen V. O., Krishnan S., Serafimova I. M., Taunton J, Electrophilic Fragment-Based Design of Reversible Covalent Kinase Inhibitors. *J Am. Chem. Soc*. **135**, 5298–5301 (2013).

5. Singh J., Petter R. C., Baillie T. A., Whitty A., The resurgence of covalent drugs. *Nat. Rev. Drug Discov*. **10**, 307-317 (2011).

6. Shannon D. A., Weerapana E. Covalent protein modification: the current landscape of residue-specific electrophiles. *Curr. Opin. Chem. Bio*. **24**, 18-26 (2015).

7. Serafimova I. M, Pufall M. A., Krishnan S., Duda K., Cohen M. S., Maglathlin R. L., McFarland J. M., Miller R. M., Frodin M., Taunton J. Reversible targeting of noncatalytic cysteines with chemically tuned electrophiles. *Nat. Chem. Bio*. **8**, 471-476 (2013).

8. Pope, A. J., Karuppiah, K., Cardounel, A. Role of the PRMT-DDAH-ADMA axis in the regulation of endothelial nitric oxide production. *J. Pharmacol. Res*. **60**, 461 (2009).

9. Johnson C. M., Monzingo A. F., Ke Z., Yoon D., Linsky T. W., Guo H., Robertus J. D., Fast W. On the Mechanism of Dimethylarginine Dimetheylaminohydrolase Inactivation by 4-Halopyridines. *J. Am. Chem. Soc*. **133**, 10951-10959 (2011).

10. Johnson, C. M., Linsky, T. W., Yoon, D. W., Person, M. D., Fast, W. Discovery

of Halopyridines as Quiescent Affinity Labels: Inactivation of Dimethylarginine Dimethylaminohydrolase. *J. Am. Chem. Soc.* **133**, 1553 (2011).

11. Y. Wang, A. F. Monzingo, S. Hu, T. Schaller, J. Robertus, W. Fast. Developing dual and specific inhibitors of dimethylarginine dimethylaminohydrolase-1 and nitric oxide synthase: toward a targeted polypharmacology to control nitric oxide. *Biochemistry*. **48**, 8624-8635 (2009).

12. MARVIN.15.11.16.0.; ChemAxon: Budapest, Hungary.

13. Szegezdi J., and Csizmadia F. Prediction of dissociation constants using microconstants. 27th ACS National Meeting, Anaheim, California, March 28-April 1 (2004).

14. Szegezdi J., and Csizmadia F. A method for calculating the pK_a values of small and large molecules. American Chemical Society Spring meeting, March 25-29th (2007).

15. Riddles P.W., Blakeley R. L., Zerner B. Reassessment of Ellman's reagent, *Methods Enzymol*. **91**, 49-60 (1983).

16. Weerasinghe J.P., Dong T, Schertzberg M. R., Kirchhof M. G., Sun Y., Schellhorn H. E. Stationary phase expression of the arginine biosynthetic operon *argCBH* in *Escherichia coli*. *BMC Microbiology*. **6**, 14 (2006).

17. Bradford M.M. A rapid and sensitive method for the quantification of microgram quantities of protein utilizing the principle of protein-dye binding. *Anal. Biochem.* **72**, 248-54 (1976).

18. Bauer R. Covalent inhibitors in drug discovery: from accidental discoveries to avoided liabilities and designed therapies. *Drug Discov. Today*. **20**, 1061-1073 (2015).

19. Mah R., Thomas J. R., Shafer C. M. Drug discovery considerations in the development of covalent inhibitors. *Bioorg. & Med. Chem. Lett*. **24**, 33-39 (2015).

20. Smyth M. S., Laidig G. J. Compounds for proteasome enzyme inhibition. US Patent No. 2015361134, August 6, 2004.

21. Bruns A., Eichner S., Lehmann F., Albrecht W., Maier A. Crystalline forms of afatinib di-maleate. US Publication Number 2013052157 A1, October 6, 2011.

22. Goldstein D. M. Formulations comprising ibrutinib. US Publication Number 2014004707 A1, June 29, 2012.

23. Kim K.B., Crews C.M., From epoxomicin to carfilzomib: chemistry, biology, and medical outcomes. *Natural Product Reports*. **30**, 600-604 (2013).

24. Cox, Brian G. Acids and Bases: Solvent Effects on Acid-base Strength. 1st ed. Oxford, UK: Oxford UP, (2013).

25. Koval I. V. Reaction of Thiols. *Russian Journal of Organic Chemistry*. **43**, 319-346 (2007).

26. Cherng YJ. Synthesis of substituted pyridines by the reactions of halopyridines with sulfur, oxygen and carbon nucleophiles under focused microwave irradiation. *Tetrahedron*. **58**, 4931-4935 (2002).

27. Kondo S., Nakanishi M., Tsuda K. Nucleophilic Substitution of Halopyridines by Benzenethiolate Anion via a Radical Chain Mechanism. *J. Heterocyclic Chem*. **21**,1243-1244 (1984).

28. Crooks G. P., Copley S. D., A Surprising Effect of Leaving Group on the Nucleophilic Aromatic Substitution Reaction Catalyzed by 4-Chlorobenzoyl-CoA Dehalogenase. *J. Am. Chem. Soc*. **115**, 6422-6423 (1993).

29. Chambers C.S. "Non-Taxifolin" Derived Flavonolignans: Phytochemistry and Biology. *Current Pharmaceutical Design*. **21**, 5489-5500 (2015).

30. Khanduja K.L., Bhardwaj A. Stable free radical scavenging and antiperoxidative properties of resveratrol compared in vitro with some other bioflavonoids. *Indian Journal of Biochemistry & Biophysics*. **40**, *416-422 (*2003).

31. Shannon D. A., Banerjee R., Webster E. R., Bak D. W, Wang C., Weerapana E. Investigating the Proteome Reactivity and Selectivity of Aryl Halides *J. Am. Chem. Soc*. **136**, 3330-3333 (2014).

32. Kathman S. G., Xu, Z., Statsyuk A. V. A Fragment-Based Method to Discover Irreversible Covalent Inhibitors of Cysteine Proteases. *Journal of Med. Chem*. **57**, 4969-4974 (2014).

Chapter 3: Evaluation and Characterization of Selected Therapeutically Relevant Protein hits from a 2- and 4-Chloropyridine Proteomic Screen

3.1 INTRODUCTION

As detailed in Chapter 2, the 4-halopyridine scaffold was first identified as a novel covalent modifier in an effort to discover structurally diverse inhibitors of dimethylarginine dimethylaminohydrolase (DDAH).[1,2] Characterization of this inactivation mechanism revealed that binding to the protein target stabilizes a more reactive protonated form of the pyridine via a correctly positioned carboxylic side chain (Asp66 in DDAH). This protonation facilitates nucelophilic aromatic substitution (SN_{Ar}) by a neighboring cysteine. Based on these requirements for covalent modification by 4-halopyridines it was hypothesized that other targets might also be susceptible to covalent modification by the 4-halopyridine scaffold and that similar compounds may be useful in the design of molecular probes, enzyme inhibitors, and therapuetics.[2]

This hypothesis was tested in our laboratory by conducting an *E. Coli* proteomic screen using 2- and 4-chloropyridines modified with an alkyne as a latent handle (unpublished). After labeling of *E. Coli* lysates and selective biotinylation of labeled proteins using standard Cu(I)-catalyzed click chemistry, proteins that were covalently labeled were partially purified using streptavidin affinity purification. Mass spectrometry (MS) was used to identify the enriched proteins. The identified proteins were treated as primary screening 'hits' and contain a variety of different protein classes.

Verification of targets within the primary hit list is sought for several reasons. First, follow-up experiments are needed to validate the ability of halopyridine(s) to covalently modifiy the target protein of interest. Affinity purification combined with mass spectrometry is a well established procedure to identify target enrichment based on a given treatment. However, nonspecific interactions with the affinity column matrix or with the retained proteins can lead to false positives.[3] Additionally, during the protomic screening procedure, parameters such as redox state and protein abundance were not explicitly controlled or normalized for.[4-6] Validation of primary 'hits' is therefore essential for confirmation. Secondly, while the initial characterization of the halopyridine scaffold indicated a correctly positioned carboxylic side chain and cystiene nucleophile were required to catalyze inactivation of DDAH it's not clear if this residue configuration is the only way to catalyze covalent bond formation. Determining if the requirments previously outlined for target modification hold true for additional targets would help to reveal if covalent modification using this scaffold is stringent with respect to the previously outlined mechanism or if there are any other sites that could be targeted by halopyridines. Together, validation and characterization of additional targets builds evidence for the application of halopyridines as a useful inhibitor scaffold.

The primary proteomic screen of *E. Coli* lysates resulted in 142 hits identified in the 2-chloropyridine (**1**) and/or 4-chloropyridine probe (**2**) samples, but not the no probe control. Narrowing these hits to fewer candidates for further validation was carried using several criteria. First, proteins were selected based on their clinical or therapeutic significance. Secondly, proteins with catalytic functions were selected to facilitate

characterization by kinetic assays. Third, similarity between each enzyme's substrate and the halopyridine scaffold was considered in an attempt to increase the likelihood of validating active site modifiers. Fourth, crystal structures of the remaining hits were inspected for carboxylic containing side chains in close spatial proximity to cysteine residues. However, this last criterion was not a stringent requirement because other residues might be able to act as nucelphiles.

Based on these criteria, 3 primary hits were selected for validation: *E. Coli* Cytidine Deaminase (CytD), *E. Coli* Uridine phosphorylase (UDP), and human KRas (Isoform 2B, 1-169). KRas did not show up in the initial proteomic screen using HEK 293T cell lysates (unpublished data), but we did observe enrichment of other purine nucleotide handling enzymes. As described below, covalent modification was observed for both UDP and KRas, but not CytD. Modificaion of KRas was characterized in detail. It was determined that the mechanism of KRas modification is similar to the mechanism previously shown for DDAH and *E. Coli* inosine monophosphate dehydrogenase (IMPDH, unpublished data). Interestingly, we find that unlike these previous targets, the covalent adduct is not stable and susceptible to subsequent hydrolysis. The effects of 4-chloropyridine treatment on cells harboring oncogenic KRas and target engagement with KRas in cell culture are also evaluated.

3.2 MATERIALS AND METHODS

Materials

Unless otherwise noted, all chemicals and reagents were purchased from Sigma-

Aldrich (St. Louis, MO, USA). K_2HPO_4, Na_2HPO_4, NaH_2PO_4, and acetonitrile, were purchased from Thermo Fisher Scientific (Waltham, MA, USA).

Cloning *Escherichia Coli* Cytidine Deaminase (CytD)

E. Coli BL21(DE3) genomic DNA was isolated from 5 mL of an overnight culture, purified using QIAGEN DNeasy Blood & Tissue Kit (Qiagen; Valencia, CA, USA). Polymerase Chain Reaction (PCR) amplification of the cytidine deaminase (*cytd*) from genomic DNA was carried out using the following primers, (gcytd-NdeI-For) 5'-TAC CAT ATG TTT CAC GCG TTG CAT AAT TAA-3' and, (gcytd-XhoI-Rev) 5'-TAC CTC GAG TTA ATA TTT TGC TGT TCC GAG CAC-3'. Breifly, a PCR mixture containing 100 ng of genomic DNA, 200 uM dNTP's, 25 pmol of primers, and 0.5 U Phusion HF polymerase in the manufacturer's buffer (New England Biolabs; Ipswich, MA, USA) was thermocycled using a temperature program of 95 °C for 30 s, followed by 20 cycles of 95 °C for 30 s, 50 – 60 °C (temperature gradient PCR) for 45 s, 72 °C for 90 s and a final step at 72 °C for 10 min. Successful amplification and purity of the PCR product was analyzed by 1% agarose gel stained with ethidium bromide. The resulting PCR product at approximately 1.25 kb was gel purified using a QIAquick Gel Extraction Kit (Qiagen; Valencia, CA, USA). The purified PCR product and a pET-28a expression vector were subjected to restriction enzyme digestion. Breifly, 1 unit of NdeI and XhoI were incubated with 500 ng pET-28a and 1000 ng PCR product in manufacturer's buffer at 37 °C for 2 h (New England Biolabs; Ipswich, MA, USA). Digested samples were purified using the QIAquick PCR Purification Kit (Qiagen; Valencia, CA, USA). The digested PCR product and pET-28a samples were then ligated using 200 units of T4

ligase in manufacturer's buffer (New England Biolabs; Ipswich, MA, USA) at a 1:3 ratio, respectively, for 18 h at 16 °C. 2 μL of the ligation reaction was transformed into electrocompetent BL23 (DE3) *E. Coli* cells and plated onto lysogeny broth (LB) agar plates with kanamycin (30 μg / mL). Several viable colonies were selected from the LB agar plates with kanamycin (30 μg / mL) after overnight incubation at 37 °C and regrown overnight as 5 mL cultures in the presence of kanamycin (30 μg / mL) at 37 °C. Plasmid from the regrown cultures was extracted and purified using a QIAprep Miniprep Kit (Qiagen; Valencia, CA, USA). DNA sequencing at the University of Texas DNA sequencing facility confirmed that the desired plasmid sequence matched that expected for *E. Coli cdd* (NCBI RefSeq: NP_416648.1).

Expression and Purification of CytD

Expression and purification of *E. Coli* CytD was carried out as previously described.[7] No affinity tag was used in the purification of the *E. Coli* CytD construct. Expression and purification resulted in approximately 70% pure protein.

Assay for CytD Enzymatic Activity and Inhibition by Halopyridines

Activity of partially purified *E. Coli* CytD was monitored by following the change in UV absorbance when a cytosine nucleoside was converted to uracil nucleoside as previously described.[7] To monitor time-dependent irreversible inactivation, CytD (60 μM) was pre-incubated with (**1**) and (**2**) (Table 1) (0-60 min, 2 mM). Aliquots of the pre-incubation mixtures were diluted 20-fold into excess cytidine substrate (10 mM) and monitored at 301 nm for 5 min.

Cloning *Escherichia Coli* Uridine phosphorylase (UDP)

E. Coli BL21(DE3) genomic DNA was isolated from a 5 mL overnight culture and purified using QIAGEN DNeasy Blood & Tissue Kit (Qiagen; Valencia, CA, USA). PCR amplification of the uridine phosphorylase gene (*udp*) from genomic DNA was carried out using the following primers, (NdeI-EcUDP For) 5'-TAC CAT ATG TAT ATG TCC AAG TCT GAT GTT-3' and (XhoI-EcUDP Rev) 5'- TAC CTC GAG GCG GGT AAA TTT ATG CAA CGC-3'. Breifly, a PCR mixture containing 100 ng of genomic DNA, 200 uM dNTP's, 25 pmol of primers, and 0.5 units Phusion HF polymerase in the manufacturer's buffer (New England Biolabs; Ipswich, MA, USA) was thermocycled using a temperature program of 95 °C for 30 s, followed by 20 cycles of 95 °C for 30 s, 50 – 60 °C (temperature gradient PCR) for 45 s, 72 °C for 90 s and a final step at 72 °C for 10 min. Successful amplification and purity of the PCR product was analyzed by 1% agarose gel stained with ethidium bromide. The resulting PCR product at approximately 1.25 kb was gel purified using a QIAquick Gel Extraction Kit (Qiagen; Valencia, CA, USA). The purified PCR product and a pET-28a expression vector were subjected to restriction enzyme digestion. Breifly, 1 unit of NdeI and XhoI were incubated with 500 ng pET-28a and 1000 ng PCR product in manufacturer's buffer at 37 °C for 2 h (New England Biolabs; Ipswich, MA, USA). Digested samples were purified using the QIAquick PCR Purification Kit (Qiagen; Valencia, CA, USA). The digested PCR product and pET-28a samples were then ligated using 200 units of T4 ligase in manufacturer's buffer (New England Biolabs; Ipswich, MA, USA) at a 1:3 ratio, respectively, for 18 h at 16 °C. 2 μL of the ligation reaction was transformed into BL23

(DE3) *E. Coli* cells and plated onto LB agar plates with kanamycin (30 μg / mL). Several viable colonies were selected from the LB agar plates with kanamycin (30 μg / mL) after overnight incubation at 37 °C and regrown overnight as 5 mL cultures in the presence of kanamycin (30 μg / mL) at 37 °C. Plasmid was extracted and purified using a QIAprep Miniprep Kit (Qiagen; Valencia, CA, USA). DNA sequencing at the University of Texas DNA sequencing facility confirmed the desired insert sequence matched that expected for *E. Coli udp* (NCBI RefSeq NP_418275.1).

Overexpression of *Escherichia Coli* UDP

500 mL of an *E. Coli* BL21(DE3) culture containing pET-28a-EcUDP was grown under agitation (250 RPM) at 37 °C until OD_{600} = 0.4-0.6 absorbance units in Lysogeny Broth containing 50 mg/L kanamycin and subsequently induced by adding 0.5 mM isopropyl-β-D-thiogalactoside (IPTG). Growth was continued overnight at 37 °C with agitation (approx. 18 hr). Bacterial culture was collected by centrifugation at 7,741 × g for 20 min, 4 C. The cell pellet was either frozen in liquid nitrogen and stored at -80 °C or used fresh.

The cell pellet was resuspended in 40 mL buffer containing 50 mM Tris, 100 mM KCl at pH 8, containing protease inhibitor cocktail (170 μg/mL phenylmethylsulfonyl fluoride (PMSF), 1 μg/mL pepstatin A, 1 μg/mL leupeptin). The resulting cell slurry was sonicated and centrifuged at 39,191 × g to pellet then discard cell debris. The remaining cell lysates were then assessed for total protein concentration via a Bradford assay and aliquots were flash frozen for storage.

***E. Coli* UDP Modification by 2- and 4-Chloropyridine Probes**

Cell lysates containing overexpressed *E. Coli* uridine phosphorylase (50 μg total protein) were treated with 1 mM (**1**) and (**2**) at room temperature for 60 min. Replicate samples with exogenous uridine added (2 mM final concentration) were treated similarly. A 'no-compound' control was also run in parallel (43 μL total reaction volume). Following incubation, a biotin tag was selectively appended to the alkyne-bearing probe by the addition of *N*-[2-[2-[2-(2-azidoethoxy)ethoxy]ethoxy]ethyl]hexahydro-2-oxo-(3*aS*,4*S*,6*aR*)-1H-thieno[3,4*d*]imidazole-4-pentanamide (Biotin-PEO_3-azide) (125 μM), tris(2-carboxyethyl)phosphine (TCEP, 1 mM), tris[(1-benzyl-1H-1,2,3-trazol-4-yl)methyl]amine (TBTA, 100 μM), and $CuSO_4$ (1 mM) bringing the final reaction volume to 50 μL. After an additional 1 h incubation, samples were quenched with freshly prepared 2 × Laemmli buffer. Samples were then subjected to sodium dodecyl sulfate polyacrylamide gel electrophoresis (SDS-PAGE) and analyzed via Western Blot as described below.

Site-directed Mutagenesis of KRas Isoform 2b (1-169)

The pJExpress411 vector encoding an N-terminally His_6-tagged recombinant human KRas (isoform 2, residues 1–169, based on construct used for PDB accession 3GFT), containing a TEV cleavage site between the His_6-tag and KRas gene, was generously provided by Daniel Gentile and Kevin Shokat (University of California San Francisco).[8] This vector was used as a template for Quikchange site-directed mutagenesis (Stratagene). For the C51A mutant, the primers were 5'-TGA TTG ATG GCG AAA CGG CCC TGT TGG ACA TCC TGG-3'and 5'-CCA GGA TGT CCA ACA GGG CCG

TTT CGC CAT CAA TCA-3'. For the C118A mutation, the primers were 5'-AGA TGT ACC TAT GGT CCT AGT AGG AAA TAA AGC TGA TTT GCC TTC TAG A-3' and 5'-TCT AGA AGG CAA ATC AGC TTT ATT TCC TAC TAG GAC CAT AGG TAC ATC T-3'. The C51A/C118A double mutant was constructed using the C118A primers on the C51A template. The E3A/C118A double mutant was constructed using primers 5'-TTT CCA GGG TAT GAC TGC GTA CAA ACT GGT TGT CG-3' and 5'-CGA CAA CCA GTT TGT ACG CAG TCA TAC CCT GGA AA-3' on the C118A template. The E49A/C118A double mutant was constructed using primers 5'-GTT GTG ATT GAT GGC GCA ACG TGC CTG TTG GAC-3' and 5'-GTC CAA CAG GCA CGT TGC GCC ATC AAT CAC AAC-3' on the C118A template. The E3A/E49A/C118A triple mutant was constructed using primers 5'-GTT GTG ATT GAT GGC GCA ACG TGC CTG TTG GAC-3' and 5'-GTC CAA CAG GCA CGT TGC GCC ATC AAT CAC AAC-3' on the E3A/C118A template. The E134A/C51A double mutant was constructed using primers 5'-GGC ATC CCG TTT ATC GCA ACG AGC GCG AAA AC-3' and 5'-GTT TTC GCG CTC GTT GCG ATA AAC GGG ATG CC-3'on the C51A template.

To construct the mutant genes a PCR mixture containing the vector template, the mutagenic primers, a dNTP mixture, and Phusion DNA polymerase in the manufacturer's buffer (New England Biolabs; Ipswich, MA, USA) was thermocycled using a temperature program of 95 °C for 30 s, followed by 20 cycles of 95 °C for 30 s, 55 – 60 °C for 1 min (temperature gradient PCR), 72 °C for 90 s and a final step at 72 °C for 10 min. DpnI (New England Biolabs; Ipswich, MA, USA) was then added to the cooled reaction mixture and incubated at 37 °C for 2 h to digest the methylated template DNA. 2

μL of the resulting sample was transformed into electrocompetent *E. Coli* BL21 (DE3) *Echerichia coli* cells. Several viable colonies were selected from LB agar plates with kanamycin (30 μg / mL) after overnight incubation at 37 °C and regrown overnight as 5 mL cultures in the presence of kanamycin (30 μg / mL) at 37 °C. Plasmid was extracted and purified using a QIAprep Miniprep Kit (Qiagen; Valencia, CA, USA). DNA sequencing confirmed the inserts contained the desired mutations and no other mutations.

Expression and Purification of KRas Constructs

An expression vector encoding an N-terminal hexahistidine-tagged recombinant human KRas (isoform 2, residues 1-169, based on construct used for PDB accession 3GFT) was transferred into *E. coli* BL21 (DE3). Bacterial culture was grown under agitation (250 RPM) at 37 °C until OD_{600} = 0.4-0.6 in Terrific Broth containing 50 mg/L kanamycin and subsequently induced by adding 0.5 mM isopropyl-β-D-thiogalactoside (IPTG). Growth was continued overnight (approx 18 h) at 18 °C under agitation. Cells were collected by centrifugation at 7,741 × g for 20 min, 4 °C. The resulting bacterial pellet was flash frozen in liquid nitrogen and stored at -80 °C, or used freshly for the following purification.

The pellet was resuspended in 25 mL of Lysis Buffer (20 mM Tris, 500 mM NaCl, 5 mM Imidazole at pH 8) supplemented with protease inhibitor cocktail (Roche complete EDTA free). β-meracptoethanol (2 mM final concentration) was added to the solution and bacteria were lysed by sonication (210 s total, 10 s pulse on/45 s pulse off, 70% amplitude). Cell debris was pelleted by centrifugation at 39,191 × g for 20 min, 4 °C and discarded. The remaining supernantant was incubated for 1 h with 2 mL Qiagen

Ni-NTA resin slurry pre-equilibrated in Lysis Buffer. The Ni-NTA resin was then transferred to a column and washed with 50 mL Lysis Buffer supplemented with 20 mM imidazole. The hexahistidine-tagged recombinant human KRas was then eluted using 10 mL Lysis Buffer supplemented with 200 mM imidazole. The hexahistidine tag was cleaved using $NHis_6$-TEV protease[9] (1 mg recombinant TEV per 25 mg crude KRas, 1 mg GDP added per 20 mg crude KRas) while dialyzing overnight against a buffer containing 20 mM Tris, 300 mM NaCl, 5 mM imidazole, 1 mM dithiothreitol (DTT) and 0.5 mM EDTA. Following dialysis, the cleaved protein was diluted five-fold with low-salt buffer containing 20 mM Tris, 50 mM NaCl, pH 8. The dialyzed solution was supplemented with 5 mM $MgCl_2$ and 1 mM GDP. 2 mL of Ni-NTA resin pre-equilibrated with low-salt buffer was added to the solution and incubated for 1 hr to remove uncleaved protein and NHis-TEV. The Ni-NTA resin was removed by centrifugation.

The remaining protein solution was further purified using an 8 mL Q Sepharose Fast Flow column (GE Healthcare Life Sciences). The column was washed using buffer containing 20 mM Tris, 100 mM NaCl at pH 8. KRas was eluted with buffer containing 20 mM Tris, 250 mM NaCl at pH 8. The resulting protein solution was then subjected to filtration using an Ultracel 50 kDa MWCO filter (Amicon Ultra 4 Centrifugal Filter) in order to remove high molecular weight impurities in the filter. The KRas solution (flow-through) underwent buffer exchange using an Ultracel 10 kDa MWCO (Amicon Ultra 4 Centrifugal Filter) and 50 mL of buffer containing 10 mM Tris, 25 mM NaCl at pH 8. The final solution was concentrated to 1-2 mg/mL as assessed by Bradford assay (≥ 95%

purity). Purified KRas yields ranged from 5-10 mg / 1 L culture. All mutants used herein were purified using the same methodology.

Stability of 2- and 4-Halopyridine Scaffold toward Nucleotides

To determine the stability of the (**1**) and (**2**) at nuetral pH in the presense of guanine nucleotides, overnight (approx. 18 h) samples were incubated in buffer containing 50 mM KH_2PO_4 at pH 7.5. Samples containing each combination of pyridine compound ((**1**), (**2**), 1 mM) and nucleotide compound (GDP, GTP, 1 mM) were created along with control samples lacking nucleotide for each individual compound.

High performance liquid chromatography (HPLC) was used to identify overnight reaction products. HPLC was carried using a Shimadzu Prominence analytical HPLC (Columbia, MD) equipped with two LC-20A pumps, a SIL-20A autosampler, a RF10AxL fluorescence detector, and a 5 μm, 4.6 x 50 mm Shimadzu-HPLC-TEST-C18 column fitted with an Alltech Analytical Direct Connect- C18 guard column. 20 μL of an overnight incubation sample was injected using the autosampler. UV-Vis absorbance of the column eluate was monitored at wavelengths of 254 and 264 nm. Analyte separation was achieved using the following gradient program between solvent A (aqueous, potassium phosphate (100 mM) at pH 7.5, 10% acetonitrile, 0.1% trifluoroacetic acid (TFA)) and solvent B (80% acetonitrile). Solvent B was increased in a linear fashion from 0 % to 5 % over 5 min, to 25 % over the next 5 min, to 100 % over the next 1 min, held at 100 % for 2 min, and decreased to 5 % over the next 2 min. All solvents were degassed daily by bath ultrasonication for 30 min prior to use.

KRas Modification *in vitro* Characterization

4-Chloro-2-((prop-2-ynyloxy)methyl)pyridine (**(2)**, 100 μM) (4-Cl-Probe) was incubated with wildtype (*wt)* and mutant KRas (10 uM) in buffer containing 20 mM Tris, 50 mM NaCl, and 10 μM GDP at pH 7.5, 25 °C for 1 h (43 μL total reaction volume). After 1 h a biotin tag was selectively appended to (**2)** by the addition of Biotin-PEO_3-azide (125 μM), tris(2-carboxyethyl)phosphine (TCEP, 1 mM), tris[(1-benzyl-1H-1,2,3-trazol-4-yl)methyl]amine (TBTA, 100 μM), and $CuSO_4$ (1 mM) bringing the final reaction volume to 50 μL. After an additional 1 h incubation, samples were quenched with freshly prepared 2 × Laemmli buffer. Samples were then incubated at 95 °C for 5 min. Upon cooling, samples were subjected to SDS-PAGE and analyzed via Western Blot as described below.

The concentration dependent labeling of KRas was carried out analogous to that described above with the following minor changes. Concentrations of (**2)** ranged from 0-250 μM with an equimolar concentration of Biotin-PEO_3-azide added to each sample during the click reaction.

Experiments that evaluate whether KRas Isoform 2 (1-169) is covalently modified by (**1)** and (**2)** in the presence of excess guanosine diphosphate (GDP) and glutathione (GSH) were also carried out. 4-Cl-Probe, 100 uM or 4-chloro-2-((prop-2-ynyloxy)PO_3-Biotin)pyridine (4-Cl-PreClicked, 200 μM) was incubated with KRas (10 uM) in buffer containing 20 mM Tris, 50 mM NaCl, and 5 GDP or 5 mM GSH at pH 7.5, 25 °C for 1 h (43 μL total reaction volume). For samples incubated with 4-Cl-Probe, a biotin tag was selectively appended to the alkyne-bearing probe as described above. For samples

incubated with 4-CL-PreClicked, samples were quenched with 2 × Laemmli buffer. Samples were then incubated at 95 °C for 5 min. Upon cooling, samples were subjected to SDS-PAGE and analyzed via Western Blot as described below.

Overnight Dialysis of 4-chloropyridine probe modified KRas

Two replicate samples containing (**2**) (500 uM) were incubated with KRas (10 uM) in buffer containing 20 mM Tris, 50 mM NaCl, and 10 μM GDP at pH 7.5, 25 °C for 1 hr (750 μL total reaction volume). One replicate was then transferred to a dialysis bag (MWCO = 10 kDa) (Spectrum Labs, Inc., Rancho Dominguez, CA; #08-667B and dialyzed against 2 L of buffer for approx. 18 h at 4 °C. The same procedure was carried out using the 4-CL-PreClicked compound. After incubation for approximately 18 h at 4 °C a biotin tag was selectively appended to (**2**) samples as described above. Samples were quenched with 2 × Laemmli buffer. Samples were then incubated at 95 °C for 5 min. Upon cooling, samples were subjected to SDS-PAGE and analyzed via Western Blot as described below.

KRas modification in MiaPaca2 cell culture

Following treatment with (**2**) (100 μM) for 1 h. MiaPaca2 (ATCC CRL-1420, pancreatic carcinoma cell line expressing KRas G12C) cell cultures were washed with 1 × PBS, harvested, and resuspended in 20 mM Tris, 50 mM NaCl, 1% TritonX-100, at pH 7.75. Cell lysates were incubated with Biotin-PEO_3-azide (125 μM), tris(2-carboxyethyl)phosphine (TCEP, 0.5 mM), tris[(1-benzyl-1H-1,2,3-trazol-4-yl)methyl]amine (TBTA, 50 μM), and $CuSO_4$ (0.5 mM) for 1 h. The Cu-catalyzed click

reaction was quenched with the addition of 500 μM EDTA. Cell lysate samples (100 μL) were split into two replicate aliquots. Input samples were mixed with 2 × Laemmli buffer. Cold acetone (50 uL) was then added to the remaining aliquot. Samples were vortexed and place on ice for 10 min and subsequently centrifuged at 16,000 × g for 10 min at 4 °C. The supernatant was carefully removed. The protein pellet was resolubilized in 200 uL of Binding Buffer (0.1 M KH_2PO_4, 0.15 M NaCl at pH 7.5). Streptavidin slurry (Thermo Fisher Scientific; Waltham, MA, USA) (400 uL, 1:1) pre-washed 3 × in binding buffer was added to each sample. Samples were then incubated under gentle shaking for 1 hr at 4 °C. Samples were then washed 4 × with Binding Buffer (2 min at 325 × g). 1.5 × Laemmli buffer was added to the resin and subsequently incubated at 95° C for 8 min. Samples were then subjected to SDS-PAGE and analyzed via Western Blot as described below.

Cell Viability of MiaPaca2 and BxPC3 cells following 4-chloropyridine probe treatment

MiaPaca2 and BxPC3 (ATCC CRL-1687, pancreatic adenocarcinoma cell line expressing KRas wt) cells were plated in 96-well plates at 2,000 cells per well in 90 ml Dulbecco's Modified Eagle Medium (DMEM) with 10% fetal bovine serum (FBS) and allowed to attach for 24 h. Cells were treated by the addition of 10 μl of 4-Cl-Probe to a final concentration of 1-100 μM or vehicle (0.1% DMSO final). After 24-72 h, media was exchanged and plates were analyzed using CellTiter-Blue Cell Viability Assay (Promega).

Percentage of Covalent Modification of KRas *in vitro*

KRas (25 μM) was incubated with (**2**) (250 μM) or DMSO control as previously described above (see Methods: KRas Modification *in vitro* Characterization). After 1 h a biotin tag was selectively appended to the (**2**) by the addition of Biotin-PEO_3-azide (125 μM), tris(2-carboxyethyl)phosphine (TCEP, 1 mM), tris[(1-benzyl-1H-1,2,3-trazol-4-yl)methyl]amine (TBTA, 100 μM), and $CuSO_4$ (1 mM). After an additional 1 h incubation, the click reaction was quenched by addition of EDTA (1 mM, final concentration). Streptavidin agarose resin slurry (0.66 mL) (Thermo Fisher Scientific; Waltham, MA, USA) was then added to each sample and the total volume of each sample was adjusted to 1 mL using Binding Buffer ((0.1 M KH_2PO_4, 0.15 M NaCl at pH 7.5). Samples were incubated under gentle agitation for 1 h. The resin was washed 8 × with Binding Buffer. Breifly, microtubes containing resin samples were brought up to 1.5 mL total volume with Binding Buffer and vortexed gently. Resin was then pelleted by centrifugation and the supernatant was removed by pipetting. Bound KRas was eluted from the resin upon addition of 1 × SDS-PAGE buffer and heating at 95 °C for 8 min to denature streptavidin. Samples were subjected to SDS-PAGE and commassie staining. The percentage of modified KRas was approximated using densitometry analysis (Bio-Rad Laboratories; Berkeley, CA).

General Western Blot Procedure

Western blots were performed by standard procedures using two primary antibodies, IgG fraction monoclonal mouse anti-biotin (1:200) (Jackson ImmunoResearch, West Grove, PA; #200-002-211) and/or when applicable, a target

specific rabbit derived primary antibody (1:1000), coupled with the two-color Odyssey IR Dye Western Blot Kit I (Li-Cor Biosciences, Lincoln, NE; #926-31081), which contains IR Dye 800CW goat anti-mouse secondary antibody and IRDye 680CW goat anti-rabbit secondary antibody (1:10000). Images were scanned using an Odyssey Infrared Imaging System (Li-Cor Biosciences, Lincoln, NE) at the core DNA Facility (University of Texas, Austin).

3.3 RESULTS AND DISCUSSION

To explore the utility of the halopyridine scaffold in targeting additional proteins of therapuetic and clincal interest, three proteins were chosen for individual characterization, two identified in the primary screen and one from accesory data. Of the three individual proteins selected, halopyridine modification of human KRas was characterized in detail.

Initial Selection and Characterization

From the primary proteomic screen, a variety of protein classes were identified as being modified by (**1**), (**2**), or both probes (Table 3.1). Categorizing the primary hits in terms of ligand binding slectivity revealed the majority (40%) of proteins identified were GTP/ATP binding proteins with the second major group (12%) identified being NAD^+ binding proteins (Figure 3.1A). This analysis led to a hypothesis that halopyridines are somewhat selective for purine binding proteins or NAD^+-binding proteins, a proposal that is under study.

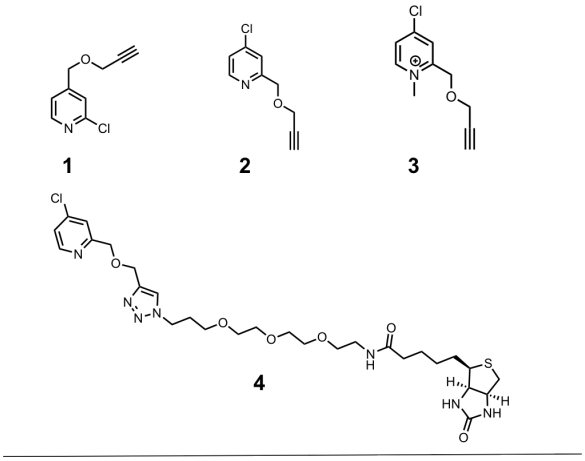

Table 3.1 Structures of halopyridine probes used for validation of primary screening hits and characterization of KRas covalent modification.

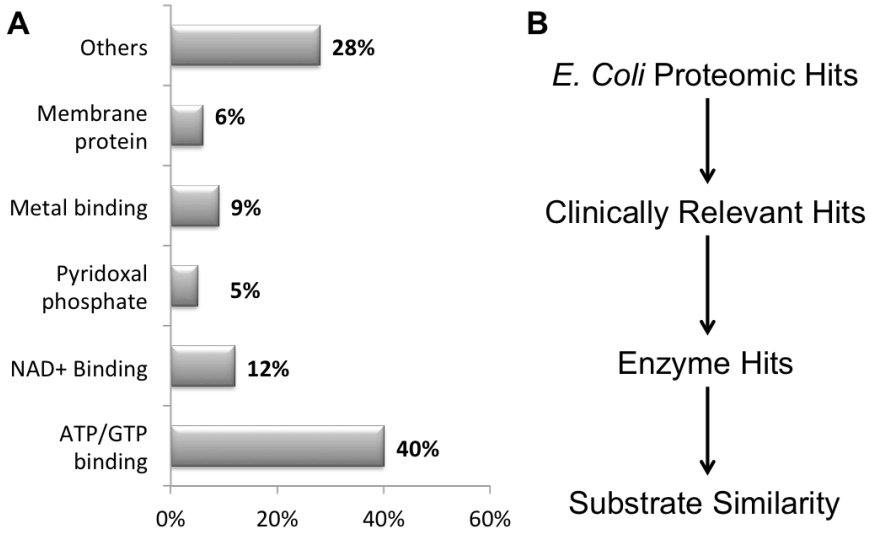

Figure 3.1 (A) E. Coli proteomic screening hits organized by binding group. (Data collected by Joyce Er) (B) Criteria used for selection of preliminary hits for validation and characterization.

The first step towards development of this scaffold as a specific modifier is the validation of primary hits. To increase the likelyhood of validating experimentally tractable targets of clinical interest, the hit list was filtered based on the critera introduced above. (Figure 3.1B) From the final list of hits, CytD and UDP were selected for characterization. CytD's clinical significance stems from its upregulation in certain adenocarcinomas and pancreatic cancers as well as its mutation-dependent role with respect to the efficacy of chemotherapuetic nucleoside analog treatments.[10-13] Similarly, UDP1 activity is elevated in various tumor types and plays an important role in the activation of chemotherapuetic agents 5-fluorouracil and 5'-deoxy-5-fluorouridine via the pyrimidine salvage pathway.[14-16]

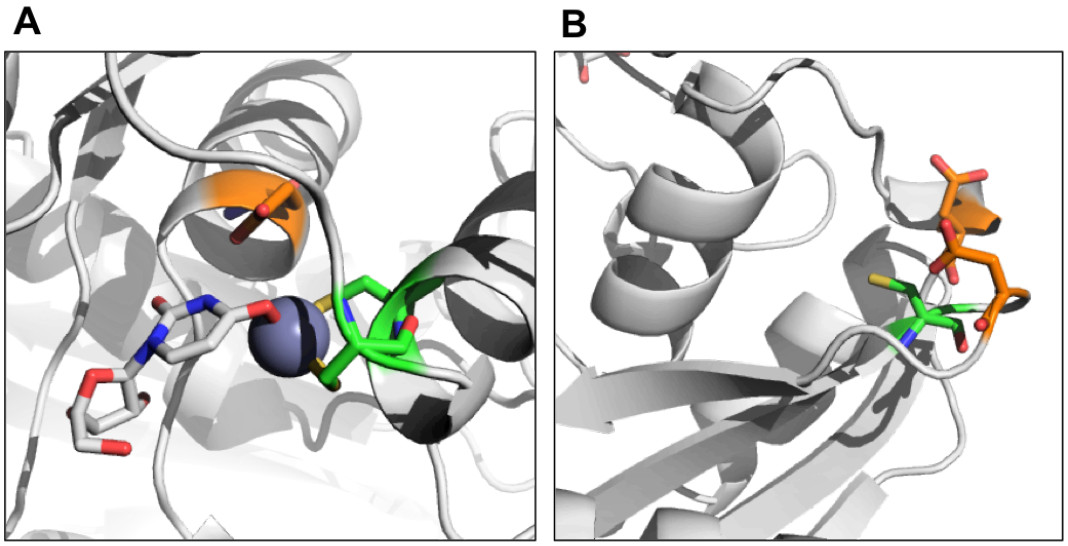

Figure 3.2 Cysteine residues in close proximity to carboxylic side chains in the CytD crystal structure (PDB: 1AF2). (A) C129 and C132 coordinate the catalytic zinc in the active site (green) and nearby E104 (orange) hydrogen bonds with N3 of the product uridine (grey). (B) C217 (green) on the distal surface is flanked by D218 and D256 (orange).

Both of these enzymes catalyze reactions involving pyrimidine nucelosides, cytidine or uridine, which resmeble the base halopyridine scaffold. As revealed in the CytD crystal structure (PDB: 1AF2), CytD contains two potential sites that fullfill the proposed modification requirements by haloypridines. One site is located at the substrate binding pocket and the other on the surface. (Figure 3.2) The homohexamieric strucutre of UDP contains only one such site, near one of the regions essential for subunit-subunit contact.[16] (Figure 3.3)

Following expression and purification of CytD, covalent modification by either (**1**) or (**2**) was tested. No modification by either probe was observed (data no shown).

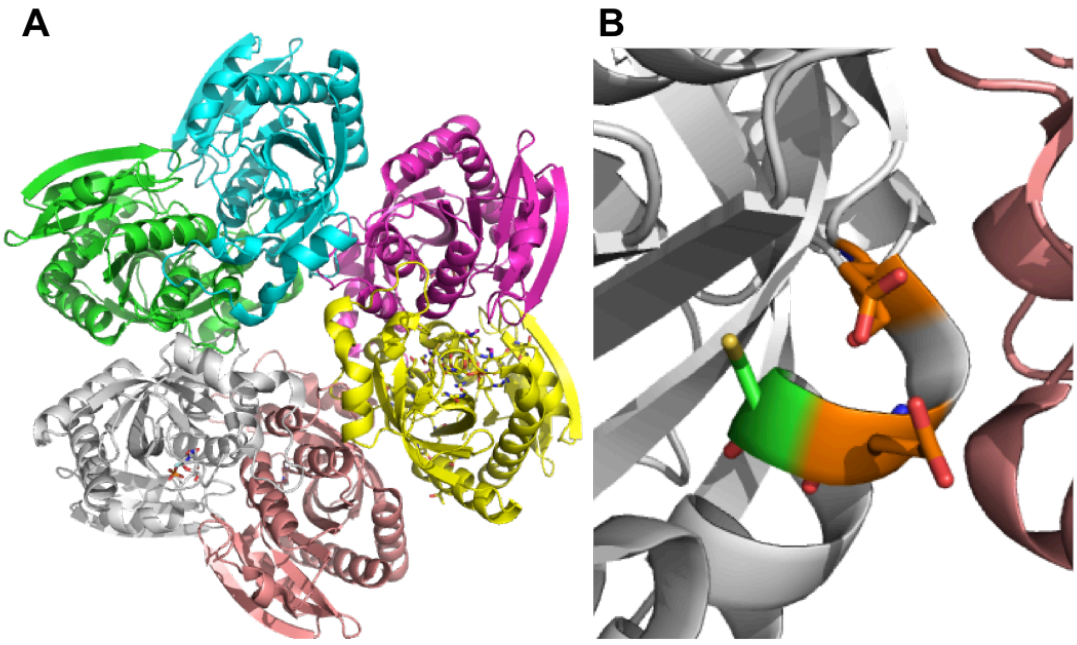

Figure 3.3 (A) Homohexameric structure of *E. Coli* UDP. (PDB: 1RXC) (B) C136 (green) flanked by D133 and E135 shown in orange located near the subunit interface.

Steady state kinetic assays were also carried out to test for any change in enzymatic activity following pre-incubation with probe. (Figure 3.4A) Again, no probe-dependent effect was observed. Based on our inability to label and the absence of any significant change in k_{cat} after pre-treatment, it was concluded that CytD was a false positive of the primary screen.

Modification of UDP by (**1**) or (**2**) in crude lysates containing overexpressed UDP was also tested. Unlike CytD, UDP did show strong labeling via Western blot (WB). (Figure 3.4B) However, modification was not blocked by the presense of excess uridine, suggesting modification may not occur at the active site (Figure 3.4C).

In parallel, modification testing was also carried out on KRas based on the abundance of purine nucleotide-binding proteins identified in the primary screen and

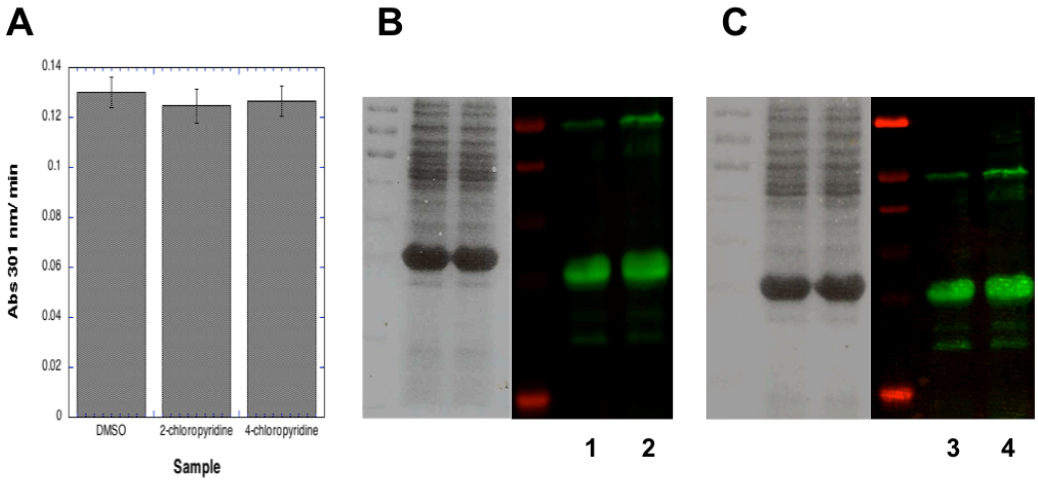

Figure 3.4 (A) CytD steady state enzymatic rates following pre-incubation with probe compounds (1) and (2) (B) WB image and coomassie stain of UDP labeling by (1) (Lane 1) and (2) (Lane 2) in *E. Coli* lysates. (C) WB image and coomassie stain of UDP labeling by (1) (Lane 3) and (2) (Lane 4) in *E. Coli* lysates in the presence of excess UDP.

recent reports of successful covalent targeting of the oncogenic mutant KRas G12C.[17-21] Western blot analysis, as described below, revealed KRas as a validated target of halopyridines. This result is of significant interest in light of the frustrating history of Ras inhibitor design efforts and may represent a new way to target KRas. For these reasons the modification of this important target by this novel scaffold was characterized in detail.

KRas Modification Site Identification

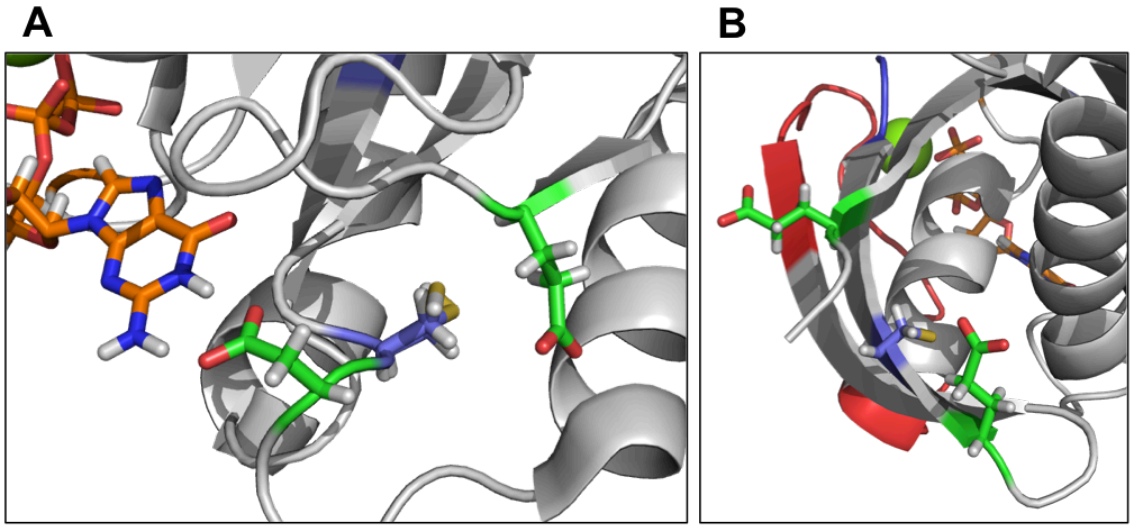

Figure 3.5 Cysteine residues in close proximity to carboxylic side chains in the KRas crystal structure (PDB: 4L8G). (A) C118 (purple) located near the nucleotide binding site, flanked by E143 and D119 (green). D119 coordinates to the guanine nucleobase. (B) C51 (purple) flanked by E3 and E49. Switch I and II are highlighted in red and blue, respectively.

In order to identify the residue(s) modified by (**2**), site-directed mutagenesis was carried out at the most likely positions, cysteine residues that are in close proximity to the acidic side chains of either glutamate or aspartate, but separated by enough space to

accommodate a pyridine ring. KRas contains two such sites on its surface. (Figure 3.5) One is near the nucleotide-binding pocket at C118. Modification experiments carried out using the purified C118A mutant still resulted in modification, albeit decreased compared to wildtype (Figure 3.6). It was then postulated that KRas contains a second site of modification. Therefore, a further mutation was carried out to create the double mutant KRas C51A/C118A (designated: DM). Modification experiments using the DM resulted in loss of all observable labeling. In addition, a construct lacking cysteine residues (C51S/C80L/C118S) was also tested for modification (Figure 3.6). This too resulted in loss of all observable labeling confirming that KRas can be modified at two distinct sites, C51 and C118, with what appears to be a higher propensity for modification at C118, although direct quantification was not assessed via Western blot.

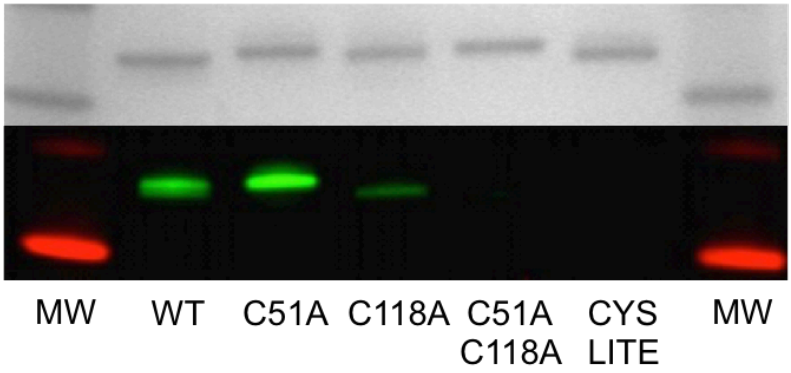

Figure 3.6 Western blot (lower) and accompanying coomassie gel (upper) of purified wild type and mutant constructs of KRas Isoform 2B (1-169) treated with (2). MW stands for Molecular Weight Marker (Fisher EZ-Run Prestained *Rec* Protein Ladder, Thermo Fisher Scientific, Waltham, MA, USA). The MW bands represent 17 kDa (lower) and 26 kDa (upper) reference proteins.

There are drawbacks to modifying residues of KRas found in non-oncogenic cells. In contrast, by targeting a specific oncogenic mutation such as G12C, one can ensure

inhibition of only hyper-activated KRas without effecting normal KRas' function in healthy tissue. However, oncogenic KRas' mutations take a variety of forms, many of which are not amenable to covalent targeting.[22] Therefore having alternative means to covalently target KRas using an inherently selective scaffold is highly advantageous.

Identification of Activating Residue(s)

Each cysteine modification site is in close proximity to two carboxylate containing side chains that each have the potential to stabilize the protonated pyridine ring and prime it for nucleophilic attack at the 4- position. The C51 site is neighbored by,

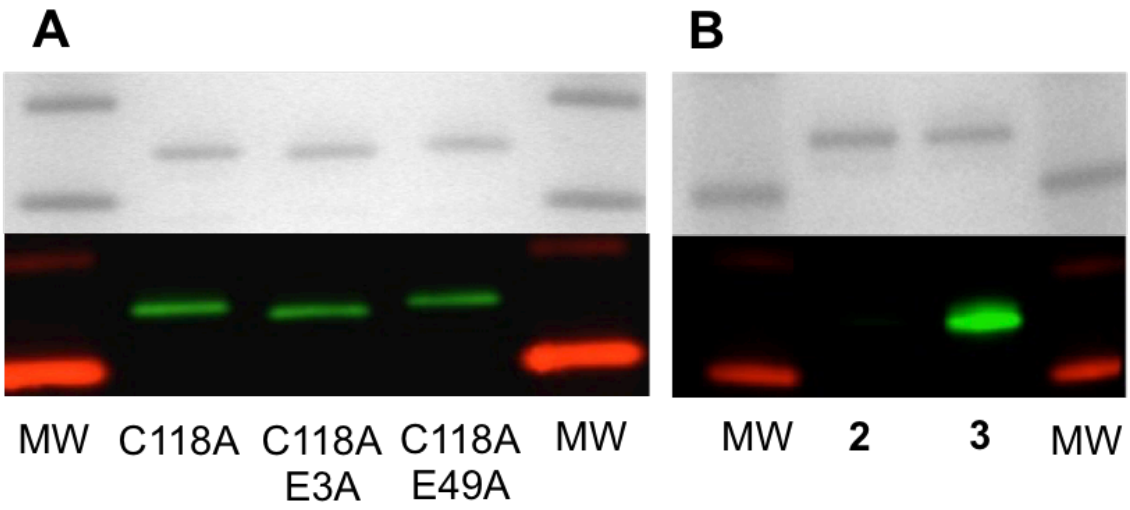

Figure 3.7 (A) Western blot (lower) and accompanying coomassie gel (upper) of mutant constructs of KRas Isoform 2B (1-169) treated with (2). (B) Western blot (lower) and accompanying coomassie gel (upper) of mutant construct KRas Isoform 2B (1-169) C118A E3A E49A (TM) treated with 2 or 3. MW stands for Molecular Weight Marker (Fisher EZ-Run Prestained *Rec* Protein Ladder, Thermo Fisher Scientific, Waltham, MA, USA). The MW bands represent 17 kDa (lower) and 26 kDa (upper) reference proteins.

glutamate residues E3 and E49. Using the KRas C118A construct as a starting point, site-directed mutagenesis was used to obtain the individual mutants E3A and E49A as well as the double mutant E3A, E49A. These constructs allowed us to study the influence of activating residues at a single site, C51. Modification experiments using the C118A, E3A or C118A, E49A purified mutants resulted in labeling equal to that found using the C118A mutant. (Figure 3.7) This result suggested one of two possibilities. Either residues E3 and E49 are compensatory with regards to 4-Cl-probe activation or modification is the result of a different mechanism. No modification was observed when the C118A, E3A, E49A mutant (designated: TM) was tested *in vitro*. As a control, incubation of the TM KRas with the fully activated 4-Cl-*N*-methyl-Probe (**3**), in which stabilization of the pyridinium form via protein binding is not necessary, resulted in strong labeling at C51 (Figure 3.7). This indicates that stabilization of the protonated form by one or both the these residues (E3 or E49) is required for modification of KRas by 4-Cl-P. To address any gross changes in overall protein structure, each mutant construct used was tested for retention of the ternary complex KRas•GDP•Mg^{2+} via native MS. In all cases, the ternary complex was conserved indicating the mutant constructs maintained the overall protein structure compared to wildtype as reflected in their ability to bind GDP and Mg^{2+} (Figure 3.8).

These experiments demonstrate a consistent mechanism for modification by (**2**), a cysteine in proximity to an activating carboxylate. However, KRas differs in that, two carboxylates have compensatory function. This flexibility may be due to labeling on the surface of KRas as opposed to an active site. In the absence of significant steric

influences or non-covalent interactions with target, the halopyridine scaffold or the carboxylate residues may have multiple confirmations that can promote covalent labeling. Future derivitization of the halopyridine scaffold to improve non-covalent interactions with KRas could influence which of these residues participate in activation.

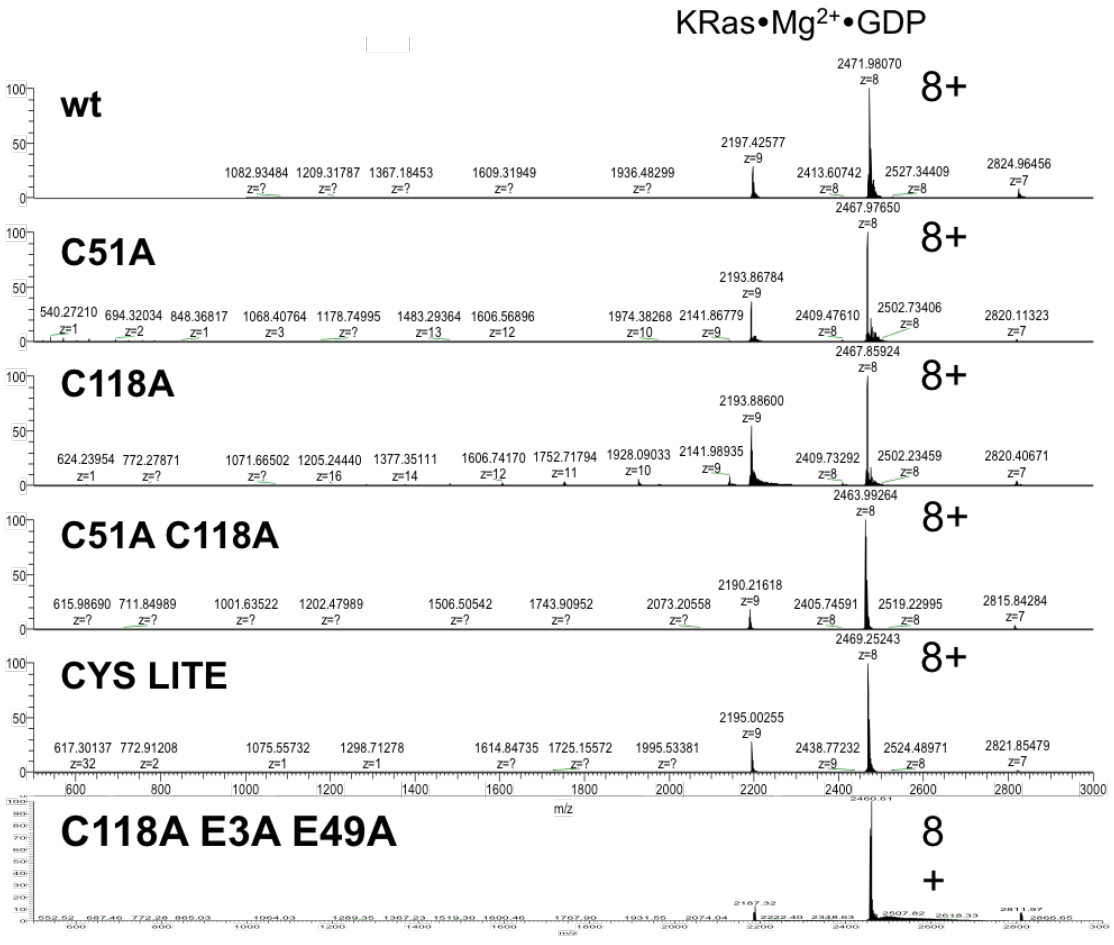

Figure 3.8 ESI mass spectrum of wild type and mutant constructs of KRas Isoform 2B (1-169) sprayed from a 50 mM ammonium acetate solution (pH 7.8). Spectrums were obtained under native spray conditions with static tip ionization, 1.4-1.7kV, capillary temperature 200°C. The complexes may contain numerous additional sodium, magnesium and ammonium adducts.

While KRas is known for its lack of obvious surface binding pockets to take advantage of, in this instance we achieve a unique selectivity due to fixed pairs of residues.

Covalent Modification of KRas by the 4-Chloropyridine Probe is Labile Over Time

Based on the Western blot detection of labeled KRas via detection of biotin appended to the probe the modification appeared to be stable under the conditions and time period tested. However, based on the solvent exposed nature of the surface modification, it was possible that the modification could be susceptible to hydrolysis over longer time periods. To test this hypothesis, KRas was incubated overnight with excess (**2)** under dialysis conditions. Loss of covalent modification was observed under dialysis conditions, but not in the control samples (no dialysis). (Figure 3.9)

These results suggest the covalent modification of KRas by (**2)** is labile over long time periods, likely due to hydrolysis of the S-C bond. Since the probe is not very reactive in solution, in the control samples where excess probe is left in the mixture, new probe has the ability to replace any that hydrolyzes over time. In contrast, under dialysis conditions, excess probe is removed and no new probe is present once hydrolysis occurs, thus leading to the loss of signal overnight. The same result was seen when using (**4)**, wherein the biotin moiety has previously been appended to the pyridine scaffold. The use of (**4**) confirms that modification is not an artifact of the click reaction or

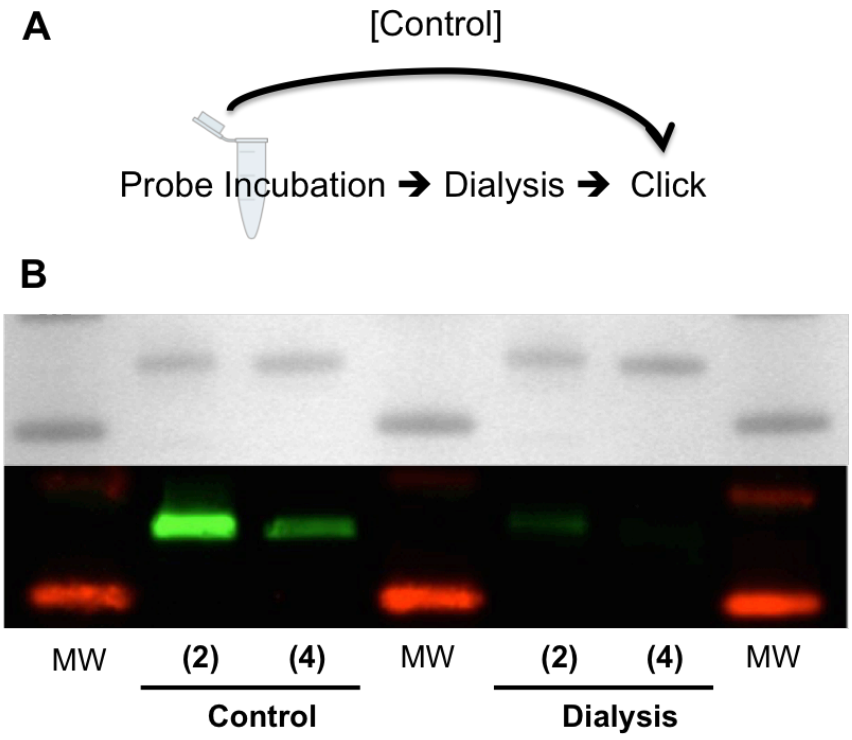

Figure 3.9 (A) Schematic representation of experimental setup. (B) Western blot (upper) and accompanying coomassie gel (lower) of wild type KRas Isoform 2B (1-169) treated with 2 or 4. MW stands for Molecular Weight Marker (Fisher EZ-Run Prestained *Rec* Protein Ladder, Thermo Fisher Scientific, Waltham, MA, USA). The MW bands represent 17 kDa (lower) and 26 kDa (upper) reference proteins.

experimental work-up, and confirms loss of label upon dialysis. Our initial efforts to detect the hydrolyzed product were not successful, possibly due to due to low abundance of the expected product (data not shown).

Probe Stability and Cu-click Chemistry Interference in the Presence of Excess GSH and GDP

Here, we determine halopyridines are stable in the presence of GDP and if modification of KRas has any dependence on GDP concentration. To investigate these

questions *in vitro*, experiments were carried out testing the stability of the probe overnight and the modification of KRas in the presence of excess (5 mM) GDP or GSH. Based on previous evidence[1, 2], it was hypothesized that neither experimental condition (overnight incubation or modification in the presence of GDP or GSH) would result in a different result. Overnight incubation with GDP resulted in no observable change as monitored by HPLC, however, modification of KRas appeared to be inhibited by both GDP and GSH. (Figure 3.10, 3.11A) To determine if GDP or GSH were inhibiting modification and not a different step in the experimental work up (**4**) was tested for its ability to modify KRas in the presence of GDP or GSH. This would eliminate any false negative due to inhibition of the click reaction. In contrast to the experiment above, use of (**4**) did result in modification. (Figure 3.11B) These results suggest that the Cu(I)-click reaction to append the biotin tag is inhibited by high concentration of GDP or GSH under these experimental conditions. However, treatment with (**4**) shows halopyridine covalent modification is even possible in the presence of these cellular effectors and that only visualization was affected.

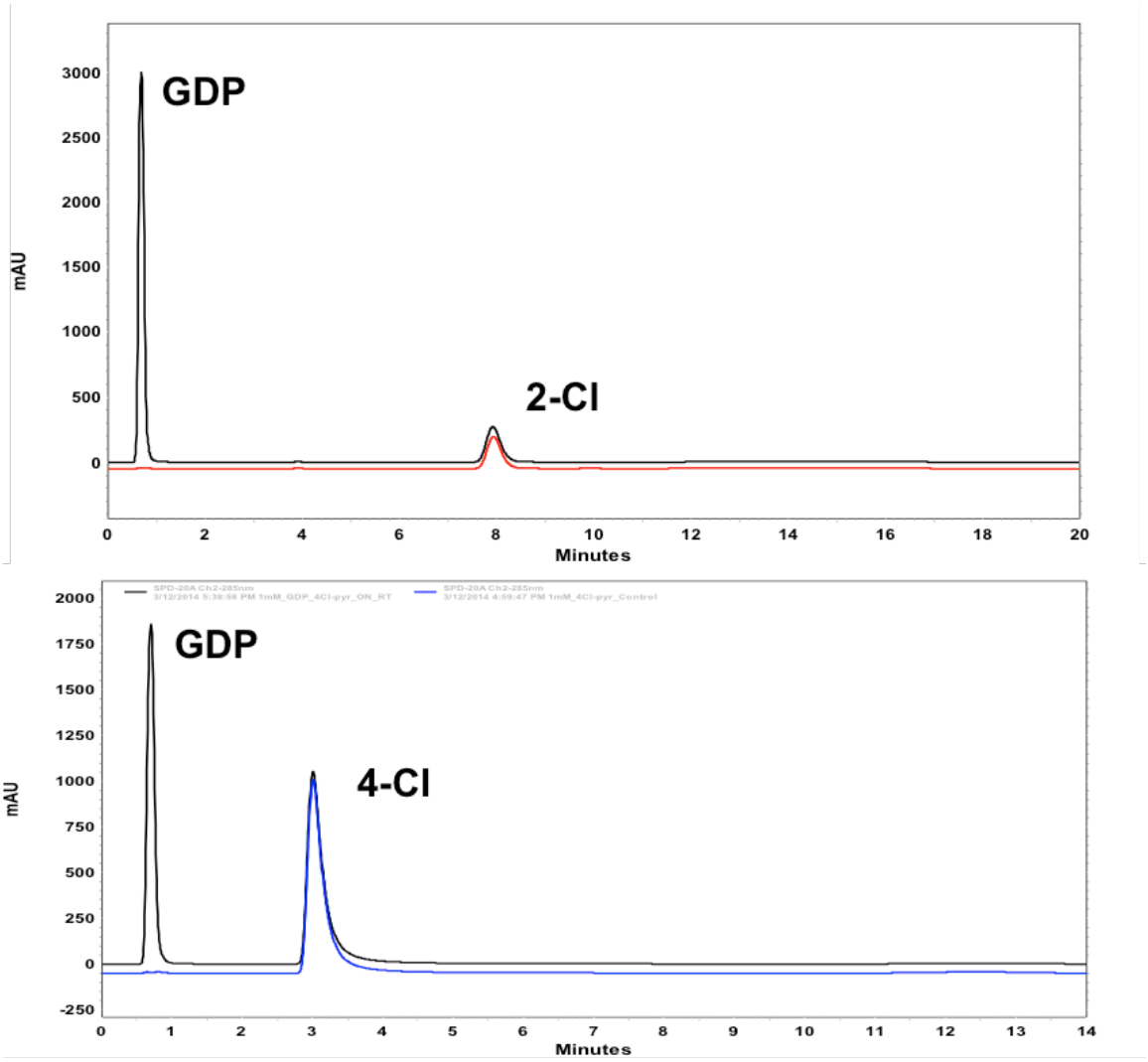

Figure 3.10 HPLC traces from overnight incubations of 2- and 4-chloropyridine probes in the presence of GDP. Peak areas and retention times remained unchanged.

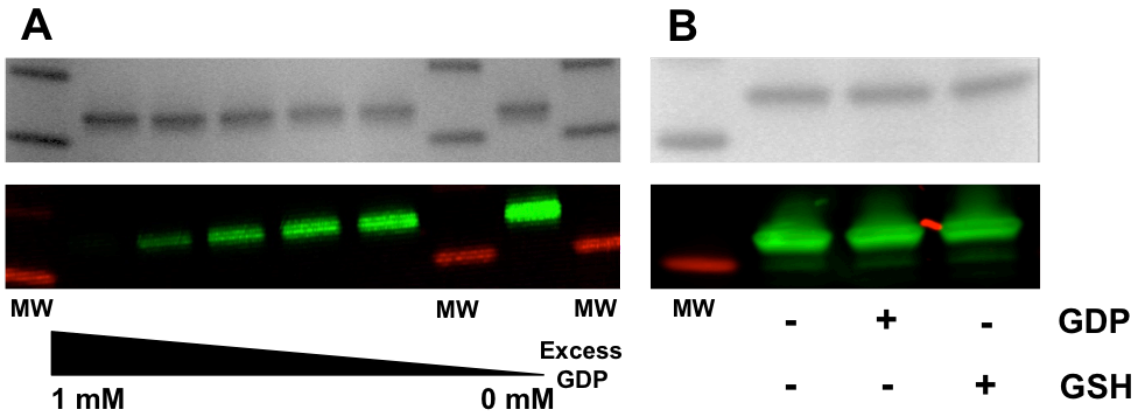

Figure 3.11 (A) Western blot (lower) and accompanying coomassie gel (upper) for labeled KRas in the presence of increasing concentrations of GDP. (B) Western blot and accompanying coomassie gel for KRas labeled with the biotin pre-clicked probe (4) in the presence of effectors GDP and GSH. MW stands for Molecular Weight Marker (Fisher EZ-Run Prestained *Rec* Protein Ladder, Thermo Fisher Scientific, Waltham, MA, USA). The MW bands represent 17 kDa (lower) and 26 kDa (upper) reference proteins.

Modification of Endogenous KRas in MiaPaca2 Cell Culture

Part of a probe compounds usefulness is its ability to modify its target in cells, so we assessed target engagement in cell culture. MiaPaca2 cells, a pancreatic carcinoma cell line, were chosen for use because 90% of pancreatic tumors harbor a KRas mutation, but the majority of these tumors do not contain the G12C mutation.[21] Therefore, validating a potential means to target other oncogenic KRas mutants would be of significant benefit. To determine whether KRas could be modified in cultured cells, MiaPaca2 cell cultures were treated with media containing (**2**) (100 μM) or vehicle control (DMSO) for 1 h. Cells were subsequently washed and harvested using standard procedures and cells were lysed by brief sonication. Biotin-PEO_3-azide, TCEP, TBTA

and $CuSO_4$ were added to lysate samples as described and incubated for an additional 1 h. The Cu-catalyzed click reaction was then quenched by addition of EDTA. Cellular

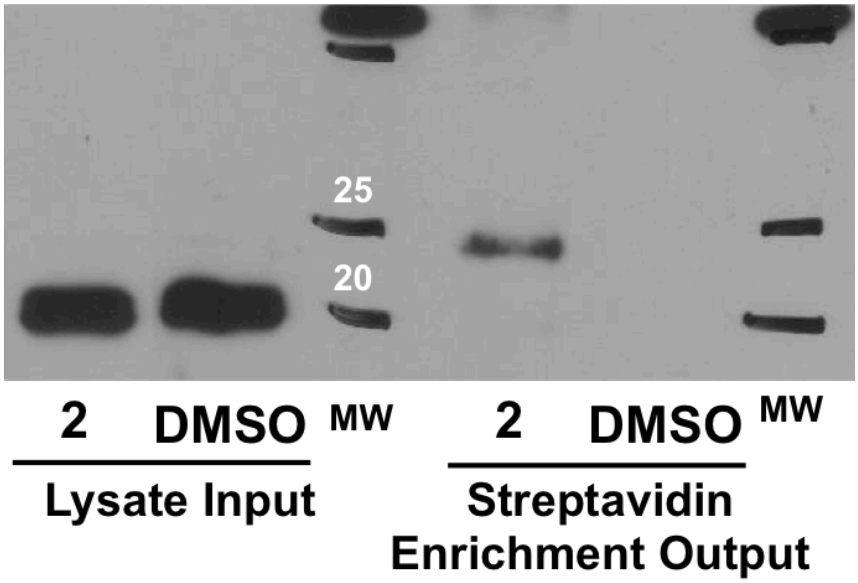

Figure 3.12 (A) Western blot for KRas in MiaPaca2 cell lysates treated with 2 or DMSO. (Left) Cell lysate input showing equal loading and (Right) KRas detection following streptavidin agarose enrichment. MW stands for Molecular Weight Marker.

proteins labeled by the probe were enriched on streptavidin agarose. The resulting enrichment was probed for KRas via Western blot. The results of this experiment demonstrate that the (**2**) does covalently modify KRas in cultured cells, suggesting it is cell permeable and is able to engage its target. (Figure 3.12)

Interestingly, there is a small shift in the mobility of the input sample and enriched sample. Small, unexpected shifts in the electrophoretic mobility of Ras isoforms have also been observed elsewhere. These shifts have been shown to correlate to single Ras point mutations and in other cellular studies, possibly reflect increased post-

translational processing.[23, 24] While not directly investigated here, it is possible that modification of KRas by (**2**) interferes with KRas processing or that additional modification in the hyper variable region (not present in the plasmid construct) cause the observed shift. While the exact nature of this shift was not determined, no other bands are apparent in either sample to suggest non-specific binding of the antibody is occurring.

Based on the previous reports of shifts in KRas' electrophoretic mobility due to small structural changes and the lack of any non-specific binding of the antibody in whole cell lysates, these experiments demonstrated target engagement in intact cultured cells. This suggests the halopyridine scaffold has the potential to be used as a starting point for covalent targeting of KRas in a cellular context.

Cell Proliferation in the presence of 4-chloropyridine probe

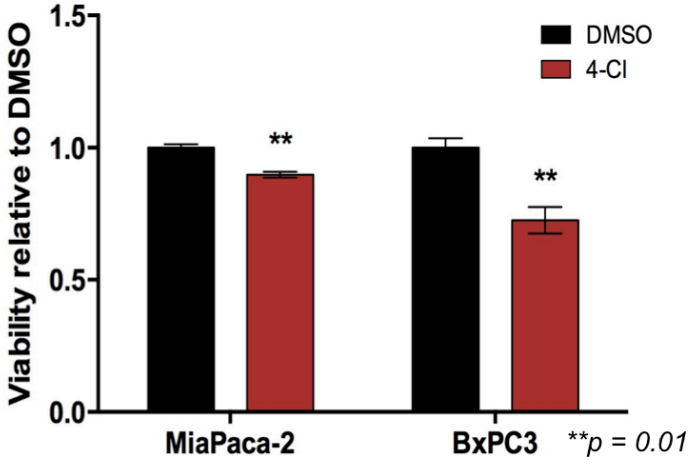

Figure 3.13 MiaPaca2 cell viability following treatment with 100 µM (2) for 72 h.

KRas functions as a cell-signaling switch through protein-protein interactions in response to external stimuli. Labeling at the C51 or C118 site may have an influence on

the ability of KRas to bind its downstream partners. It was recently shown that small molecule labeling at C118 on the Ras:SOS complex can be used to prevent the reloading of Ras with GTP *in vitro*.[25] This represented a new approach to Ras pathway inhibition, however, these compounds utilized a highly reactive maleimide to target C118. The use of (**2**) could represent a way to target this same site, using a much more selective electrophilic fragment.

To determine if labeling of KRas in MiaPaca2 cells had any effect on cell proliferation, cell viability assays using CellTiter-Blue were conducted. Viability was assessed at 0, 24, 48, and 72 h at treatments with (**2**) over a concentration range of 0.1 – 1000 μM. In MiaPaca2 cells, treatments with (**2**) at 100 μM resulted in very modest, but statistically significant, decreases in viable cells at 72 h. (Figure 3.13) To make sure this decrease in viability was due to decreased cell growth and not to cell death due to toxicity at the time of treatment, viability was monitored at several time points (0 – 72 h). It was determined that no significant cell death occurred upon treatment and is consistent with (**2**) the probe not being inherently toxic in cell culture (data not shown). This modest effect could also suggest that modified KRas does not disrupt signaling, only a small fraction of KRas is covalently modified, or other signaling pathways resulting in proliferation may be activated in response to probe treatment.

***In vitro* quantification of modified KRas**

In order to address one of the possible reasons for the lack of a strong functional effect on cell viability, the fraction of KRas covalently labeled *in vitro* was determined. Analogous to treatment of cell culture, recombinant KRas was treated with 100 μM 4-Cl-

Probe for 1 h. Biotin-PEO_3-azide, TCEP, TBTA and $CuSO_4$ were added to each sample as described and incubated for an additional 1 h. The Cu-catalyzed click reaction was then quenched by the addition of EDTA. Labeled KRas was enriched using streptavidin

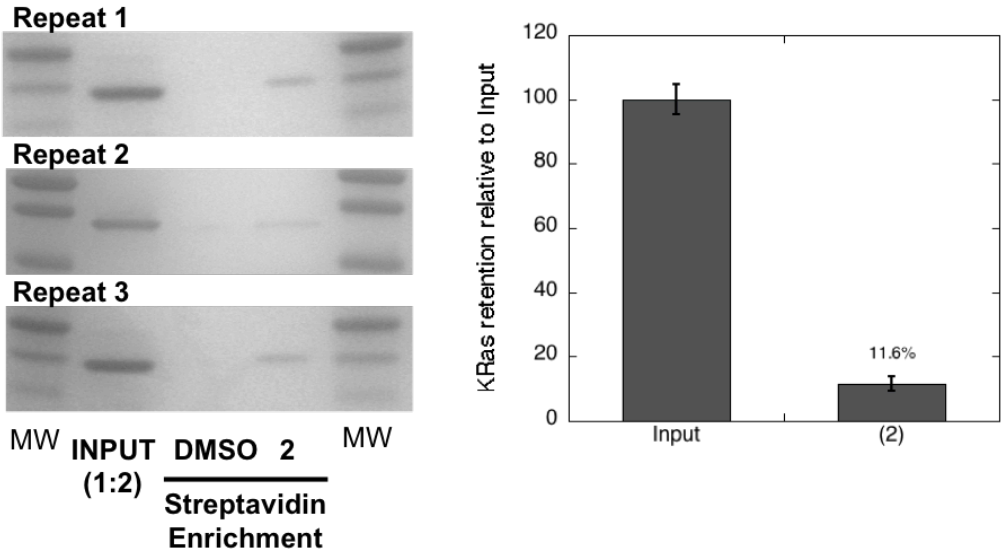

Figure 3.14 (A) *In vitro* streptavidin enrichment of KRas treated with (2) or DMSO. Triplicate coomassie stained gels. (B) Densitometry measurements of coomassie stained gels in A. MW stands for Molecular Weight Marker (Precision Plus Protein All Blue Prestained Protein Standards, Bio Rad, Hercules, CA, USA). The MW bands represent 25 kDa (upper), 20 kDa (middle) and 15 kDa (lower) reference proteins.

agarose. To directly assess the extent of labeled protein the resulting enrichment was analyzed by SDS-PAGE and visualized by coomassie staining. Enrichment of probe-treated KRas only resulted in a small percentage (approx. 11%) of labeled protein as compared to the experimental input (Figure 3.14). Therefore covalent targeting of KRas using 4-halopyridines only occurs to a minor extent.

The observation that only a small fraction of KRas is modified by (**2**) may be partly a consequence of labeling at the surface of the protein. A key determinant in the covalent modification of proteins by 4-halopyridines is the ability to stabilize the pyridinium form. With respect to DDAH, this stabilization takes place in the active site away from bulk solvent. While structurally divergent from DDAH's native substrates, steric constraints imparted by the active site in conjunction with interaction of Asp66 (*Pa*DDAH) with the pyridinium form to orient the 4-carbon for attack most likely contributes to the significantly faster and more efficient modification of DDAH compared to KRas.[1,2] The influence of these active site dependent constraints on modification are lost at the surface of the protein. Multiple residues that may serve to activate the probe are present near the sites of modification on KRas, but without the addition of other favorable interactions imparted by the target-binding site, the interactions that lead to stabilization of the active probe would be expected to be transient in nature. This has important implications for further development of 4-halopyridine based probes. When modifying at the surface of the protein, there may be limits to how much affinity can be improved through non-covalent interactions because of the lack of structural features to take advantage of as described. In these cases, the use of both target specific derivitization to the extent it may be applied at the surface as well as modulation of the pyridinium switch to increase reactivity (as discussed in Chapter 2) will be important tools for improved efficacy.

3.4 CONCLUSION

Three clinically relevant enzymes (CytD, UDP and KRas) were tested for their ability to be labeled by (**1**) and (**2**). Only one of the two enzymes selected from the initial proteomic screen (UDP) was validated as a target. The 4-chloropyridine probe also labeled KRas, which was tested based on its therapeutic interest and structural properties. It was demonstrated that the 4-chloropyridine probe uses a similar modification mechanism with KRas as previously shown for DDAH and has the ability to label both C51 and C118. Unexpectedly, the adduct was shown to be unstable and susceptible to hydrolysis overnight. Experiments in MiaPaca2 cell culture demonstrate KRas can also be modified in cultured cells. Treatment of cells, even at high concentrations of 4-chloropyridine probe, only resulted in very modest decreases in MiaPaca2 cell proliferation. One possible reason for the modest effect is incomplete KRas modification illustrated by the *in vitro* tests. Scaffold optimization will be essential to increase both the percentage of KRas labeled and to enhance any functional downstream effect of KRas targeting. These results illustrate a conserved mechanism for selectively targeting cysteine residues with neighboring carboxylates and represent a promising start for KRas targeting using a 'quiescent' electrophilic moiety.

2.5 REFERENCES

1. Johnson, C. M., Linsky, T. W., Yoon, D. W., Person, M. D., Fast, W. Discovery of Halopyridines as Quiescent Affinity Labels: Inactivation of Dimethylarginine Dimethylaminohydrolase *J. Am. Chem. Soc.* **133**, 1553 (2011)**.**

2. Johnson, C. M., Monzingo, A. F., Ke, Z., Yoon, D. W., Linsky, T. W., Guo, H., Robertus, J. D., Fast, W. On the Mechanism of Dimethylarginine Dimetheylaminohydrolase Inactivation by 4-Halopyridines *J. Am. Chem. Soc.* 133, 10951 (2011)**.**

3. Mellacheruvu, D., Wright, Z., Couzens, A. L., Lambert, JP., St-Denis, N. A., Li, Tuo, Miteva, Y. V., Hauri, S., Sardiu, M. E., Low, T. Y., Halim, V. A., Bagshaw, R. D., Hubner, N. C., al-Hakim, A., Bouchard, A., Faubert, D., Fermin, D., Dunham, W. H., Goudreault, M., Lin, Z., Badillo, G., Pawson, T., Durocher, D., Coulombe, B. & Aebersold, R. The CRAPome: a contaminant repository for affinity purification-mass spectrometry data. *Nat. Meth.* **10**, 730-736 (2013).

4. Klomsiri, C., Karplus, P. A., Poole, L. B., Cysteine-Based Redox Switches in Enzymes. *Antiox. Redox Signal.* **14,** 1065-1077 (2011).

5. Ishihama, Y., Oda, Y., Tabata, T., Sato, T., Nagasu, T., Rappsilber, J. & Mann M. Exponentially Modified Protein Abundance Index (emPAI) for Estimation of Absolute Protein Amount in Proteomics by the Number of Sequenced Peptides per Protein. *Molecular and Cellular Proteomics.* **4,** 1265-1272 (2005).

6. Oda, Y., Owa, T., Sato, T., Boucher, B., Daniels, S., Yamanaka, H., Shinohara, Y., Yokoi, A., Kuromitsu, J., & Nagasu, T. Quantitative Chemical Proteomics for Identifying Candidate Drug Targets. *Anal. Chem.* **75,** 2159-2165 (2003).

7. Carlow, D. C., Short, S. A., Wolfenden R. Complementary Truncations of a Hydrogen Bond to Ribose Involved in Transition-State Stabilization by Cytidine Deaminase. *Biochemistry.* **37,** 1199-1203 (1998)

8. Ostrem, J. M., Peters, U., Sos, M. L., Wells, J. A., & Shokat, K. M. K-Ras (G12C) inhibitors allosterically control GTP affinity and effector interactions. *Nature.* **503.** 548-551 (2013)

9. Kapust R.B., Tozser J., Fox J.D., Anderson D. E., Cherry S., Copeland T. D., Waugh D. S. Tobacco etch virus protease: mechanism of autolysis and rational design of stable mutants with wild-type catalytic proficiency. *Protein Eng.* **12,** 993-1000 (2001).

10. Mekras, J. A., Boothman, D. A. & Greer, S. B. Use of 5-trifluoromethyldeoxycytidine and tetrahydrouridine to circumvent catabolism and exploit high levels of cytidine deaminase in tumors to achieve DNA- and target-directed therapies. *Cancer Res.* **45,** 5270-80 (1985).

11. Boothman, D. A., Briggle, T. V. & Greer S. B. Protective, Tumor-selective Dual Pathway Activation of 5-Fluoro-2'-deoxycytidine Provided by Tetrahydrouridine in Mice Bearing Mammary Adenocarcinoma-755. *Cancer Research*. **47,** 2344-2353 (1987).

12. Shin, G., Kang, T., Yang, S., Baek, S., Jeong, Y. & Kin, S. GENT: Gene Expression Database of Normal and Tumor Tissues. *Cancer Informatics*. **10,** 149-157 (2011).

13. Zauri, M., Berridge, G., Thezenas, M. L., Pugh, K. M., Goldin, R., Kessler, B., M., Kriaucionis, S. CDA directs metabolism of epigenetic nucleosides revealing a therapeutic window in cancer. *Nature*. **6,** 114-8 (2015).

14. Cao, D. & Pizzorno, G. Uridine phosphorylase: An important enzyme in pyrimidine metabolism and fluoropyrimidine activation. *Drugs Today (Barc)*. **40,** 431-43 (2004).

15. Yan, R., Wan, L., Pizzorno, G. & Cao, D. Uridine phosphorylase in breast cancer: a new prognostic factor? *Front. Biosci*. **11,** 2759-66 (2006).

16. Caradoc-Davies, T. T., Cutfield, S., M., Lamont, I. L. & Cutfield, J., F. Crystal Structures of *Escherichia coli* Uridine Phosphorylase in Two Native and Three Complexed Forms Reveals Basis of Substrate Specificity, Induced Conformational Changes and Influence of Pottasium. *J. Mol. Bio*. **337,** 337-354 (2004).

17. Baines, A. T., Xu, D. & Der, C. J. Inhibition of Ras for cancer treatment: the search continues. *Future Med. Chem*. ***3***, 1787-1808 (2011)

18. Mattingly, R. R. Activated Ras as a Therapeutic Target: Constraints on Directly Targeting Ras Isoforms and Wild-Type versus Mutated Proteins. *ISRN Oncology*, ID: 536529 (2013).

19. Tsimberidou, A. M., Chandhasin, C. & Kurzrock, R. Farnesyltransferase inhibitors: where are we now? *Expert Opin. Investig. Drugs*. ***19***, 1569-1580 (2010).

20. Ostrem, J. M.; Peters, U.; Sos, M. L.; Wells, J. A.; Shokat, K. M.: K-Ras(G12C) inhibitors allosterically control GTP affinity and effector interactions. *Nature*. ***503***, 548-551 (2013).

21. Lim, S. M., Westover, K. D., Ficarro, S. B., Harrison, R. A., Choi, H. G., Pacold, M. E., Carrasco, M., Hunter, J., Kim, N. D., Xie, T., Sim, T., Janne, P. A.,

Meyerson, M., Marto, J. A., Engen, J. R. & Gray, N. S. Therapeutic Targeting of Oncogenic K-Ras by a Covalent Catalytic Site Inhibitor. *Angew. Chem. Int. Ed.*, ***53***, 199-204 (2014).

22. Prior, I. A., Lewis, P. D. & Mattos, C. A comprehensive survey of Ras Mutations in Cancer. *Cancer Res.* **72**, 2457 (2012).

23. Kim K., Kuo T., Cai J., Murnane M. J. N-ras protein: Frequent quantitative and qualitative changes occur in human colorectal carcinomas. *Int. J. Cancer.* **71,** 767-75 (1997).

24. Tabin C. J., Bardley S. M., Bargmann C. I., Weinberg, R. A. Mechanism of activation of a human oncogene. *Nature.* **300,** 143-149 (1982).

25. Winter J.G., Anderson M., Blades K., Brassington C., Breeze A. L., Christine C., Embrey K., Fairley G., Faulder P., Finlay R. V., Kettle J. G., Nowak T., Overman R., Patel J., Perkins P., Spadola L., Tart J., Tucker J. A., Wrigley G. Small Molecules Binding Sites on the Ras:SOS complex Can Be Exploited for Inhibition of Ras Activation. *J. Med. Chem.* **58,** 2265-2274 (2015).

Chapter 4: Characterization of the Catalytic Activity of *Pa*DDAH T165L and it's Application Toward ADMA Quantification

4.1 INTRODUCTION

The methylated arginines, asymmetric N^{ω}- N^{ω}-L-dimethylarginine (ADMA), N^{ω}-monomethyl-L-argnine (NMMA) and symmetric N^{ω}- N^{ω}-L-dimethylarginine (SDMA) are produced by the degradation of post translationally methylated proteins. In cells, both ADMA and NMMA act as endogenous inhibitors of all three forms of Nitric Oxide Synthase (NOS). NOS is responsible for synthesis of nitric oxide (NO), a short-lived signaling molecule that initiates diverse signaling cascades based on tissue type.[1-3] In the endothelium, NO helps to maintain vascular homeostasis.[4] Because of its central role in regulating blood pressure, proper NOS function is of utmost importance. To date, several regulatory mechanisms of NOS activity have been uncovered.

One such mechanism is regulation of ADMA and NMMA levels through their catabolism by the enzyme dimethylarginine dimethylaminohydrolase-1 (DDAH-1). While ADMA and NMMA can be eliminated by renal excretion, the vast majority is catabolyzed by DDAH-1.[5] So, DDAH serves an important role as an indirect regulator of NOS. Interestingly, DDAH-1 activity has been shown to be decreased during oxidative stress, a cellular condition commonly associated with cardiovascular disease. This decrease in DDAH1 activity is concomitant with ADMA accumulation.[6-8] And while impairment of the NOS pathway is multifactorial, increased levels of circulating ADMA have been suggested to play a role in endothelial dysfunction.[9] The exact role ADMA

plays is still a matter of debate, but regardless of if it is a causative agent or a byproduct of cardiovascular disease progression, research in this area has led to the understanding that the concentration of circulating ADMA can be used as an independent biomarker, with strong prognostic value, for cardiovascular morbidity and total mortality.[10]

As both a biomarker for and possible mediator of cardiovascular disease, ADMA quantification is of significant clinical interest.[11] Currently, the three most established methods for quantification of ADMA are HPLC, LC-MS, and ELISA each of these methods has its own distinct advantages and disadvantages.[12] In the case of HPLC and LC-MS, both of these methods have the advantage of being able to simultaneously quantify not only ADMA, but NMMA and SDMA as well. While often requiring sample enrichment (LC-MS, HPLC) and/or pre-column derivitization (HPLC), these methods are considered the most reliable analysis methods. Unfortunately, these methods also require instrumentation that may not be available or is prohibitively expensive depending on the clinical setting.[13] Comparatively, ELISA kits utilizing an anti-ADMA antibody can quantify ADMA in a plate based format using common laboratory equipment, and do not require sample enrichment, but do require derivitization (*N*-acylation). Unfortunately, this analysis method can suffer from matrix dependent effects (comparison of plasma/serum samples vs. standard controls) relegating its effective use to clinical investigations in which groups of samples are compared and the endpoint is the shift in ADMA concentrations in response to an intervientionn.[13]

ADMA quantification methods require a high level of both sensitivity and accuracy due to the low concentrations of ADMA that need to be quantified (0.3-0.7 μM

for healthy individuals, ≥ 1 μM for at risk individuals) and the observation that even slightly elevated concentrations are correlated with cardiovascular risk.[13] For example, even a 0.13 μM increase in ADMA levels was correlated with a 21% risk increase in cardiovascular disease.[14] Again, the significant risk associated with even these small deviations demonstrates the importance of methods that can accurately and precisely determine ADMA concentrations as well as the difficulty in comparing values derived from different quantification methods. Progress continues to be made, but improved methods to quantify ADMA are of interest.

Based on preliminary characterization of *Pseudomonas aeruginosa* DDAH (PaDDAH) T165L conducted by Dr. Tom Linsky and Dr. Corey Johnson in our laboratory, it has been proposed herein that this specific mutant may be applicable as a tool for ADMA quantification. Briefly, through investigation of the role of Thr165 in the catalytic mechanism it was found that *Pa*DDAH T165L had a dramatic effect on catalysis.[15] The mutant *Pa*DDAH T165L was shown to be covalently inactivated by its own substrate in a time-dependent manner. Mass spectrometry studies indicated the possible formation of a thiocarbamate adduct which is only hydrolyzed slowly and much less efficiently than the normal thiouronium adduct (Scheme 4.1). Because of *Pa*DDAH T165L's partitioning between substrate turnover and self-inactivation, in conjunction with the slow rate of hydrolysis to regenerate the resting enzyme, we hypothesize here that this mutant represents a means by which ADMA, its natural substrate, can be quantified. Specifically, the percentage of inactivated *Pa*DDAH

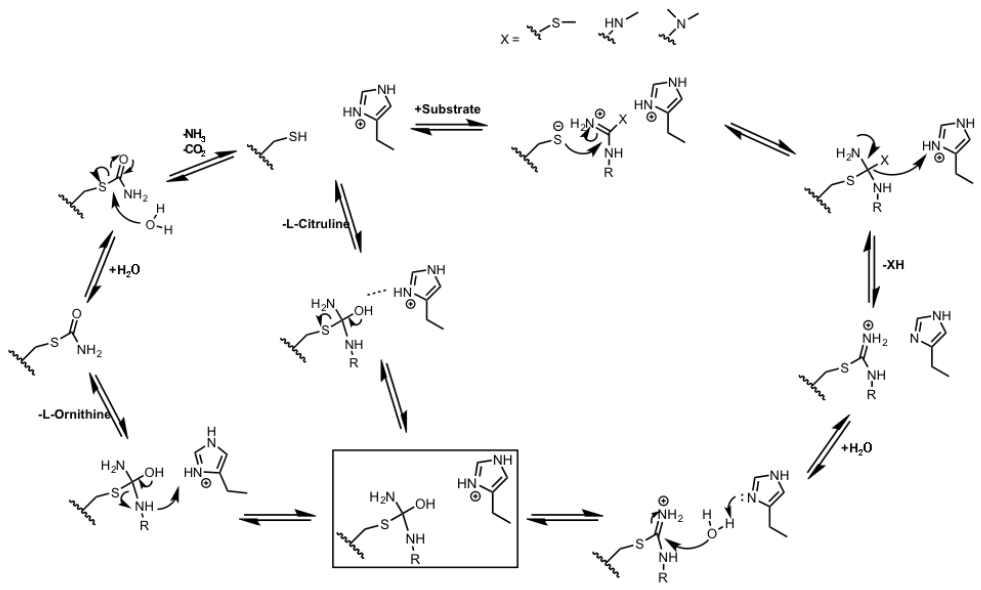

Scheme 4.1 Proposed scheme of *Pa*DDAH T165L catalytic activity. The proposed partitioning step is boxed.

T165L after incubation with a sample containing ADMA should be proportional to the amount of ADMA present in the given sample. Following incubation of *Pa*DDAH T165L with ADMA samples, a signal amplification step can be used to quantify the remaining activity of *Pa*DDAH T165L, representing a method that is not dependent on expensive instrumentation, is inherently specific for methylated argnines, and has the potential to be more cost-effective than ELISA (Figure 4.1).

In this chapter, a methodology to quantify ADMA using *Pa*DDAH T165L is developed. The experimental partition ratios for ADMA, NMMA, and SMTC are measured and proof-of-principal experiments that demonstrate the feasibility of this approach are preformed. To the best of our knowledge, this is the first time a mutation-induced inactivation partitioning has been applied to quantify a substrate, which in this

case is a clinically relevant biomarker. Each step in this method is experimentally optimized in order to maximize accuracy and sensitivity. Although rigorous validation of the proposed method will be required prior to clinical use, the experiments presented here support our hypothesis that the unique partitioning of *Pa*DDAH T165L can be utilized for quantification of a clinically significant biomarker. During the development of this method, insights into the mechanisms governing self-inactivation were also revealed.

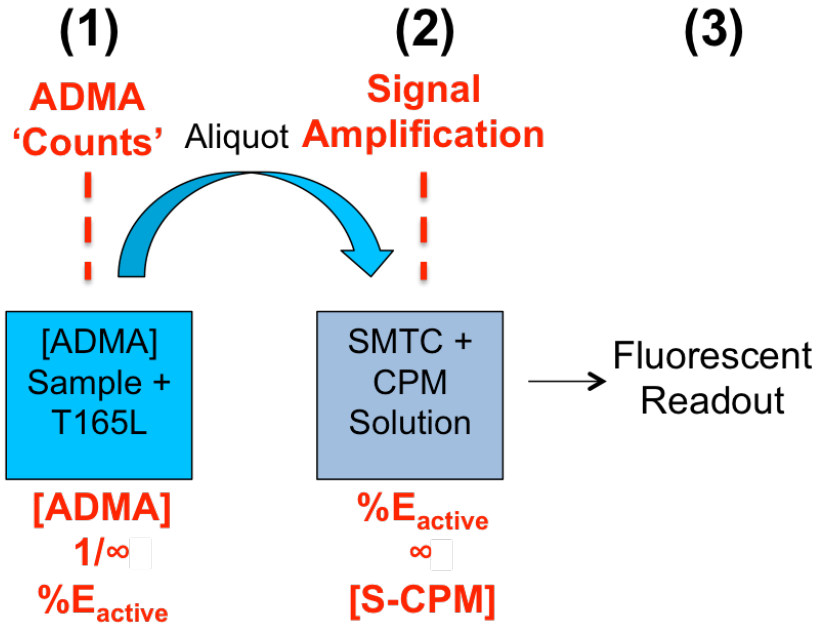

Figure 4.1 ADMA quantification using *Pa*DDAH T165L workflow. The method is composed of three individual steps, (1) Incubation of *Pa*DDAH T165L with the sample of interest. (2) Sample aliquot dilution into a secondary incubation containing excess substrate *S*-Methyl-*L*-thiocitrulline (SMTC) and 7-diethylamino-3-(4-maleimidophenyl)-4-methylcoumarin (CPM). (3) Fluorescence measurement for the quantification of the reaction of methanethiol with CPM (Excitation λ: 384 nm, Emission λ: 470 nm).

4.2 MATERIALS AND METHODS

Materials

Unless otherwise noted, all chemicals and reagents were purchased from Sigma-Aldrich (St. Louis, MO, USA). K_2HPO_4, Na_2HPO_4, NaH_2PO_4, dimethylsulfoxide (DMSO) and trifluoroacetic acid (TFA) were from Thermo Fisher Scientific (Waltham, MA, USA). 96-well and 384-well black bottom polystyrene microplates were from Corning (Corning, NY, USA). Expression and purification of each *Pa*DDAH mutant was carried out as previously described.[16]

Construction of Vector for *Pa*DDAH T165L, C249S

The pET-28a vector with N-terminally His_6-tagged recombinant PaDDAH T165L, was previously cloned by Tom Linsky.[16] This vector was used as a template for Quikchange site-directed mutagenesis (Stratagene; La Jolla, CA, USA). For the C249S mutant, the primers were 5'- GAC GGC GGC GTC AGT AGC ATG TCG CT-3'and 5'-AGC GAC ATG CTA CTG ACG CCG CCG TC -3'. To construct the mutant genes, a PCR mixture containing the template vector, the mutagenic primers, a dNTP mixture, and Phusion DNA polymerase in the manufacturer's buffer (New England Biolabs; Ipswich, MA, USA) was run using a temperature program of 95 °C for 30 s, followed by 20 cycles of 95 °C for 30 s, 55 – 60 °C for 1 min (temperature gradient PCR), 72 °C for 90 s and a final step at 72 °C for 10 min. DpnI (New England Biolabs; Ipswich, MA, USA) was then added to the cooled reaction mixture and incubated at 37 °C for 2 h to digest the methylated template DNA. 2 μL of the resulting sample was transformed into BL21

(DE3) *Echerichia coli* cells. Viable colonies were selected from Lysogeny Broth (LB) agar plates with kanamycin (30 μg / mL) after overnight incubation at 37 °C. Plasmid was extracted and purified using a QIAprep Miniprep Kit (Qiagen; Valencia, CA, USA). Mutations were confirmed by DNA sequencing of the insert sequence.

Determination of Partition Ratios for Substrates ADMA, NMMA, and SMTC

Partition ratios, defined as the number of moles of product per mole enzyme inactivated, were determined for each substrate using the COLDER protocol to quantify L-citrulline formation. The partition ratio for SMTC was also determined using the continuous CPM based fluorescence assay utilizing the synthetic substrate SMTC. [17,18]

To determine partition ratios, purified recombinant *Pa*DDAH T165L (0.3-1 μM) was incubated with the substrate of interest (ADMA, NMMA, or SMTC, 1 mM) in Assay Buffer (KCl (100 mM), Na_2HPO_4 (100 mM), EDTA (0.05 mM), and Tween20 (0.01% w/v) at pH 6.5) at 25 C (100 μL total reaction volume). At varying time points (0-180 min) reactions were quenched with 10 μL of 6 N TFA and analyzed for L-ctirulline production as previously described.[17] All experiments were run in triplicate in a 96-well plate format. To determine the partition ratio (y_0), the calculated turnover number versus time plots were fit to the exponential decay function below using Kaleida Graph (Synergy Software, Reading, PA). Variables are defined as follows: P; Number of turnovers, y_0; Partition Ratio, A; burst phase amplitude, $kobs$; observed inactivation rate, *t;* time.

$$P = y_0 + A \cdot e^{-kobs \cdot t} \quad \text{(Eq. 3.1)}$$

pH Dependence on Enzyme Reactivation from the Thiocarbamate Adduct

To test the pH dependence of *Pa*DDAH T165L activity, experiments were set up as outlined above for partition ratio determination using the COLDER assay. Assay conditions were equivalent for all experiments, excluding pH adjustments. Experiments were carried out at pH values 6.5 and 7.5. Data were fit to the following equation to model burst phase and steady state turnover at pH 7.5.). Variables are defined as follows: P; Number of turnovers, y_0; Partition Ratio, A; burst phase amplitude, $kobs$; observed inactivation rate, *t;* time, *m;* steady state turnover.

$$P = y_0 + A \cdot e^{-kobs \cdot t} + m \cdot t \text{ (Eq. 3.2)}$$

Blood Plasma Sample Preparation

ADMA standard solutions (0 – 2.5 μM) or human blood plasma samples from normal and arteriosclerosis donor backgrounds were obtained from a commercial vendor (ProteGenex, Inc.; Culver City, CA, USA). 2 mL Acetonitrile (ACN) was added to each 1 mL plasma sample to precipitate proteins. Samples were vortexed for 2 min and centrifuged to pellet insoluble material (16 × g, 10 min). The resulting supernatant was transferred and split between 3 microtubes. The samples were concentrated to dryness under vacuum at 45 °C. At this point, some samples were tested as is after reconstitution in Assay Buffer. Samples were then reconstituted in phosphate buffered saline (PBS; 137 mM NaCl, 2.7 mM KCl, 10 mM Na_2HPO_4, 1.8 mM KH_2PO_4) at pH 7.4. Samples were enriched for methylated arginines by solid phase extraction (SPE) using Oasis MCX 1cc

vacuum cartridges (Waters Coorporation; Milford, MA,USA). Briefly, samples were applied to the SPE column, washed with 1 mL 100 mM HCl and 1 mL MeOH sequentially. Bound small molecules were then eluted using a freshly prepared solution of 50% MeOH/40% H_2O/10% concentrated NH_4OH (v/v/v). The eluted samples were again concentrated to dryness under vacuum at 45 °C. The final samples were reconstituted in Assay Buffer (80 uL total volume, concentrated approx 12.5-fold).

General Assay Procedure

The methodology developed was based on the following steps. (1) Incubation of *Pa*DDAH T165L with the ADMA containing. (2) The incubation was then diluted into a secondary incubation containing excess SMTC and 7-diethylamino-3-(4-maleimidophenyl)-4-methylcoumarin (CPM). (3) Fluorescence measurement for the quantification of the product methanethiol reacting with CPM (Excitation λ: 384 nm, Emission λ: 470 nm). The raw RFU signal versus time data was fit to equation 3.1 in order to determine the relative fluorescence units (RFU) end point. Calculated end points were used as is or converted to number of turnovers per enzyme and plotted versus ADMA μM.

Assay Optimization

In order to determine the parameters, concentrations, and incubation times needed for ADMA quantification in clinical samples, *Pa*DDAH T165L (10 – 500 nM) was incubated with various concentrations of ADMA (0-150 uM) in Assay Buffer. At varying time points (0-18 h) aliquots (25 or 50 μL) were diluted into a solution (30 or 60

μL) containing SMTC (0.5 - 2 mM), CPM (20 – 200 μM), and DMSO (5 - 10%) in Assay Buffer. Fluorescence was measured (every 30 – 90 sec) for a total of 20 min. The final parameters chosen for testing of clinical samples were: [*Pa*DDAH T165L] = 250 nM, [ADMA] ≥ 5 μM (after sample enrichment), Incubation time = 3 h, [SMTC] = 545 uM, [CPM] = 60 μM, and 9% DMSO.

ADMA Quantification in EDTA Stabilized Blood Plasma Samples

Blood plasma samples were prepared for use as described above. *Pa*DDAH T165L was added to each enriched plasma sample or a standard ADMA solution to a final concentration of 0.25 μM (80 uL total volume). Samples were incubated at 25 °C for 3 h. 25 μL was pipetted into a 384-well black bottom polystyrene microplate. 30 μL of substrate solution containing SMTC (1 mM), CPM (110 μM), and DMSO (10%) was added to each well using an Rainin® AutoRep E repeater pipette (Mettler-Toledo LLC, Columbus, OH, USA). The final concentrations for all components were 0.114 μM *Pa*DDAH T165L, 545 μM SMTC, 60 μM CPM, and 9% DMSO. Each sample or standard was run in triplicate. Fluorescence was read on a Wallac Victor 1420 Plate Reader (PerkinElmer; Waltham, MA, USA) equipped with filters for excitation at 340 nm and emission at 470 nm.

4.3 RESULTS AND DISCUSSION

Previously, Dr. Tom Linsky, carried out site-directed mutagenesis at Thr165 to learn more about the role this residue played in catalysis. His results indicated Thr165

might not play a significant role in the reaction. However, one of the mutants tested, T165L, slowly became inactivated when incubated with substrate (SMTC and ADMA).[15] Herein, the potential utility of *Pa*DDAH T165L as a tool to quantify the clinically important biomarker ADMA was evaluated. Through method development and optimization, further insights on the mechanism of inactivation are also revealed.

Determination of Substrate Partition Ratios

In order to develop an ADMA quantification methodology using *Pa*DDAH T165L, experimental determination of the partition ratio(s), for each substrate, was needed. This partition ratio describes the number of moles of product per mole enzyme inactivated and is essential to determine the assay conditions needed to achieve observable inactivation. Previously, Dr. Tom Linsky had estimated the partition ratio of SMTC based on ratios of rate constants derived from global fitting of kinetic data.[16] Herein, the partition ratios for ADMA, NMMA, and SMTC were all determined experimentally based on quantifying product formation over time. Experiments were carried out using excess substrate at three different enzyme concentrations (0.3, 0.5, and 1 μM). The final concentration of L-citrulline produced was used to determine the number of turnovers per enzyme at varying time points (Figure 4.2). The partition ratio was shown to be independent of total enzyme concentration, an important factor with respect to its ability to quantify ADMA (*vide infra*).

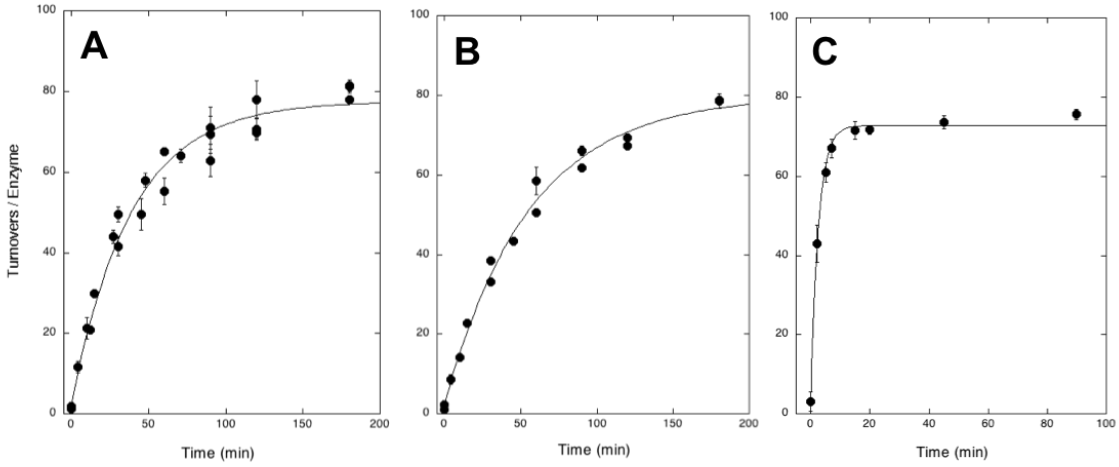

Figure 4.2 Determination of partition ratio (y_0) for (A) ADMA, (B) NMMA, and (C) SMTC. Turnovers per enzyme with respect to time as determined by the COLDER assay with T165L DDAH (1 μM) at pH 6.5 were plotted for each substrate. (A) ADMA data fit to a single exponential with A = -75 ± 2, k_{obs} = 2.3 ± 0.2 × 10^{-2}, and y_0 = 78 ± 2. (B) NMMA data fit to a single exponential with A = -77 ± 2, k_{obs} = 1.8 ± 0.1 × 10^{-2}, and y_0 = 80 ± 2. (C) SMTC data fit to a single exponential with A = -69 ± 2, k_{obs} = 3.8 ± 0.3 × 10^{-1}, and y_0 = 73 ± 1.

Determination of partition ratios for all three substrates also provided potential clues as to the nature of substrate inactivation and if substrate partitioning takes place at a common step in all three cases. If different partition ratios were found for each substrate, this difference might suggest partitioning occurs at a step influenced by different substrate substituents. The partition ratios (product formed: inactivated enzyme) for ADMA (78 ± 2 :1) and NMMA (80 ± 2 :1) are within error suggesting a common portion step (Figure 3.1). SMTC was observed to have a slightly lower partition ratio at 73 ± 1: 1. This might suggest a different partition step for SMTC, however, this decreased value could also arise from another factor (see below). The burst phase for SMTC is much more rapid than that of ADMA or NMMA.[20] In fitting to equation 3.1, the derived k_{obs} is

approximately 30-fold higher for SMTC and reaches an end point value in approx. one tenth of the time. Because no terms in the equation take into consideration reactivation of the enzyme, which may take place to a minor extent over the timescale of the reaction (180 min), any reactivation would be reflected in a reduction in k_{obs} and an approximate increase in the partition ratio (y_0).

While the differences in the calculated partition ratios of ADMA, NMMA and SMTC were outside of error, we believe the differences are due to reactivation and not different partitioning steps (see below). Based on the current experimental data, a single partitioning step is proposed that takes place upon collapse of the second tetrahedral intermediate (Scheme 4.1). Here we suggest a mechanism where by the T165L mutant could cause this inactivation. The bulkier leucine residue may influence the conformation of the active site histidine (H162). If the protonated His is positioned closer to the δ-nitrogen in the mutant (T165L), this could activate the δ-nitrogen as a leaving group promoting the loss of L-ornithine and formation of the thiocarbamate adduct. Regardless of mechanism, these experiments revealed the necessary details for application of *Pa*DDAH T165L for ADMA quantification. Specifically, we demonstrated that in bulk solution, on average, under these experimental conditions, *Pa*DDAH T165L is inactivated approximately once every 80 turnovers when ADMA or NMMA is used as substrate. When SMTC is used as substrate, inactivation is completed at a much faster rate than when ADMA or NMMA is used (20 min versus 180 min). This information is essential for determining the working concentration of *Pa*DDAH to use in the assay to

ensure both observable inactivation and sufficient signal during the signal amplification step.

Influences on *Pa*DDAH T165L Reactivation

Previous mass spectrometry evidence suggested the formation of a common inhibitory thiocarbamate adduct (+ 42 Da) when either SMTC or ADMA was used as the substrate.[15] A slow reactivation rate was assigned to hydrolysis of this long-lived adduct. In order to accurately quantify ADMA it would be advantageous to completely eliminate or at least minimize the amount of enzyme that undergoes this reactivation reaction during the time period of the assay. Identifying what factors influence *Pa*DDAH T165L reactivation following adduct formation would allow us to control these potentially complicating factors during method development.

It was hypothesized that, if the enzyme adduct is hydrolyzed to regenerate the active enzyme, the pH of the solution should have an influence on the rate of reactivation. To test the effects of pH, partition experiments were repeated at pH 7.5. These experiments revealed that reactivation of T165L was increased at higher pH, as reflected by the increase in steady state enzyme turnover at longer time periods when the data was fit to equation 3.2 (Figure 4.3).

Unexpectedly, the increased steady state rate of turnover at higher pH was different for each substrate (ADMA > NMMA > SMTC). This was an unexpected result since, mass spectrometry evidence suggested that a common 42 Da adduct accumulates over time when either SMTC or ADMA was used as the substrate. If the adduct is the

same, why do we observe different reactivation rates? Furthermore, this unidentified influence on enzyme reactivation rates is substrate specific.

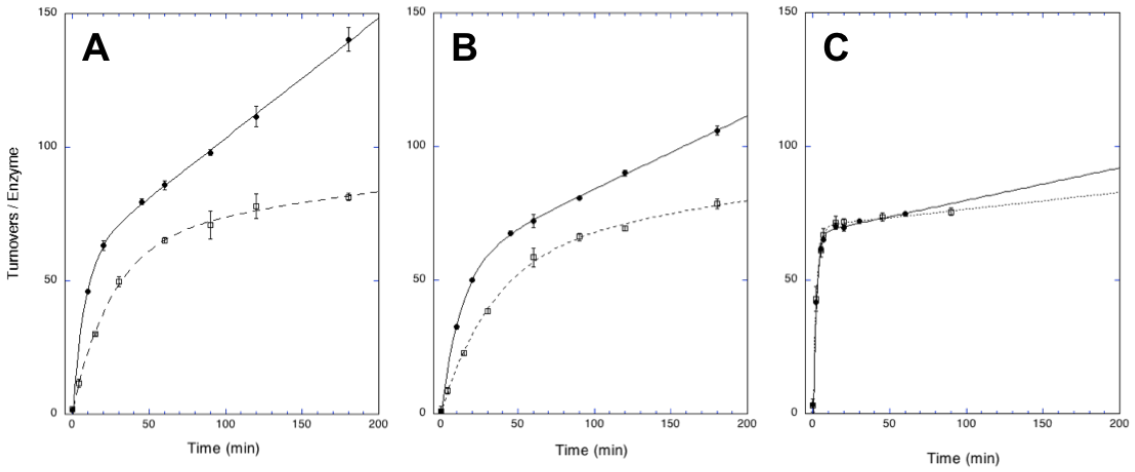

Figure 4.3 Influence of pH on steady state turnover for (A) ADMA, (B) NMMA, and (C) SMTC. Turnovers per enzyme with respect to time as determined by a uriedo assay with T165L DDAH (1 μM) at pH 6.5 (□) and 7.5 (●) were plotted for each substrate and fit to equation 3.2. (A) ADMA steady state turnover at pH 7.5, m = 0.45 ± 0.01 min^{-1}. (B) NMMA steady state turnover at pH 7.5, m = 0.27 ± 0.01 min^{-1}. (C) SMTC steady state turnover at pH 7.5, m = 0.12 ± 0.02 min^{-1}.

We reasoned that the alkyl-containing product (methanethiol, methylamine, or dimethylamine) produced during normal turnover might accelerate reactivation. If this were true, nucleophilic attack by the product (methanethiol, methylamine, or dimethylamine) at the thiocarbamate carbon would contribute to the increased rate of reactivation to different extents, explaining the observed differences. Dr. Tom Linsky had previously shown that the adduct was susceptible to attack by hydroxylamine, but these experiments were conducted with high (mM) concentrations of hydroxylamine, well above the concentrations of product that would be produced during hydrolysis of ADMA

at the concentrations of *Pa*DDAH T165L used (3 - 5 μM).[16] Because ADMA showed the highest steady state reactivation rates, we tested whether the addition of exogenous dimethyl amine, now at lower concentrations, to SMTC-inactivated T165L could increase the rate of steady state turnover. SMTC inactivated *Pa*DDAH T165L was used because of its relatively low basal reactivation rate as compared to ADMA inactivated *Pa*DDAH T165L. Addition of dimethylamine at the concentrations expected to be produced (70 uM) during inactivation under our assay conditions did not result in any change in reactivation of the enzyme. Moreover, at double the concentration expected to be produced, a slight negative effect was seen (Figure 4.4A). From these experiments, we concluded that the presence of the alkyl-containing product did not have an effect on enzyme reactivation.

Another factor that was unique in each experimental sample was the identity of the excess substrate present in the inactivation mixture. To test whether the identity of the excess substrate had any effect on reactivation, T165L was again inactivated using SMTC at pH 7.5. Aliquots of inactivated enzyme were then diluted into excess ADMA, NMMA, or SMTC. Reactions were quenched at varying time points and the partition ratio was calculated. In these experiments, three unique steady state rates were observed (Figure 4.4B). The rates of reactivation were closely related to the steady state rates observed in the original experiments at pH 7.5. These results suggest that substrate binding to inactivated protein, either at the active site or at an allosteric site, are the most likely factors that affect the rate of adduct hydrolysis and subsequent reactivation.

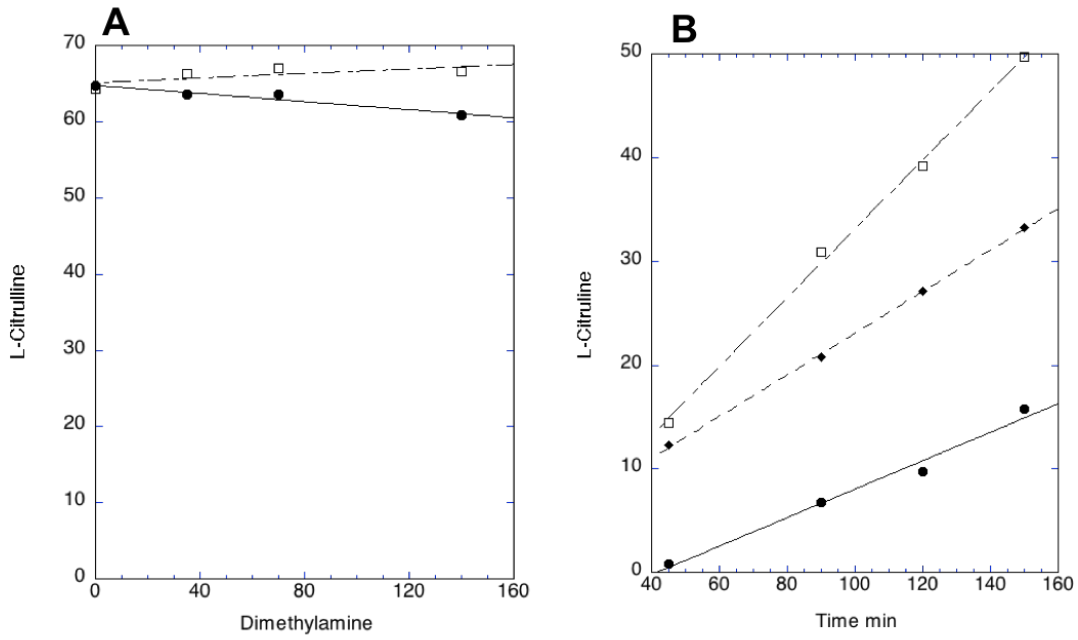

Figure 4.4 Influence of dimethylamine and excess substrate identity on steady state L-Citruline production. (A) SMTC-inactivated T165L in the presence of excess SMTC and dimethylamine (●) or no dimethylamine control (□) at pH 7.5. (B) SMTC-inactivated T165L in the presence of excess SMTC (●), ADMA (□), or NMMA (◆). Steady state *L*-Citrulline production in the presence of SMTC at pH 7.5 fit to a line with y-intercept = -5.6 ± 1.4 and slope m = 0.13 ± 0.01 min^{-1}. Steady state *L*-Citrulline production in the presence of NMMA at pH 7.5 fit to a line with y-intercept = 3.0 ± 0.4 and slope m = 0.20 ± 0.01 min^{-1}. Steady state *L*-Citrulline production in the presence of ADMA at pH 7.5 fit to a line with y-intercept = -0.1 ± 1.3 and slope m = 0.33 ± 0.01 min^{-1}.

Unlike the human DDAH1 isoform, *Pa*DDAH is known to dimerize with an apparent K_d ~500 nM.[19] Substitution of residues R40 and R98 to glutamate and histidine, respectively, shifts the equilibrium position towards the monomer. In the monomeric form, *Pa*DDAH (E40, H98) still retains greater than 95% activity suggesting that cooperativty between active sites in the dimer form is unlikely. Still, the lack of

cooperativity in the enzyme does not exclude the possibility that binding of substrate to one T165L monomer may induce small active site rearrangements in the paired T165L monomer, which might better position the adduct for hydrolysis. Alternatively, it may be possible for substrate to bind to the same active site with the adduct and induce rearrangements dependent on the identity of the substrate. Recently obtained crystallographic data is currently being reviewed to determine possible active site rearrangements induced by the T165L mutation, the possibility of T165L cooperativity or 'half-sites' reactivity in the dimer form, and whether or not substrate is able to bind at the active site already containing the thiocarbamate adduct.

Determining what influences enzyme reactivation rates was of significant importance with respect to developing a *Pa*DDAH T165L ADMA quantification method. Based on these results, the pH of assay samples should be kept low (pH 6.5) and the products of normal enzyme turnover are not expected to effect reactivation at the concentrations produced. Additionally, the fact that SMTC displays the lowest rate(s) of reactivation is advantageous for signal amplification and endpoint analysis. Furthermore, if future study finds that dimerization has an influence on the rate of reactivation, use of a monomer form of *Pa*DDAH T165L (Triple mutant: T165L, E40, H98) may represent a means to further improve the robustness of the assay.

Proof of Principle Demonstrating Application of *Pa*DDAH T165L for ADMA Quantification

To test for the ability of *Pa*DDAH T165L to be inactivated by ADMA in a concentration dependent manner, *Pa*DDAH T165L (0.5 μM) was incubated with varying

concentrations of ADMA (0 – 150 μM) for 3 h. Aliquots of each sample were transferred to a 96-well plate containing SMTC (545 μM) and CPM (60 μM) and the fluorescence

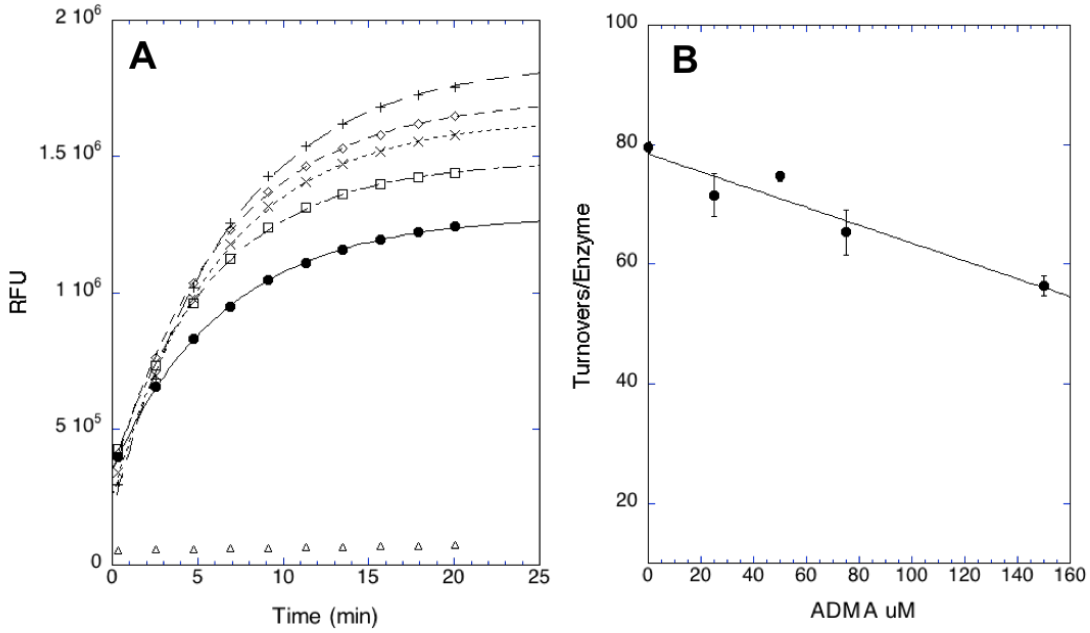

Figure 4.5 ADMA concentration dependence on remaining activity of *Pa*DDAH T165L. (A) Reactions of T165L (0.114 μM) with SMTC (545 μM) upon rapid dilution following 1 h pre-incubation with various concentrations of ADMA (0; + , 25; ◇ , 50; × , 75; □ , 150 μM; ●), fit to equation 3.1. (B) Turnovers/Enzyme as a function of the concentration of ADMA in pre-incubation mixture fit to a line with y-intercept of 78.5 ± 2 and slope of -0.15 ± 0.03.

was monitored every 90 s for 20 min. The results demonstrate that the end point of the fluorescence assay decreases as the concentration of ADMA in the original sample increases (Figure 4.5A). Plotting the assay end point fit as a function of ADMA reveals a linear relationship over the concentration range tested (Figure 4.5B). Additionally, the apparent partition ratio calculated here, in the absence of ADMA, is in good agreement with the partition ratio calculated using the color-developing reagent (COLDER) to derivitize and quantify the urea group of the L-Citrulline product. These results

demonstrate the ability to discriminate various ADMA concentrations utilizing T165L's unexpected catalytic partitioning and provided evidence for further method development based on these principles.

Evaluation of *Pa*DDAH T165L Sample Incubation Conditions

Upon demonstrating the ability of *Pa*DDAH T165L to be inactivated by ADMA in a concentration dependent manner, we sought to optimize the methodology for quantification of ADMA in clinical samples. Ideal properties of an ADMA quantification method would include the ability to quantify ADMA directly from the sample of interest (e.g. blood plasma or serum). Concentrations of ADMA in blood plasma are in the low micromolar range, much lower than the concentrations used in the proof of principle experiments above. Still, based on *Pa*DDAH T165L's specificity for ADMA, and its slow rate of reactivation we sought to evaluate if differences could be observed at these low concentrations of ADMA.

To test if *Pa*DDAH T165L could be used to discriminate ADMA levels at the concentrations found in blood plasma, *Pa*DDAH T165L (15 nM) was incubated with varying concentrations of ADMA (0 – 2.5 μM) for 18 h. Aliquots of each sample were transferred to a 96-well plate containing SMTC (545 μM) and CPM (60 μM) and the fluorescence was monitored every 90 s for 20 min total. End point RFU values were calculated using equation 3.1 and plotted as a function of ADMA concentration (Figure 4.5). Compared to the experimental conditions above (See: Proof of Principle for *Pa*DDAH T165L ADMA Quantification), a reduction in enzyme concentration was required in order to ensure each enzyme molecule would undergo an adequate number of

turnovers to promote inactivation as defined by the partition ratio. Samples were incubated overnight to account for the low reaction velocity at concentrations below K_M. These experiments also revealed a linear correlation between fluorescence signal and ADMA concentration (Figure 4.6). However, the slope of this line is on the same order of magnitude as the average standard deviation between triplicate samples tested (-7200: 6800). Therefore, skipping a concentration step under these conditions will not result in sufficient accuracy for clinical samples and suggests the concentration or enrichment of

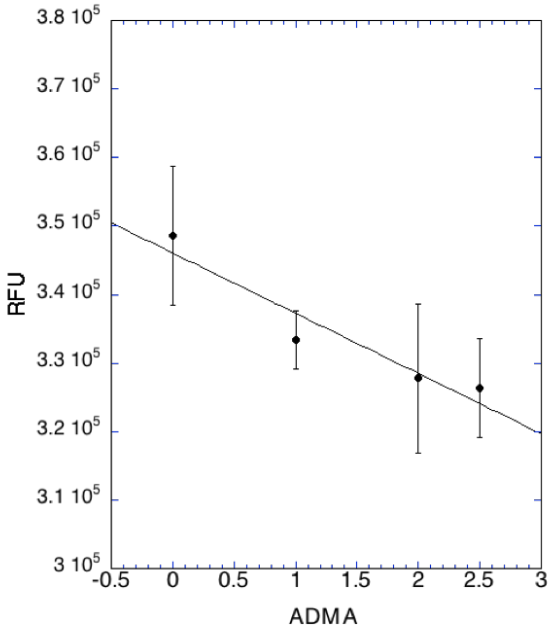

Figure 4.6 End point RFU from reactions of T165L (15 nM) with SMTC (545 µM) upon rapid dilution following 18 h pre-incubation with various concentrations of ADMA (0 – 2.5 µM). The RFU values were plotted against ADMA concentration and fit to a line with y-intercept 3.4 ± 0.3 × 10^5 RFU and a slope of -0.7 ± 0.1 × 10^5 RFU / ADMA µM.

ADMA from blood plasma samples will be needed for accurate quantification.

To test the minimal concentration of ADMA needed for accurate and sensitive quantification, *Pa*DDAH T165L (0 - 500 nM) was incubated with varying concentrations of ADMA (0 – 75 μM) for 0-5 h. Aliquots of each sample were transferred to a 96-well plate containing SMTC (545 μM) and CPM (60 μM) and the fluorescence was monitored every 90 s for 20 min total. Based on the analysis of these experiments, a minimum of 5 μM of ADMA was needed for accurate quantification. This would entail a ten-fold enrichment of ADMA. Sample concentration to this degree is possible through centrifugal evaporation with or without solid phase extraction.

Sample Preparation and Evaluation of ADMA in Human Blood Plasma

To prepare samples for centrifugal evaporation, 2 mL acetonitrile was added to each 1 mL blood plasma sample in order to precipitate proteins that might interfere with the signal amplification step. Following centrifugation, the supernatant was removed and subjected to centrifugal evaporation using a speed vacuum instrument. Samples were reconstituted in 80 μL Assay Buffer and were incubated with 0.25 μM *Pa*DDAH for 3 h. Aliquots (25 μL) of each sample were transferred to a 384-well plate containing SMTC (545 μM) and CPM (60 μM) and the fluorescence was monitored every 90 s for 20 min total (Figure 4.7A).

These tests revealed differential signals between control human blood plasma and human blood plasma with an arteriosclerosis medical background (ProteGenex, Inc.; Culver City, CA, USA). However, the fit values lie out of range of expected values when compared to the standard curve and do not reach an end point over the same timescale at the standard solutions. These results could indicate a background reaction of free plasma

thiols (e.g. glutathione, cysteine, and homocysteine) with CPM. The total concentration of free thiols in blood plasma can be as high as 10 μM, ten fold higher than that of ADMA, and would complicate the assay.[21] Additionally, the amount of unwanted

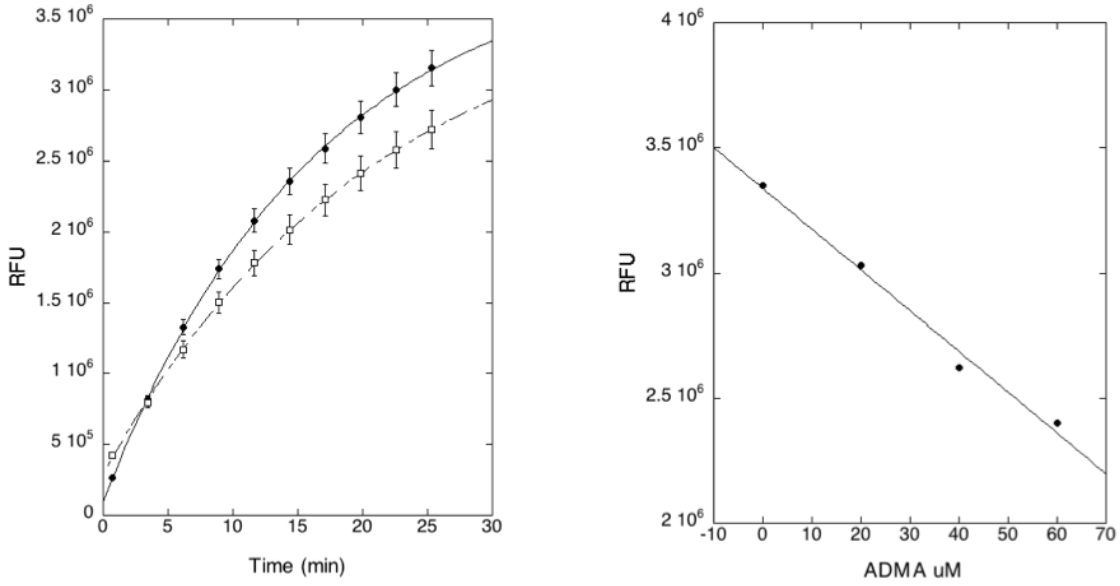

Figure 4.7 Evaluation of assay design in human blood plasma samples levels. (A) RFU as a function of time following pre-incubation with reconstituted plasma samples. (Arteriosclerosis; □ , Control; ●). (B) Standard curve produced using ADMA in Assay Buffer. End point values for Control (4.0 ± 0.5 × 10^6 RFU) and Arteriosclerosis (3.6 ± 0.4 × 10^6 RFU) do not correlate with the standard curve.

reaction of plasma free thiols and CPM may be further complicated by other medical conditions of the individuals from whom the samples were taken. For example, elevated levels of homocysteine have also been identified as a marker for atherosclerosis.[22] If not properly adjusted for, these background contributions may result in overestimation of the concentration of ADMA. While it was encouraging to see differentiation between control samples and those with a cardiovascular disease background (arteriosclerosis) the

plasma dependent effects limit the usefulness of this methodology (in its current form) in the same way as has been reported for ADMA quantification using ELISA. Specifically, matrix dependent effects limit the ability to accurately quantify samples based on a standard curve and often lead to an overestimation of ADMA levels.[13]

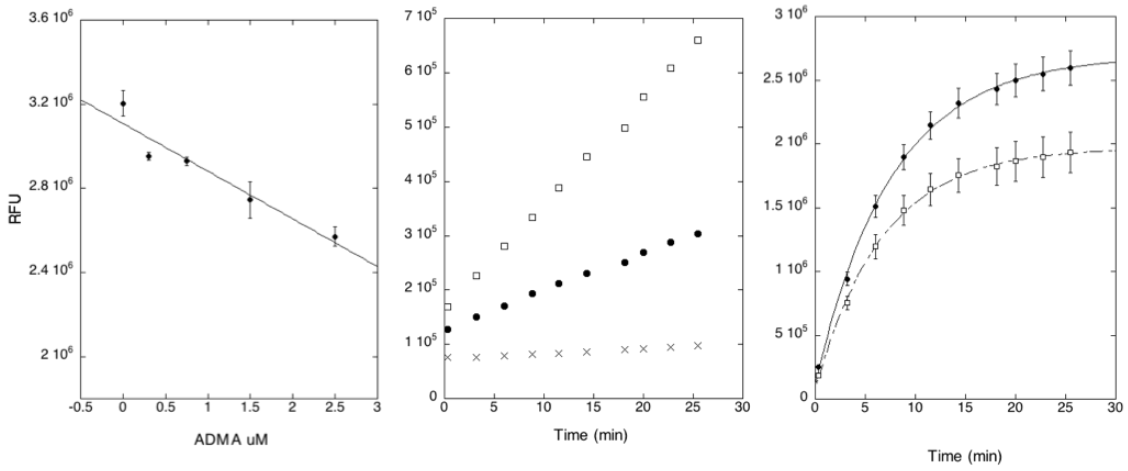

Figure 4.8 Evaluation of blood plasma samples and standard solutions of ADMA following SPE treatment. (A) Standard curve produced by standard solutions of ADMA (0 – 2.5 μM). (B) Sample dependent background signal over the timescale of the assay following SPE treatment (Arteriosclerosis; □ , Control; ●, Buffer; ×). (C) Background corrected RFU as a function of time following pre-incubation with SPE treated plasma samples. (Arteriosclerosis; □ , Control; ●).

These limitations prompted us to test whether or not incorporating solid phase extraction could improve or eliminate the background signal associated with direct sampling of reconstituted blood plasma. In theory, solid phase extraction using a cation exchange resin, such as the Oasis MCX SPE cartridges (Waters Coorporation; Milford, MA,USA), should result in the selective isolation of basic amino acids and concomitant elimination of unwanted free thiols. In order to assess any other effects based on addition of the SPE protocol, standard solutions of ADMA (0 – 2.5 μM) were also treated in the

same way for direct comparison. Once reconstituted in Assay Buffer following centrifugal evaporation of the SPE eluent, samples were assayed as the blood plasma samples described above.

The results of these experiments revealed enrichment and concentration of standard solutions (0 – 2.5 μM) by centrifugal evaporation and SPE treatment can achieve observable differentiation (Figure 4.8A) Furthermore, SPE does not introduce additional background signal within the standard solutions. To test whether or not plasma samples still maintain significant background signal following SPE treatment, fluorescence of plasma sample incubations lacking SMTC were monitored for 20 min. These experiments showed a significant contribution to background signal from plasma components even after SPE. Furthermore, the background signal was observed to be condition dependent (Figure 4.8B). When background corrected, a similar result is observed as seen when assaying samples without SPE pre-treatment. Specifically, differences in control and arteriosclerosis samples are observed, but the values do not correlate to the expected concentration range as defined by the standard curve (Figure 4.8C).

These sample-dependent background contributions are a major challenge in the development of a *Pa*DDAH T165L based assay for ADMA quantification because, as presented, the inactivation of *Pa*DDAH T165L is ADMA specific, but the final fluorescence readout is indiscriminate of the source of the thiol. Currently, the methodology described here has the potential to be suitable for investigations in which groups of samples are compared and the endpoint is the shift in ADMA concentration in

response to an intervention. Still, possible solutions to these problems are currently being evaluated to extend the method's usefulness to absolute quantification of ADMA concentration. For example, pre-treatment of samples with a non-fluorescent thiol reactive molecule such as N-ethylmaleimide (NEM) could minimize the background signal contribution. However, sample dependent effects make addition of a standardized amount of compound for pre-treatment unreliable as excess NEM could compete with CPM for reaction with methanethiol. Alternatively, pre-treatment with a thiol scavenging resin (Sigma Aldrich, St. Louis, MO, USA, Cat# 569909) could eliminate the influence of plasma thiols in a sample independent manner. Further development of this assay along with a direct comparison of the method outlined here with a commercially available ADMA ELISA Kit ALX-850-323-K101 (Enzo Life Sciences, Inc., Farmingdale, NY, USA) is underway.[23]

Based on our results, it is likely further improvement will be required to increase the sensitivity and accuracy of this methodology for clinical use. Comparison to the current standards of clinical measurement during continued optimization, especially with the only other plate-based methodology (ELISA), will be an essential part of the evaluation of our assay. While ELISA is currently the most accessible method for quantification, the cost-savings associated with production and use of a recombinant *Pa*DDAH T165L based assay compared with using α-ADMA monoclonal (or polyclonal) antibodies (Ab) for ADMA quantification would be significant.[24, 25] With small increases in sensitivity and accuracy, a *Pa*DDAH T165L based assay has the potential to overcome the limitations of analytical methods (HPLC/LC-MS) in terms of accessibility and

represents a significant cost reduction with respect to plate based consumable reagents (*Pa*DDAH T165L vs. α-ADMA Abs).

Comparison to Other Examples of Substrate Inactivation

The result that *Pa*DDAH T165L slowly becomes inactivated when incubated with substrate was unexpected, but the observation of substrate inactivation is not completely novel. Substrate inactivation of enzymes haw also been reported elsewhere. Meely and Martin reported the substrate dependent inactivation of brain Glutamate Decarboxylase (GAD).[26,27] The authors proposed that through the GAD's decarboxylation dependent transamination mechanism, the substrate glutamate promotes formation of inactivated enzyme via dissociation of the co-factor PLP. This mechanism is proposed to contribute to the physiological regulation of GAD, which involves a cycle of formation of apoenzyme and its reactivation to holoezyme by binding PLP.[27] Substrate induced inactivation has also been reported for *E. Coli N*-acetylmuramoyl-L-alanine amidase (AmiD). In this case, transient-substrate induced inactivation was interpreted in terms of conformational isomerization of the enzyme in the presence of substrate.[28] However, compared with our studies, both of these mechanisms of inactivation are shown to be non-covalent in nature and are a function of natural regulation of enzyme activity.

Substrate inactivation of mutant enzymes has also been reported elsewhere and in one case was discovered as a result of site directed mutational studies probing the substrate specificity of FEZ-1 metallo-β-lactamase, a study directly analogous to the one that led to the characterization of *Pa*DDAH T165L.[29] In this example, evidence suggested that the replacement of active site Y228 with alanine in FEZ-1 changes the position of the

subsrate in the catalytic pocket. This allows a direct interaction between C200 and the hydrolyzed substrate leading to the formation of a covalent and irreversibly inactivated complex. Inactivation of a specific point mutant enzyme during steady state turnover has also been reported for the diheme enzyme MauG (P107V) from *Paracoccus denitrificans*.[30] Here, the point mutation enhances the rate of a detrimental oxidative side reaction most likely caused by altered positions of amino acids at the heme site.

These studies, along with our own, suggest that catalytic partitioning of mutant enzymes is not limited to enzymes that use covalent intermediates, nor is it limited to enzymes that require cofactors. In all three cases, these branched pathways were discovered unexpectedly through active site mutational analysis. However, our work represents a novel advance in that this is the first time an unexpected substrate partitioning has been applied to quantify a substrate. The discovery of mutation-induced inactivation partitioning in a variety of enzyme classes suggests that it may be possible to use mutagenesis to purposefully engineer enzymes for substrate inactivation and quantification purposes for a wider array of small molecules.

4.4 CONCLUSIONS

In this chapter, a methodology for ADMA quantification using the catalytic partitioning of *Pa*DDAH T165L was explored. The experimental partition ratios for DDAH's endogenous substrates (ADMA and NMMA) and the synthetic substrate SMTC are defined. Based on this data and the proposed assay workflow, a methodology to quantify ADMA was developed. The method outlined was tested for the ability to

quantify ADMA in clinically-relevant blood plasma samples. Differences in signal amplification were seen between control plasma and those from individuals with an arteriosclerosis medical background. However, sample-dependent background contributions did not allow for absolute quantification of ADMA by use of a standard curve, although optimization of the protocol is continuing. The results described here show the feasibility of using *Pa*DDAH T165L as a means to quantify ADMA, but the assay must be further optimized and other complicating factors must be accounted for if the methodology is to be used in a clinical setting.

REFERENCES

1. Stuehr D., Griffith O. Mammalian Nitric Oxide Synthases. *Adv. Enzym. Relat. Areas Mol. Biol.* **65**, 287–346 (1993).

2. Shaul PW. Regulation of endothelial nitric oxide synthase: location, location, location. *Annu. Rev. Physiol.* **64**, 749–74 (2002).

3. Susswein AJ, Katzoff A, Miller N, Hurwitz I. Nitric oxide and memory. *Neuroscience Review J Bringing Neurobiol Neurol Psychia*try. **2**,153–62 (2004).

4. Tousoulis D, Kampoli A., Tentolouris C., Papageorgiou N. and Stefanadis C. The Role of Nitric Oxide on Endothelial Function. *Curr. Vasc. Pharmacol.* **14** 4-18 (2016).

5. Pope AJ, Karuppiah K, Cardounel AJ. Role of the PRMT–DDAH–ADMA axis in the regulation of endothelial nitric oxide production. *Pharmacol. Res.* **60**, 461–5 (2009).

6. Ito A, Tsao PS, Adimoolam S et al. Novel mechanism for endothelial dysfunction. Dysregulation of dimethylarginine dimethylaminohydrolase. *Circulation.* **99**, 3092–95 (1999).

7. Lin KY, Ito A, Asagami T et al. Impaired nitric oxide synthase pathway in diabetes mellitus: role of asymmetric dimethylarginine and dimethylarginine dimethylaminohydrolase. *Circulation*. **106**, 987–92 (2002).

8. Dhalla, NS, Temsah RM, Netticadan T, Role of oxidative stress in cardiovascular diseases. *J. Hypertens*. **18**, 655-73 (2000).

9. Cooke, J. P., Ghebremariam, Y. T., DDAH says NO to ADMA. *Arterioscler. Thromb. Vasc. Biol*. **31**, 1462-1464 (2011).

10. Mittermayer F, Krzyzanowska K, Exner M, Mlekusch W, Amighi J, Sabeti S, Minar E, Müller M, Wolzt M, Schillinger M. Asymmetric dimethylarginine predicts major adverse cardiovascular events in patients with advanced peripheral artery disease. *Arterioscler. Thromb. Vasc. Biol*. **26**, 2536-40 (2006).

11. Szuba, A., Podgorski, M. Asymmetric dimethylarginine (ADMA) a novel cardiovascular risk factor--evidence from epidemiological and prospective clinical trials. *Pharmacol. Rep*. **58**, 16- 20 (2006).

12. Bouras G, Deftereos S, Tousoulis D, Giannopoulos G, Chatzis G, Tsounis D, Cleman MW, and Stefanadis C. Asymetric Dimethylareginine (ADMA): A Promising Biomarker for Cardiovascular Disease? *Curr. Top. Med. Chem*. **13**, 180-200 (2013).

13. *Martens-Lobenhoffer J, Westphal S, Awiszus F, Bode-Bo ̈ger SM, Luley C*. Determination of Asymmetric Dimethylarginine: Liquid Chromatography–Mass Spectrometry or ELISA? *Clin. Chem*. **51**, 2188-2189 (2005).

14. Boger, R. H.; Sullivan, L. M.; Schwedhelm, E.; Wang, T. J.; Maas, R.; Benjamin, E. J.; Schulze, F.; Xanthakis, V.; Benndorf, R. A.; Vasan, R. S. Plasma asymmetric dimethylarginine and incidence of cardiovascular disease and death in the community. *Circulation,* **119**, 1592-1600 (2009).

15. Linsky, T. W. Studies on the mechanism and inhibition of enzymes in the pentein superfamily. Ph. D. Dissertation, University of Texas, Austin, TX, 2012.

16. Stone E.M., Person M.D., Costello N.J., Fast,W. Characterization of a transient covalent adduct formed during dimethylarginine dimethylaminohydrolase catalysis. *Biochemistry* **2005**, 44, 7069.

17. Knipp, M. & Vasák, M. A colorimetric 96-well microtiter plate assay for the determination of enzymatically formed citrulline. *Anal. Biochem*. 286, 257–264 (2000).

18. Linsky ,T Fast, W. A continuous, fluorescent, high-throughput assay for human dimethylarginine dimethylaminohydrolase-1. *J Biolmol Screen*. **16**, 1089-97 (2011).

19. Plevin M. J., Magalhaes B. S., Harris R., Sankar A., Perklins S. J., Driscoll P. C. Characterization and Manipulation of the *Pseudomonas aeruginosa* Dimethylarginine Dimethylaminohydrolase Monomer-Dimer Equilibrium. *J. Mol. Bio*. **341,** 171-184 (2004).

20. Birdsey, G. M., Leiper, J. M., and Vallance, P. Intracellular localization of dimethylarginine dimethylaminohydrolase overexpressed in an endothelial cellline. *Acta Physiol Scand* **168**, 73-9 (2000).

21. Andersson A., Lindgren A., Arnadottir M., Prytz H., Hutlberg B. Thiols as a Measure of Plasma Redox Status in Healthy Subjects and in Patients with Renal or Liver Failure. *Clin. Chem*. **45,** (1999).

22. Sreckovic B., Sreckovic V. D., Soldatovic I., Colak E., Sumarac-Dumanovic M., Janeski H., Janeski N, Gacic J., Mrdovic I. Homocysteine is a marker for metabolic syndrome and arteroscIerosis. *Diabetes & Metabolic Syndrome: Clin. Res. Rev*. doi: 10.1016/j.dsx.2016.08.026. [Epub ahead of print] (2016).

23. Bland JM, Altman DG. Statistical methods for assessing agreement between two methods of clinical measurement. *Lancet* **1,** 307–10 (1986).

24. Kelley B. Industrialization of mAb production technology The bioprocessing industry at a crossroads. *MAbs*. **5,** 443-452 (2009).

25. Wakayama T., Kato Y., Utsumi R., Tsuji A., Iseki S. A Time and Cost-Saving Method of Producing Rat Polyclonal Antibodies. *Acta Histochem Cytochem,* **39,** 79-87 (2006).

26. Meely M. P., Martin D. L. Reactivation of Substrate-Inactivated Brain Glutamate Decarboxylase. *Cell Mol. Neurobiol*. **3,** 55-68 (1983).

27. Martin D. L., Meeley M. P., Martin S. B., Pedersen S. Factors influencing the activation and inactivation of glutamate decarboxylase. *BRB*. **5,** 57-61 (1980).

28. Pennartz A., Genereux C., Parquet C., Mengin-Lecreulx D., Joris B. Substrate-Induced Inactivation of the *Escherichia coli* AmiD *N*-Acetylmuramoyl-L-Alanine Amidase Highlights a New Strategy To Inhibit This Class of Enzyme. *Antimicrob. Agents Chemother*. **53,** 2991-2997 (2009).

29. Mercuri P. S., Garcia-Saez I., Vriendt K., Thamm I., Devreese B., Beeumen J. V.,

Dideberg O., Rossolini G. M., Frere J. M., Galleni M. Probing the Specificity of the Subclass B3 FEZ-1 Metallo-β-lactamase by Site-directed Mutagenesis. *J. Bio. Chem*. **279,** 33630-33638 (2004).

30. Ma Z., Williamson H. R., Davidson V. L. A suicide Mutation Affecting Proton Transfers to High-Valent Hemes Causes Inactivation of MauG during Catalysis. *Biochemistry*. **55,** 5738-5745 (2016).

Appendix

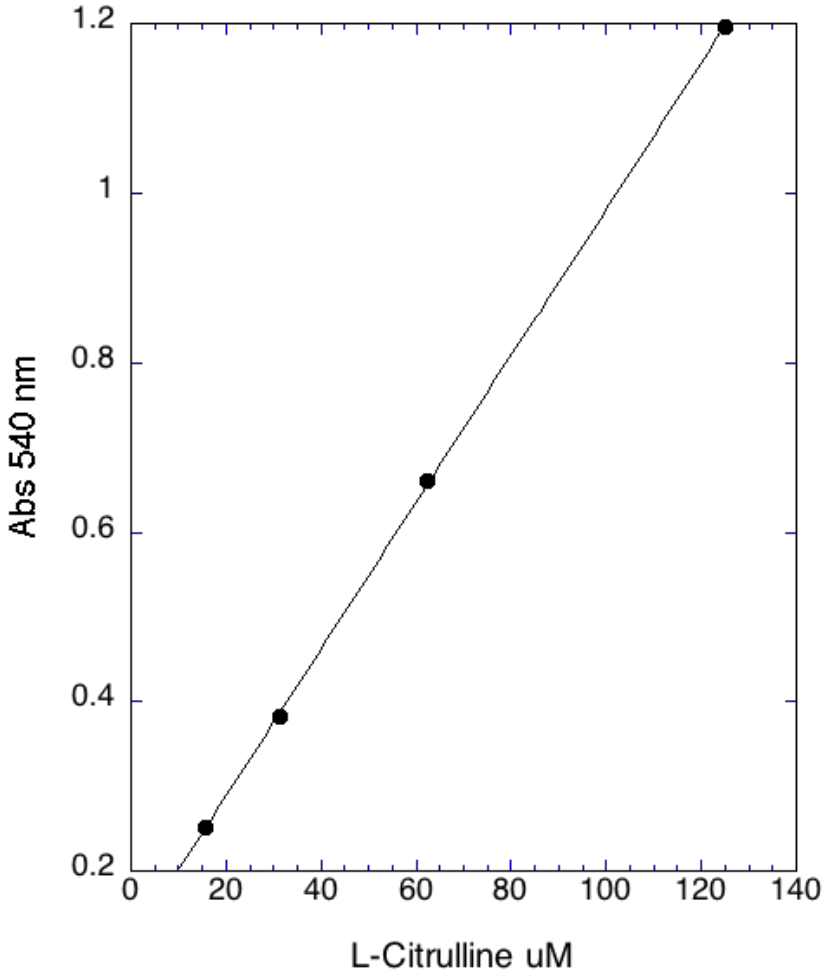

Figure A.1 L-Citrulline standard curve using the color-developing reagent (COLDER) to derivatize the urea group of the *L*-Citrulline product The data was fit to the line $y = 1.15 \pm 0.03 \times 10^{-1} + 8.65 \pm 0.04 \times 10^{-3}$.

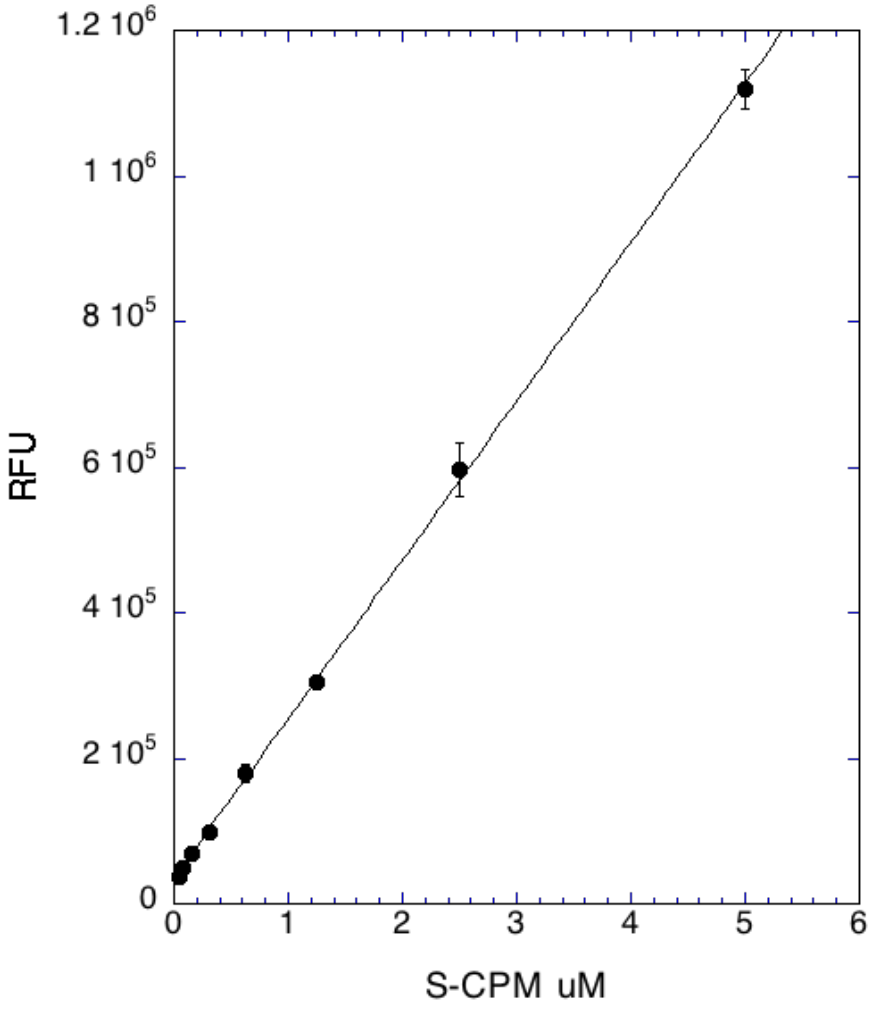

Figure A.2 Standard curve for the reaction of free thiol with CPM in a 96-well plate format. Data was fit to the line $y = 3.5 \pm 0.4 \times 10^4 + 2.2 \pm 0.2 \times 10^5$

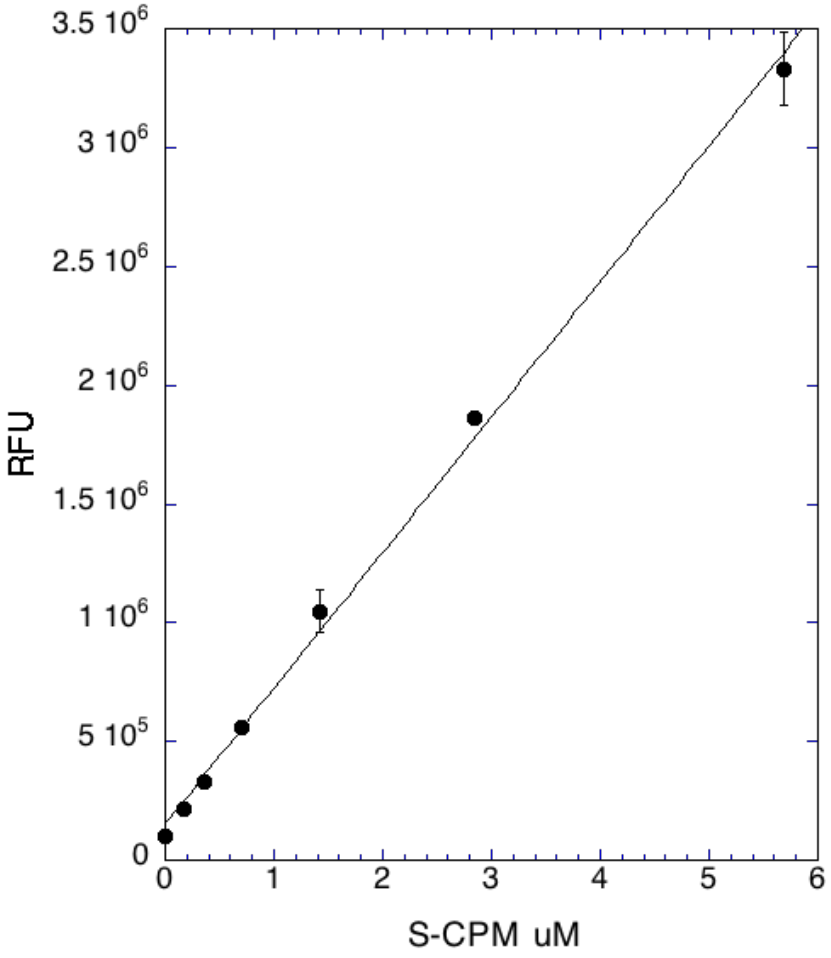

Figure A.3 Standard curve for the reaction of free thiol with CPM in a 384-well plate format. Data was fit to the line $y = 1.5 \pm 0.3 \times 10^5 + 5.8 \pm 0.1 \times 10^5$

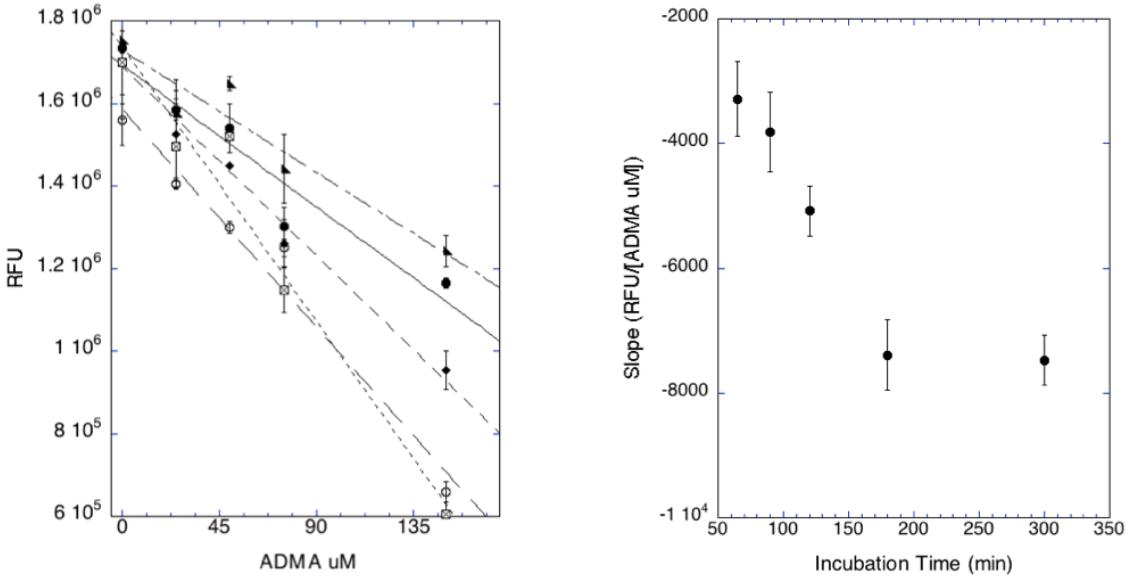

Figure A.4 Incubation time dependence on remaining activity of *Pa*DDAH T165L. (A) RFU as a function of the concentration of ADMA in pre-incubation mixtures assayed at various time points (65 min; + , 90 min; ◇ , 120 min; × , 180 min; □ , 300 min; ●). (B) Calculated slopes from (A) replot versus incubation time.

Bibliography

Amann R., Peskar B. A. Anti-inflammatory effects of aspiring and sodium salicylate. *Eur. J. Pharmacol.* **447,** 1-9 (2002).

Andersson A., Lindgren A., Arnadottir M., Prytz H., Hutlberg B. Thiols as a Measure of Plasma Redox Status in Healthy Subjects and in Patients with Renal or Liver Failure. *Clin. Chem.*. **45,** (1999).

Baines, A. T., Xu, D. & Der, C. J. Inhibition of Ras for cancer treatment: the search continues. *Future Med. Chem.* ***3***, 1787-1808 (2011)

Bauer R. Covalent inhibitors in drug discovery: from accidental discoveries to avoided liabilities and designed therapies. *Drug Discov. Today*. **20**, 1061-1073 (2015).

Birdsey, G. M., Leiper, J. M., and Vallance, P. Intracellular localization of dimethylarginine dimethylaminohydrolase overexpressed in an endothelial cellline. *Acta. Physiol. Scand.* **168**, 73-9 (2000).

Bland JM, Altman DG. Statistical methods for assessing agreement between two methods of clinical measurement. *Lancet* **1,** 307–10 (1986).

Boger, R. H.; Sullivan, L. M.; Schwedhelm, E.; Wang, T. J.; Maas, R.; Benjamin, E. J.; Schulze, F.; Xanthakis, V.; Benndorf, R. A.; Vasan, R. S. Plasma asymmetric dimethylarginine and incidence of cardiovascular disease and death in the community. *Circulation,* **119**, 1592-1600 (2009).

Boothman, D. A., Briggle, T. V. & Greer S. B. Protective, Tumor-selective Dual Pathway Activation of 5-Fluoro-2'-deoxycytidine Provided by Tetrahydrouridine in Mice Bearing Mammary Adenocarcinoma-755. *Cancer Res.* **47,** 2344-2353 (1987).

Bouras G, Deftereos S, Tousoulis D, Giannopoulos G, Chatzis G, Tsounis D, Cleman MW, and Stefanadis C. Asymetric Dimethylareginine (ADMA): A Promising Biomarker for Cardiovascular Disease? *Curr. Top. Med. Chem.* **13**, 180-200 (2013).

Bradford M.M. A rapid and sensitive method for the quantification of microgram quantities of protein utilizing the principle of protein-dye binding. *Anal. Biochem.* **72***,* 248-54 (1976).

Bruns A., Eichner S., Lehmann F., Albrecht W., Maier A. Crystalline forms of afatinib di-maleate. US Publication Number 2013052157 A1, October 6, 2011.

Cao, D. & Pizzorno, G. Uridine phosphorylase: An important enzyme in pyrimidine metabolism and fluoropyrimidine activation. *Drugs of Today (Barc)*. **40,** 431-43 (2004).

Caradoc-Davies, T. T., Cutfield, S., M., Lamont, I. L. & Cutfield, J., F. Crystal Structures of *Escherichia coli* Uridine Phosphorylase in Two Native and Three Complexed Forms Reveals Basis of Substrate Specificity, Induced Conformational Changes and Influence of Pottasium. *J Mol. Bio*. **337,** 337-354 (2004).

Carlow, D. C., Short, S. A., Wolfenden R. Complementary Truncations of a Hydrogen Bond to Ribose Involved in Transition-State Stabilization by Cytidine Deaminase. *Biochemistry*. **37,** 1199-1203 (1998)

Chambers C.S. "Non-Taxifolin" Derived Flavonolignans: Phytochemistry and Biology. *Curr. Pharm. Des*. **21**, 5489-5500 (2015).

Cherng YJ. Synthesis of substituted pyridines by the reactions of halopyridines with sulfur, oxygen and carbon nucleophiles under focused microwave irradiation. *Tetrahedron*. **58**, 4931-4935 (2002).

Congreve, M., Aharony, D., Albert, J., Callaghan, O., Campbell, J., Carr, R. A., Chessari, G., Cowan, S., Edwards, P. D., Frederickson, M., McMenamin, R., Murray, C. W., Patel, S., and Wallis, N. Application of fragment screening by X-ray crystallography to the discovery of amino pyridines as inhibitors of β-secretase *J. Med. Chem*. **50**, 1124–1132 (2007).

Cooke, J. P., Ghebremariam, Y. T., DDAH says NO to ADMA. *Arterioscler Thromb Vasc Biol*. **31**, 1462-1464 (2011).

Cox, Brian G. Acids and Bases: Solvent Effects on Acid-base Strength. 1st ed. Oxford, UK: Oxford UP, (2013).

Crooks G. P., Copley S. D., A Surprising Effect of Leaving Group on the Nucleophilic Aromatic Substitution Reaction Catalyzed by 4-Chlorobenzoyl-CoA Dehalogenase. *J. Am. Chem. Soc*. **115**, 6422-6423 (1993).

Dhalla, NS, Temsah RM, Netticadan T, Role of oxidative stress in cardiovascular diseases. *J Hypertens*. **18**, 655-73 (2000).

Drahl C., Cravatt B. F., Sorensen E. J. Protein-Reactive Natural Products. *Angew. Chem. Int. Ed*. **44,** 5788-5809 (2005).

Dreser H. Pharmacologisches über Aspirin (Acetylsalicyl-saüre). *Pflügers Arch Gesamte Physiol Menschen Tiere*, **76**, 306–318 (1899).

Er, J. A. The design of halopyridine-based activity-based probes and mechanistic studies of succinylarginine dihydrolase. Ph. D. Dissertation, University of Texas, Austin, TX, 2015.

Goldstein D. M. Formulations comprising ibrutinib. US Publication Number 2014004707 A1, June 29, 2012.

Huth, J. R., Park, C., Petros, A. M., Kunzer, A. R., Wendt, M. D., Wang, X., Lynch, C. L., Mack, J. C., Swift, K. M., Judge, R. A., Chen, J., Richardson, P. L., Jin, S., Tahir, S. K., Matayoshi, E. D., Dorwin, S. A., Ladror, U. S., Severin, J. M., Walter, K. A., Bartley, D. M., Fesik, S. W., Elmore, S. W., and Hajduk, P. J. Discovery and Design of Novel HSP90 Inhibitors Using Multiple Fragment-based Design Strategies. *Chem. Biol. Drug Des.* **70**, 1–12 (2007).

Ishihama, Y., Oda, Y., Tabata, T., Sato, T., Nagasu, T., Rappsilber, J. & Mann M. Exponentially Modified Protein Abundance Index (emPAI) for Estimation of Absolute Protein Amount in Proteomics by the Number of Sequenced Peptides per Protein. *Mol. Cell Proteomics*. **4,** 1265-1272 (2005).

Ito A, Tsao PS, Adimoolam S et al. Novel mechanism for endothelial dysfunction. Dysregulation of dimethylarginine dimethylaminohydrolase. *Circulation*. **99**, 3092–95 (1999).

Jeffreys D. *Aspirin: The Remarkable Story of a Wonder Drug*. Bloomsbury, 2004.

Johnson, C. M., Linsky, T. W., Yoon, D. W., Person, M. D., Fast, W. Discovery of Halopyridines as Quiescent Affinity Labels: Inactivation of Dimethylarginine Dimethylaminohydrolase. *J. Am. Chem. Soc.* **133**, 1553 (2011).

Johnson C. M., Monzingo A. F., Ke Z., Yoon D., Linsky T. W., Guo H., Robertus J. D., Fast W. On the Mechanism of Dimethylarginine Dimetheylaminohydrolase Inactivation by 4-Halopyridines. *J. Am. Chem. Soc.* **133**, 10951-10959 (2011).

Kathman S. G., Xu, Z., Statsyuk A. V. A Fragment-Based Method to Discover Irreversible Covalent Inhibitors of Cysteine Proteases. *J. Med. Chem.* **57**, 4969-4974 (2014).

Kapust R.B., Tozser J., Fox J.D., Anderson D. E., Cherry S., Copeland T. D., Waugh D. S. Tobacco etch virus protease: mechanism of autolysis and rational design of stable mutants with wild-type catalytic proficiency. *Protein Eng*. **12,** 993-1000 (2001).

Kelley B. Industrialization of mAb production technology The bioprocessing industry at a crossroads. *MAbs*. **5,** 443-452 (2009)

Khanduja K.L., Bhardwaj A. Stable free radical scavenging and antiperoxidative properties of resveratrol compared in vitro with some other bioflavonoids. *Indian J. Biochem. Biophys*. **40***, 416-422 (*2003**)**.

Kim K., Kuo T., Cai J., Murnane M. J. N-ras protein: Frequent quantitative and qualitative changes occur in human colorectal carcinomas. *Int. J. Cancer*. **71,** 767-75 (1997).

Kim K.B., Crews C.M., From epoxomicin to carfilzomib: chemistry, biology, and medical outcomes. *Natural Product Reports*. **30***,* 600-604 (2013).

Klomsiri, C., Karplus, P. A., Poole, L. B., Cysteine-Based Redox Switches in Enzymes. *Antioxidants & Redox Signaling*. **14,** 1065-1077 (2011).

Knipp, M. & Vasák, M. A colorimetric 96-well microtiter plate assay for the determination of enzymatically formed citrulline. *Anal. Biochem*. 286, 257–264 (2000).

Kondo S., Nakanishi M., Tsuda K. Nucleophilic Substitution of Halopyridines by Benzenethiolate Anion via a Radical Chain Mechanism. *J. Heterocyclic Chem*. **21**,1243-1244 (1984**)**.

Koval I. V. Reaction of Thiols. *Russian Journal of Organic Chemistry*. **43***,* 319-346 (2007**)**.

Lim, S. M., Westover, K. D., Ficarro, S. B., Harrison, R. A., Choi, H. G., Pacold, M. E., Carrasco, M., Hunter, J., Kim, N. D., Xie, T., Sim, T., Janne, P. A., Meyerson, M., Marto, J. A., Engen, J. R. & Gray, N. S. Therapeutic Targeting of Oncogenic K-Ras by a Covalent Catalytic Site Inhibitor. *Angew. Chem. Int. Ed.*, ***53***, 199-204 (2014).

Lin KY, Ito A, Asagami T et al. Impaired nitric oxide synthase pathway in diabetes mellitus: role of asymmetric dimethylarginine and dimethylarginine dimethylaminohydrolase. Circulation. **106**, 987–92 (2002).

Linsky ,T Fast, W. A continuous, fluorescent, high-throughput assay for human dimethylarginine dimethylaminohydrolase-1. *J Biolmol. Screen*. **16**, 1089-97 (2011)

Linsky, T. W. Studies on the mechanism and inhibition of enzymes in the pentein superfamily. Ph. D. Dissertation, University of Texas, Austin, TX, 2012.

Ma Z., Williamson H. R., Davidson V. L. A suicide Mutation Affecting Proton Transfers to High-Valent Hemes Causes Inactivation of MauG during Catalysis. *Biochemistry*. **55,** 5738-5745 (2016).

Mah R., Thomas J. R., Shafer C. M. Drug discovery considerations in the development of covalent inhibitors. *Bioorg. Med. Chem. Lett*, **24**, 33-39 (2015).

Martens-Lobenhoffer J, Westphal S, Awiszus F, Bode-Bo ̈ger SM, Luley C. Determination of Asymmetric Dimethylarginine: Liq- uid Chromatography–Mass Spectrometry or ELISA? *Clin. Chem*. **51**, 2188-2189 (2005).

Martin D. L., Meeley M. P., Martin S. B., Pedersen S. Factors influencing the activation and inactivation of glutamate decarboxylase. *BRB*. **5,** 57-61 (1980).

MARVIN.15.11.16.0.; ChemAxon: Budapest, Hungary.

Mattingly, R. R. Activated Ras as a Therapeutic Target: Constraints on Directly Targeting Ras Isoforms and Wild-Type versus Mutated Proteins. *ISRN Oncology*, ID: 536529 (2013).

Meely M. P., Martin D. L. Reactivation of Substrate-Inactivated Brain Glutamate Decarboxylase. *Cell Mol. Neurobiol*. **3,** 55-68 (1983).

Mekras, J. A., Boothman, D. A. & Greer, S. B. Use of 5-trifluoromethyldeoxycytidine and tetrahydrouridine to circumvent catabolism and exploit high levels of cytidine deaminase in tumors to achieve DNA- and target-directed therapies. *Cancer Res*. **45,** 5270-80 (1985).

Mellacheruvu, D., Wright, Z., Couzens, A. L., Lambert, JP., St-Denis, N. A., Li, Tuo, Miteva, Y. V., Hauri, S., Sardiu, M. E., Low, T. Y., Halim, V. A., Bagshaw, R. D., Hubner, N. C., al-Hakim, A., Bouchard, A., Faubert, D., Fermin, D., Dunham, W. H., Goudreault, M., Lin, Z., Badillo, G., Pawson, T., Durocher, D., Coulombe, B. & Aebersold, R. The CRAPome: a contaminant repository for affinity purification-mass spectrometry data. *Nat. Meth*. **10**, 730-736 (2013).

Mercuri P. S., Garcia-Saez I., Vriendt K., Thamm I., Devreese B., Beeumen J. V., Dideberg O., Rossolini G. M., Frere J. M., Galleni M. Probing the Specificity of

the Subclass B3 FEZ-1 Metallo-β-lactamase by Site-directed Mutagenesis. *J. Bio. Chem.* **279,** 33630-33638 (2004).

Miller R. M., Paavilainen V. O., Krishnan S., Serafimova I. M., Taunton J, Electrophilic Fragment-Based Design of Reversible Covalent Kinase Inhibitors. *J. Am. Chem. Soc.* **135**, 5298–5301 (2013).

Mittermayer F, Krzyzanowska K, Exner M, Mlekusch W, Amighi J, Sabeti S, Minar E, Müller M, Wolzt M, Schillinger M. Asymmetric dimethylarginine predicts major adverse cardiovascular events in patients with advanced peripheral artery disease. *Arterioscler. Thromb. Vasc. Biol.* **26**, 2536-40 (2006).

Mizuno K., Yamamoto S., Lands W. E. Effects of non-steroidal anti-inflammatory drugs on fatty acid cyclooxygenase and prostaglandin hydroperoxidase activities. *Prostaglandins.* **23,** 743-757 (1982).

Oda, Y., Owa, T., Sato, T., Boucher, B., Daniels, S., Yamanaka, H., Shinohara, Y., Yokoi, A., Kuromitsu, J., & Nagasu, T. Quantitative Chemical Proteomics for Identifying Candidate Drug Targets. *Anal. Chem.* **75,** 2159-2165 (2003).

Ostrem, J. M.; Peters, U.; Sos, M. L.; Wells, J. A.; Shokat, K. M.: K-Ras(G12C) inhibitors allosterically control GTP affinity and effector interactions. *Nature.* ***503***, 548-551 (2013).

Park B. K., Boobis A., Clarke S., Goldring C. E., Jones D., Kenna J.G., Lambert C., Laverty H. G., Naisbitt D. J. , Nelson S, Nicoll-Griffith D. A., Obach R. S., Routledge P., Smith D. A., Tweedie D. J., Vermeulen N., Williams D. P., Wilson I. D. & Baillie T. A. Managing the challenge of chemically reactive metabolites in drug development. *Nat. Rev. Drug Discov.* **10**, 292-306 (2011).

Pennartz A., Genereux C., Parquet C., Mengin-Lecreulx D., Joris B. Substrate-Induced Inactivation of the *Escherichia coli* AmiD *N*-Acetylmuramoyl-L-Alanine Amidase Highlights a New Strategy To Inhibit This Class of Enzyme. *Antimicrob Agents Chemother.* **53,** 2991-2997 (2009).

Plevin M. J., Magalhaes B. S., Harris R., Sankar A., Perklins S. J., Driscoll P. C. Characterization and Manipulation of the *Pseudomonas aeruginosa* Dimethylarginine Dimethylaminohydrolase Monomer-Dimer Equilibrium. *J. Mol. Bio.* **341,** 171-184 (2004).

Piria R. Sur de neuveaux produits extraits de la salicine (On new products extracted from salicine). *Comptes rendus.* **6**, 620-624 (1838).

Pope AJ, Karuppiah K, Cardounel AJ. Role of the PRMT–DDAH–ADMA axis in the regulation of endothelial nitric oxide production. *Pharmacol. Res.* **60**, 461–5 (2009).

Prior, I. A., Lewis, P. D. & Mattos, C. A comprehensive survey of Ras Mutations in Cancer. *Cancer Res.* **72**, 2457 (2012).

Riddles P.W., Blakeley R. L., Zerner B. Reassessment of Ellman's reagent, *Methods Enzymol.* **91**, 49-60 (1983).

Scott D. E., Coyne A. G., Hudson S. A., Abell C. Fragment-Based Approaches in Drug Discovery and Chemical Biology. *Biochemistry.* **51**, 4990-5003 (2012).

Serafimova I. M, Pufall M. A., Krishnan S., Duda K., Cohen M. S., Maglathlin R. L., McFarland J. M., Miller R. M., Frodin M., Taunton J. Reversible targeting of noncatalytic cysteines with chemically tuned electrophiles. *Nat. Chem. Bio.* **8**, 471-476 (2013).

Shannon D. A., Weerapana E. Covalent protein modification: the current landscape of residue-specific electrophiles. *Curr. Opin. Chem. Bio.* **24**, 18-26 (2015).

Shannon D. A., Banerjee R., Webster E. R., Bak D. W, Wang C., Weerapana E. Investigating the Proteome Reactivity and Selectivity of Aryl Halides *J. Am. Chem. Soc.* **136**, 3330-3333 (2014).

Shaul PW. Regulation of endothelial nitric oxide synthase: location, location, location. *Annu. Rev. Physiol.* **64**, 749–74 (2002).

Shin, G., Kang, T., Yang, S., Baek, S., Jeong, Y. & Kin, S. GENT: Gene Expression Database of Normal and Tumor Tissues. *Cancer Informatics.* **10,** 149-157 (2011).

Singh J., Petter R. C., Baillie T. A., Whitty A., The resurgence of covalent drugs. *Nature Reviews Drug Discovery.* **10**, 307-317 (2011).

Smyth M. S., Laidig G. J. Compounds for proteasome enzyme inhibition. US Patent No. 2015361134, August 6, 2004.

Sreckovic B., Sreckovic V. D., Soldatovic I., Colak E., Sumarac-Dumanovic M., Janeski H., Janeski N, Gacic J., Mrdovic I. Homocysteine is a marker for metabolic syndrome and arterosclerosis. *Diabetes & Metabolic Syndrome: Clinical Research & Reviews*. doi: 10.1016/j.dsx.2016.08.026. [Epub ahead of print] (2016).

Stone E.M., Person M.D., Costello N.J., Fast,W. Characterization of a transient covalent adduct formed during dimethylarginine dimethylaminohydrolase catalysis. *Biochemistry* **2005**, 44, 7069.

Stuehr D., Griffith O. Mammalian Nitric Oxide Synthases. *Adv. Enzym. Relat. Areas Mol. Biol.* **65**, 287–346 (1993).

Susswein AJ, Katzoff A, Miller N, Hurwitz I. Nitric oxide and memory. *Neuroscience Review J Bringing Neurobiol. Neurol. Psych.* **2**,153–62 (2004).

Szegezdi J., and Csizmadia F. A method for calculating the pK_a values of small and large molecules. American Chemical Society Spring meeting, March 25-29th (2007).

Szegezdi J., and Csizmadia F. Prediction of dissociation constants using microconstants. 27th ACS National Meeting, Anaheim, California, March 28-April 1 (2004).

Szuba, A., Podgorski, M. Asymmetric dimethylarginine (ADMA) a novel cardiovascular risk factor--evidence from epidemiological and prospective clinical trials. *Pharmacol Rep*. **58**, 16- 20 (2006).

Tabin C. J., Bardley S. M., Bargmann C. I., Weinberg, R. A. Mechanism of activation of a human oncogene. *Nature*. **300,** 143-149 (1982).

Tousoulis D, Kampoli A., Tentolouris C., Papageorgiou N. and Stefanadis C. The Role of Nitric Oxide on Endothelial Function. *Curr. Vasc. Pharma*. **14** 4-18 **(**2016**)**.

Tsimberidou, A. M., Chandhasin, C. & Kurzrock, R. Farnesyltransferase inhibitors: where are we now? *Expert Opin. Investig. Drugs*. ***19***, 1569-1580 **(**2010).

Vane J. R. *Nat. New Biol*. **231**, 232 –235 (1971).

Wakayama T., Kato Y., Utsumi R., Tsuji A., Iseki S. A Time and Cost-Saving Method of Producing Rat Polyclonal Antibodies. *Acta. Histochem. Cytochem*. **39,** 79-87 (2006)

Wang Y., Monzingo A. F., Hu S., Schaller T., Robertus J., Fast W. Developing dual and specific inhibitors of dimethylarginine dimethylaminohydrolase-1 and nitric oxide synthase: toward a targeted polypharmacology to control nitric oxide. *Biochemistry*. **48**, 8624-8635 (2009**)**.

Weerasinghe J.P., Dong T, Schertzberg M. R., Kirchhof M. G., Sun Y., Schellhorn H. E. Stationary phase expression of the arginine biosynthetic operon *argCBH* in *Escherichia coli*. *BMC Microbiology*. **6**, 14 (2006**)**.

Winter J.G., Anderson M., Blades K., Brassington C., Breeze A. L., Christine C., Embrey K., Fairley G., Faulder P., Finlay R. V., Kettle J. G., Nowak T., Overman R., Patel J., Perkins P., Spadola L., Tart J., Tucker J. A., Wrigley G. Small Molecules Binding Sites on the Ras:SOS complex Can Be Exploited for Inhibition of Ras Activation. *J. Med. Chem.* **58,** 2265-2274 (2015).

Wright P.M., Seiple I. B., Myers A. G. The evolving role of chemical synthesis in antibacterial drug discovery. *Angew. Chem. Int. Ed.* **53**, 8840–8869 (2014).

Yan, R., Wan, L., Pizzorno, G. & Cao, D. Uridine phosphorylase in breast cancer: a new prognostic factor? *Front. Biosci.* **11,** 2759-66 (2006).

Zauri, M., Berridge, G., Thezenas, M. L., Pugh, K. M., Goldin, R., Kessler, B., M., Kriaucionis, S. CDA directs metabolism of epigenetic nucleosides revealing a therapeutic window in cancer. *Nature.* **6,** 114-8 (2015).

Vita

Christopher Lee Schardon received his BS (Biochemistry) in 2010 from Trinity University, where he split his time between the classroom and the pitch as part of the Trinity University Men's Soccer Team. During his undergraduate studies, he was involved in multiple research projects. He both identified novel flavonoid and sinapate secondary metabolites produced by plants in response to UV irradiation and examined the molecular recognition of peptides using the synthetic receptor cucurbit[7]uril. In 2011, he was accepted by the Department of Chemistry and Biochemistry at The University of Texas at Austin for graduate study in Biochemistry. In the lab of Dr. Walter Fast he was able to work to expand our understanding at the interface of enzymology and drug discovery.

Permanent email address: cschardon@gmail.com

This dissertation was typed by Christopher Lee Schardon